Mathematical Models For Educational Simulation of Cardiovascular Pathophysiology

(Modelos matemáticos para a simulação educativa da patofisiologia cardiovascular)

Carla Sá Couto

Dissertation submitted in fulfilment of the requirements for the degree of Doctor in Biomedical Engineering by the Faculty of Engineering of the University of Porto, Portugal

FEUP, 2009

Thesis prepared under the supervision of:

Professor Doutor Willem Lambertus van Meurs
Instituto de Engenharia Biomédica (INEB)
Faculdade de Engenharia da Universidade do Porto (FEUP)

Professor Doutor Diogo de Matos Graça Ayres de Campos
Faculdade de Medicina da Universidade do Porto (FMUP)
Instituto de Engenharia Biomédica (INEB)

Reviewing board

Doutor Aurélio Joaquim de Castro Campilho
Prof. Catedrático, Dept. Engenharia Electrotécnica e de Computadores, FEUP

Doutor Mark Tooley
Professor, Bath University, UK

Doutor Hans van Oostrom
Associate Professor, University of Florida, USA

Doutor Peter Andriessen
Neonatologist, Máxima Medical Centre, Veldhoven, The Netherlands

Doutor João Bernardes
Professor Catedrático, Dept. Ginecologia e Obstetrícia, FMUP

Doutor Willem van Meurs
Investigador Principal, INEB

Doutor Diogo Ayres de Campos
Professor Associado, Dept. Ginecologia e Obstetrícia, FMUP

Study supported by

Instituto de Engenharia Biomédica (INEB), Porto, Portugal

Máxima Medical Center (MMC), Veldhoven, The Netherlands

Medical Education Technologies, Inc (METI), Florida, USA

Host institution

Instituto de Engenharia Biomédica (INEB), Porto, Portugal

To Pedro, Beatriz, and Matilde

Acknowledgements

I would like to express my sincere gratitude to those who, directly or indirectly, have contributed to this long term project, and made possible the completion of this thesis.

Firstly, I would like to acknowledge my supervisors, Prof. Willem van Meurs and Prof. Diogo Ayres de Campos, for the guidance, suggestions, and constructive criticism. Thank you for the friendship, trust and the given opportunities throughout these years.

My appreciation also goes to Dr. Peter Andriessen, for the stimulating collaboration and the many valuable discussions on several topics of this thesis.

To the co-authors of the papers presented in this thesis, my many thanks for their contribution to this research.

I also would like to acknowledge to the Modeling and Simulation team of INEB, for the motivating discussions that have contributed to this work.
To my colleagues and friends Luísa Bastos, Mariana Lobo, Gabriela Afonso, and Alexandra Oliveira, thank you for your friendship inside and outside INEB.

There are no words to express my deep gratitude to my family for their unconditional support and encouragement. To my husband (and colleague) Pedro, for his infinite patience, companionship and love, and for always believe in me. To my adorable daughter Beatriz, who, with the innocence of a three years-old child, gave me inspiration to overcome the insipid moments. To my newborn daughter Matilde, for giving me a delightful pregnancy and for demonstrate such strength and courage in her early complicated beginning. A special thanks to my parents for their constant encouragement and for everything they have done for me.

Abstract

In several areas of acute care medicine, such as anesthesia, intensive care, and emergency medicine, simulator based training has been shown to reduce human error and save lives. Full-body model-driven patient simulators provide the technology that can be used in immersive medical training in a controlled environment, without risks to real patients.

The work presented in this thesis fits within the general framework of model-driven simulator design. Its ultimate goals are to contribute to medical training and patient safety. The specific purpose of this study was to provide a consistent set of mathematical models for educational simulation of cardiovascular pathophysiology. The same uncontrolled cardiovascular model was used as a basis for deriving models for different patients (fetus, neonate, and infant), different pathologies (aortic stenosis and several other congenital heart defects), an incident (blood loss), and a natural transition (birth). The presented models may serve as simulation engines for screen-based or full-body simulators.

The *introductory chapter* presents background information considered relevant for the understanding of subsequent chapters. An historical overview of cardiovascular modeling is given, with special emphasis on lumped-parameter models for the complete circulation. A brief description of selected cardiovascular physiology and pathologies are also presented. Considerations on the evolution and benefits of using simulation in medical training, together with a short description of available tools, conclude this chapter.

Chapter 2 illustrates the run-time information flow in a script-controlled model-driven medical simulator and introduces different types of requirements for models of physiology and pharmacology, part of the simulation engine of a medical educational simulator.

In *chapter 3* existing models for the uncontrolled cardiovascular system and the adult baroreflex are described in detail and combined, and a new parameter set representing a 6-month old infant is derived. Simulated vital signs match published target data, the model reacts appropriately to blood loss, and incorporation of aortic stenosis is straightforward.

In *chapter 4*, using the same underlying model as for the infant, a complete set of parameters reflecting a normal 1-week old neonate is derived. The hemodynamic model is then expanded to reflect selected pathologies. Simulation results for the baseline patient, blood loss, and congenital heart defects match published target data. Simulated waveforms are considered realistic enough for educational simulation.

Chapter 5 identifies and corrects errors in the software implementation of the previous model. One of the errors masked a model shortcoming. The model is improved through further investigation and adaptation of the baroreflex model. Simulation results of the improved model closely match published target data. A procedure for model and code verification is presented.

Chapter 6 presents an original combination of a physiological model with scripted parameter changes for educational simulation of hemodynamic transitions at birth. Simulation results match published target data and demonstrate that the model is capable of correctly representing fetal hemodynamics and the evolution of neonatal hemodynamics during the first 24 hours of life.

To facilitate future parameter estimation for additional simulation patients, *chapter 7* proposes a systematic sensitivity analysis of the adult hemodynamic model in its baseline operating point. It highlights the parameters with significant effects and those with minor ones, and helps to distinguish parameters with a more isolated effect on specific monitored signals from those that affect the entire circulation.

The *closing chapter* places the presented research in its model-driven simulator context, lists the main conclusions, and presents suggestions for future work.

Sumário

Em diversas áreas da medicina de cuidados agudos, como a anestesia, os cuidados intensivos, e a medicina de emergência, o uso de simuladores no ensino tem demonstrado reduzir o erro humano e salvar vidas. Simuladores de pacientes de corpo-inteiro e baseados em modelos proporcionam a tecnologia necessária para o treino médico, num ambiente imersivo e controlado, sem risco para os pacientes reais.

O trabalho apresentado nesta tese enquadra-se no contexto geral do desenho de simuladores baseados em modelos, tendo como objectivo final contribuir para o treino médico e para a segurança dos pacientes. Como objectivo específico, este estudo visa estabelecer um conjunto consistente de modelos matemáticos para a simulação educativa da pato-fisiologia cardiovascular. O mesmo modelo cardiovascular (sem inclusão de controlo) foi usado como base para a derivação de outros modelos para diferentes pacientes (feto, recém-nascido e bebé de 6 meses), para diferentes patologias (estenose da aorta e várias outras cardiopatias congénitas), para um incidente (hemorragia) e uma transição natural (nascimento). Os modelos apresentados poderão servir de base para motores de simulação de simuladores de corpo-inteiro ou baseados em computadores.

O *capítulo introdutório* apresenta informação de base considerada relevante para a compreensão dos capítulos subsequentes. Uma revisão histórica da modelação cardiovascular é apresentada, dando especial ênfase aos modelos da circulação completa baseados em parâmetros. É ainda apresentada uma descrição breve de aspectos seleccionados da pato-fisiologia cardiovascular. Considerações sobre a evolução e os benefícios do uso da simulação no treino médico, incluindo uma breve descrição das ferramentas disponíveis, concluem este capítulo.

O *capítulo 2* ilustra a evolução do fluxo de informação durante a utilização de um simulador médico baseado em modelos e controlado por scripts. Ainda introduz diferentes tipos de requisitos para modelos fisiológicos e farmacológicos que constituem o motor de simulação de um simulador médico educativo.

No *capítulo 3*, modelos existentes para o adulto do sistema cardiovascular (sem a inclusão de controlo) e do baroreflexo são descritos detalhadamente e combinados. Um novo conjunto de parâmetros representando um bebé de 6 meses é derivado. Os sinais vitais

simulados correspondem a dados-alvo publicados, o modelo responde apropriadamente a uma hemorragia e a incorporação de uma estenose da aorta é directa.

No *capítulo 4*, usando o mesmo modelo de base, é derivado um novo conjunto de parâmetros reflectindo um recém-nascido de uma semana. O modelo hemodinâmico é então expandido de modo a reproduzir patologias seleccionadas. Os resultados de simulação do paciente basal, de hemorragias e de várias cardiopatias congénitas correspondem a dados-alvo publicados. As curvas simuladas foram consideradas suficientemente realísticas para a simulação educativa.

O *capítulo 5* identifica e corrige erros na implementação em *software* do modelo anterior. Um desses erros camuflou uma incorrecção do modelo. Uma investigação aprofundada e consequente adaptação do modelo do baroreflexo conduziu a um modelo melhorado. Os resultados de simulação do modelo melhorado correspondem a dados-alvo publicados. Ainda é apresentado um procedimento para a verificação de modelos e sua implementação em *software*.

O *capítulo 6* apresenta uma combinação original de um modelo fisiológico com um script que controla mudanças de parâmetros específicos, visando a simulação educativa das transições hemodinâmicas á nascença. Os resultados de simulação correspondem a dados-alvo publicados e demonstram que o modelo é capaz de correctamente representar a hemodinâmica fetal e a evolução da hemodinâmica neonatal durante as primeiras 24 horas de vida.

Para facilitar a estimação de parâmetros para novos pacientes simulados, o *capítulo 7* propõe uma análise de sensibilidade sistemática do modelo hemodinâmico do adulto, no seu ponto de operação. Esta análise evidência quais os parâmetros com um efeito significativo e quais os parâmetros com um efeito minoritário. Ainda permite distinguir os parâmetros com um efeito isolado em sinais monitorizados específicos dos que afectam toda a circulação.

O *capítulo final* situa a conducente investigação no contexto dos simuladores baseados em modelos, enuncia as principais conclusões e apresenta sugestões para trabalho futuro.

Résumé

Dans plusieurs spécialités de la médecine traitant des situations critiques et urgentes, telles que l'anesthésie, les soins intensifs, et les urgences, il a été démontré que l'entraînement par simulateur pouvait réduire l'erreur humaine et sauver des vies. Les simulateurs de patient de taille humaine et activés par modèles (anglais: full-body model-driven), fournissent la technologie permettant un entraînement immersif dans un environnement contrôlé et sans risques pour les vrais patients.

Le travail présenté dans cette thèse s'intègre dans le contexte général du design des simulateurs activés par modèles. Son but ultime est de contribuer à l'entraînement médical et à la sécurité des patients. L'objectif spécifique de cette étude était de proposer un ensemble de modèles mathématiques consistants pour la simulation pédagogique des pathophysiologies cardiovasculaires. Le même modèle cardiovasculaire sans baroréflexe (anglais: uncontrolled cardiovascular model) a été utilisé comme base pour dériver des modèles pour différents patients (fœtus, nouveau-né et nourrisson), différentes pathologies (sténose aortique et plusieurs autres défauts congénitaux), un incident (hémorragie), et une transition naturelle (naissance). Les modèles présentés peuvent être utilisés comme moteur de simulation pour des simulateurs sur ordinateur personnel ou pour des simulateurs de taille humaine.

Le *chapitre d'introduction* présente des informations de base nécessaires pour la compréhension des chapitres suivants. Un historique global des modèles cardiovasculaires est donné en insistant plus particulièrement sur les modèles à paramètres localisés pour la circulation complète. Une brève description d'aspects sélectionnés de la physiologie et des pathologies cardiovasculaires est également présentée. Des considérations sur l'évolution de la simulation et les bénéfices de son utilisation pour l'entraînement médical, ainsi qu'une brève description des outils disponibles, concluent ce chapitre.

Le *chapitre 2* illustre le flux d'informations durant l'opération d'un simulateur médical activé par modèles et contrôlé par scripts (anglais: script-controlled model-driven medical simulator). Il introduit les éléments type d'un cahier des charges pour les modèles de la physiologie et de la pharmacologie qui font partie du moteur de simulation dans un simulateur pédagogique médical.

Dans le *chapitre 3* des modèles existants du système cardiovasculaire et du baroréflexe chez l'adulte sont décrits en détail et associés. Un nouvel ensemble de paramètres représentant

un nourrisson de 6 mois est dérivé. Les signes vitaux simulés correspondent aux données visées publiées, le modèle réagit correctement à l'hémorragie, et l'incorporation d'une sténose aortique est simple.

Au *chapitre 4*, utilisant le même modèle de base que pour le nourrisson, un ensemble complet de paramètres pour un nouveau-né d'une semaine est dérivé. Le modèle hémodynamique est alors étendu pour représenter des pathologies sélectionnées. Les résultats de la simulation du patient de base, de l'hémorragie et des défauts cardiaques congénitaux correspondent aux données visées publiées. Les courbes simulées sont considérées comme suffisamment réalistes pour la simulation pédagogique.

Le *chapitre 5* identifie et corrige des erreurs dans le logiciel du modèle précédent. Une des erreurs masquait un défaut du modèle. Le modèle a été amélioré par une recherche plus approfondie et l'adaptation du modèle du baroréflexe. Les résultats de la simulation du modèle amélioré se rapprochent des données visées publiées. Une procédure pour la vérification du modèle et du logiciel est présentée.

Le *chapitre 6* présente une combinaison originale du modèle physiologique et d'un script pour les changements de paramètres pour la simulation pédagogique des transitions hémodynamiques à la naissance. Les résultats de la simulation correspondent aux données visées publiées et démontrent que le modèle est capable de représenter correctement l'hémodynamique du fœtus et l'évolution de l'hémodynamique néo-natale durant les premières 24 heures de vie.

Pour faciliter l'estimation de paramètres pour la simulation de nouveaux patients, le *chapitre 7* propose une analyse de sensibilité du modèle hémodynamique adulte dans son point d'opération de base. Elle souligne les paramètres qui ont des effets significatifs et ceux aux moindres effets. Elle aide à distinguer les paramètres avec des effets plus isolés sur des signaux spécifiques de ceux qui affectent la circulation totale.

Le *dernier chapitre* place la recherche présentée dans le contexte des simulateurs activés par modèles, cite les conclusions principales et propose des suggestions pour la recherche future.

Contents

Chapter 1

Introduction

This introductory chapter presents background information considered relevant for the understanding of subsequent articles and chapters. A brief historical overview of cardiovascular modeling is given, with special emphasis on lumped-parameter models for the complete circulation. Models for specific parts of the circulation or those based on other mathematical formulations, such as transmission line models or neural network models, are considered beyond the scope of this thesis. Relevant cardiovascular physiology and selected pathologies are presented. The evolution and benefits of using simulation in medical training are considered, together with a short description of available tools. The main research objectives and the thesis outline conclude this chapter.

Historical overview and cardiovascular modeling

The physiology of the cardiovascular system was elucidated gradually over the last 2400 years. Aristotle (384–322 B.C.) identified the role of blood vessels in transferring "animal heat" from the heart to the periphery of the body, although he was not aware of blood circulation[1].

Galen (c. 130–200 A.D.), an anatomist and experimental physiologist, was the first to observe the presence of blood in the arteries[1]. Galen believed that there were two distinct types of blood: *Nutritive blood* that was thought to be made by the liver and carried through veins to the organs, where it was consumed; and *vital blood* that was thought to be made by the heart and pumped through arteries to carry the "vital spirits". The lungs served to cool the heart and remove sooty impurities from the new blood. The heart was thought to contain pores to allow spirit or gaseous exchange across the septum[2]. His discoveries exerted a profound influence on medicine and were commonly accepted during the next 1400 years[3].

Almost 15 centuries later, in the 1600s, Sir William Harvey inaugurated modern cardiovascular research with his publication *De Motu Cardis e Sanguinis Animalibus* (About the Motion of the Heart and Blood in Animals), in which he wrote "*I began privately to consider if it* (the blood) *had a movement, as it is, it would be in a circle.*" He was probably the first to demonstrate clearly and convincingly the role of the heart as a pump which caused blood to flow in a unidirectional closed circuit through the systemic and pulmonary circulations[1,4]. He also identified the venous valves and understood their functioning. Harvey based most of his conclusions on careful observations recorded during vivisections made of various animals during controlled experiments, being the first person to study the cardiovascular system quantitatively. Among other results, he was able to quantify the total amount of blood in the body.

Nearly one century later, Reverend Stephen Hales, in his Statistical Essays[5], introduced quantitative studies of blood pressure. He considered arterial elasticity and asserted its buffering effect on the pulsatile nature of blood flow. He likened the depulsing effect to the fire engines of his time. In such engines, water was forced into a closed, domelike chamber (windkessel) thus compressing the entrapped elastic air; the compressed air then served to force the water out of the hose in a steady stream. This analogy became the basis of the first modern cardiovascular model[4].

Near the beginning of the 20th century, the Windkessel theory was developed and propounded by the German physiologist Otto Frank. The Windkessel model has been a useful analogy for illustrating the concept that the arteries store energy during systole and release it during diastole[6]. The work of Otto Frank spawned the interest of many subsequent investigators and led to a proliferation of modified Windkessel-type models[4]. The major

criticism of the pure Windkessel theory was that it ignored spatial considerations and instead lumped all the vasculature into a single point or compartment. Attempts to correct this shortcoming included adding inertial and damping factors as well as collapsible components. Despite its limitations, the pure Windkessel theory is still useful as a teaching tool because of its simplicity and clear, intuitive descriptions.

Even before Otto Frank, there was great interest in the mathematics of blood flow in distensible vessels. Many of the famous mathematicians, such as, Bernoulli, Euler, Young, Poiseuille, Navier and Stokes explored wave propagation, reflection and pressure-flow relationships in blood vessels[4].

Models of the complete circulation

In the mid 1950s, Arthur Guyton was the first to consider a closed circulatory system with a constant amount of blood[7,8]. In his early studies, he proposed a derivation of the venous return and cardiac output based on the right atrial pressure.

Towards the end of same decade, Fred Grodins, following Guyton, developed a systematic approach to describe the cardiovascular system[9]. In his approach, systemic arteries and veins, pulmonary arteries and veins, and the two sides of the heart were distinguished. With 23 simultaneous equations, he described the uncontrolled closed circulatory system. The heart used a Frank-Starling mechanism[1] wherein stroke volume was a variable fraction of end-diastolic volume; stroke volume increased with increasing heart strength and decreasing aortic pressure.

At the same time, Homer Warner proposed a model for describing the closed circulatory system[10]. It consisted of six compartments: left ventricle, arterial bed, right atrium and systemic veins, right ventricle, pulmonary arteries, and left atrium and pulmonary veins. Two states were considered for the ventricles: systole and diastole. Each compartment was described with 3 time-dependent equations, expressing relationships between volumes, flows and pressures. The 18 equations that compose this model were solved by an analog computer. The major disadvantage of this model was the abrupt transition between systolic and diastolic states.

In the first half of the 1960s, several simple electrical analogs of human circulation were constructed[11,12]. These systems included ventricular pumps, and distinct pulmonary and systemic circulations.

[1] ***Frank-Starling mechanism*** (or Frank-Starling law of the heart) states that the greater the volume of blood in the heart at the end of diastole (end-diastolic volume), the greater the volume of blood ejected during systolic contraction (stroke volume).

In 1965, Jan Beneken presented a complete mathematical description for a normal, closed, uncontrolled circulation[13]. Using an analog computer, physiologic signals and pulsatile waveforms were simulated. The linearized, improved version of this model is still widely used today and will be revisited in this thesis. This ten-compartment pulsatile model reflects the systemic circulation, differentiating among intra- and extrathoracic arteries and veins. It also reflects separate pulmonary arteries and veins. Each of these compartments is characterized by a hydraulic resistance, a compliance, and an unstressed volume. Inertial effects of blood are included only between the systemic arterial compartments. This model does not represent the accumulation of blood in tissue, nor does it reflect distinct parallel vascular beds. The pressure drops over the systemic and pulmonary vascular beds are each represented by a single resistance. The four heart chambers are represented by time varying compliances and by a constant unstressed volume. Ideal unidirectional valves, in series with a resistance, mimic the heart valves. Backflow from the atria is limited by non-linear resistances.

In 1967, Beneken and DeWit presented a detailed version of the above model[14]. The result was a model composed by 19 compartments and described by 57 equations (39 of which representing the right and left ventricles and 18 the pulmonary and systemic circulations). The model generated very acceptable and highly detailed pulsatile hemodynamics. Other features included in this model were: the baroreceptor control of heart rate, ventricular contractility and arterial resistance; nonlinear pressure-flow relationships; effect of coronary flow on ventricular performance; and fluid shifts across the capillaries between vascular and extravascular spaces.

Around the same time, John McLeod published a model of the closed circulation, known as PHYSBE, which was intended to serve as a benchmark for evaluating simulation systems[15,16]. This is a pulsatile model incorporating nine compartments: four are assigned to the heart-lung system and five to the peripheral circulation (aorta, head, arms, trunk, and legs). Both the circulation of blood and of heat are modeled, thus allowing for the simulation of thermodilution phenomena. Although the model was initially designed for implementation on an electronic analog computer, it has more recently been implemented in digital computers, one of which is currently available on The MathWorks™ website[17].

In the 1970s, the arrival of inexpensive digital computers led to several refinements in cardiovascular modeling, with ever-increasing detail and extent of application. Several models for qualitatively and quantitatively different cardiovascular systems (such as those of the fetus and the pregnant woman) were developed[18-22]. More recently, models for human pathological conditions (e.g. hypertension) were derived[23-26]. The complexity of these

models is closely related to their intended application: research, educational simulation or clinical.

Selected cardiovascular pathophysiology

For a description of the normal circulation and baroreflex control we refer to physiology textbooks[27,28].

Fetal circulation and hemodynamic transitions at birth

In the normal circulation systemic and pulmonary circulations are arranged in series. In the fetus, however, the lungs are non-functional and gas exchange occurs in the placenta. The placenta receives blood from the fetus via the descending aorta and two umbilical arteries. The blood returns from the placenta via the umbilical vein, into the hepatic veins and inferior vena cava. There are three vascular shunts which are exclusive to the fetal circulation – the foramen ovale[2], ductus arteriosus[3] and ductus venosus[4]. The first two give rise to a parallel system, where both ventricles eject into the systemic circulation. Consequently, fetal cardiac output is expressed as the total output of both ventricles - combined ventricular output (CVO)[29].

Transitions to postnatal circulation begin to occur shortly after birth. With expansion of the lungs there is a reduction in pulmonary blood vessels compression, and pulmonary resistance to blood flow decreases several fold[29]. Hypoxia of the lungs during fetal life also causes considerable tonic vasoconstriction, which is reversed shortly after aeration of the lungs. These two changes bring about a reduction in pulmonary arterial pressure, right ventricular pressure and right atrial pressure[28]. Another important change is the almost immediate cessation of placental circulation after birth, which leads to an almost twofold increase in systemic vascular resistance. This increases aortic, left ventricular and left atrial pressures[28].

With pulmonary circulation and cessation of placental flow, the fetal shunts begin to close. Without umbilical venous flow, the ductus venosus closes by loss of function[29]. The combination of increased left atrial volume resulting from pulmonary venous return and diminished inferior vena cava return to the right atrium causes left atrial pressure to exceed that of the right side, thereby causing the valve like foramen ovale to functionally close[30]. Driven by increased systemic pressure, resulting from the loss of the placental circulation, and by decreased pulmonary pressure, resulting from lung expansion, ductus arteriosus flow reverses, becoming predominantly left to right. Closure of the ductus arteriosus depends on other – non

[2] **Foramen ovale** - Oval opening between the two fetal atria, acting as a valve allowing for right-to-left passage of blood.

[3] **Ductus arteriosus** - Vessel connecting the pulmonary artery with the ascending aorta.

[4] **Ductus venosus** – Vessel connecting the umbilical vein, through the liver, to the inferior vena cava.

hemodynamic – factors: Increase in oxygen tension, decrease of prostaglandin E_2, and other vasoactive substances[29,30]. The ductus arteriosus constricts rapidly after birth and in mature infants functional closure generally occurs within the first 12-36 hours[30-34].

Pathologies: Congenital heart disease

A congenital heart defect occurs when the heart or closely associated vessels are malformed during fetal life. Congenital heart diseases are among the most common causes of morbidity and mortality in pediatric hospitals[30]. Congenital anomalies of the heart can be classified into four basic types: left-to-right shunts, right-to-left shunts, obstructive lesions, and complex shunts.

Left-to-right shunts. A left-to-right shunt is a cardiac abnormality that allows blood to flow directly from the left heart or aorta to the right heart or pulmonary artery, thus bypassing the systemic circulation. Patients usually display right-sided heart failure because of increased pulmonary blood flow[28,35]. Patent ductus arteriosus is an example of a left-to-right shunt. In children with this disease, as much as a half to two thirds of aortic blood crosses the ductus arteriosus to the pulmonary circulation. It will pass through the lungs two or more times for every time it will enter the systemic circulation. No cyanosis (bluish coloring of the extremities due to lack of blood oxygenation) occurs until heart failure develops or the lungs become congested. The major effect of disease is high left ventricular cardiac output, which is often two to three times in excess of normal[28]. Other examples of left-to-right shunts are atrial and ventricular septal defects, or a patent foramen ovale.

***Right-to-left shunts*.** Right-to-left shunts are abnormalities characterized by connections allowing blood flow from the right to the left heart chambers, thus bypassing the lung. The left ventricle then ejects less well oxygenated blood into the systemic circulation, causing patients to exhibit marked hypoxemia and cyanosis[28,35]. An example of a right-to-left shunt is tetralogy of Fallot. In this condition, four different heart abnormalities occur simultaneously[28]:

1. The aorta originates from the right ventricle rather than from the left, or it overrides the septum, receiving blood from both ventricles.
2. The pulmonary artery exhibits stenosis, so that instead of allowing the passage of a normal amount of blood into the lungs, right ventricular flow is predominantly to the aorta.
3. Blood from the left ventricle flows either through a ventricular septal defect into the right ventricle and from there into the aorta, or directly into the overriding aorta.

4. Because the right side of the heart pumps large quantities of blood against a high pressure aorta and stenosed pulmonary artery, its musculature is highly developed, and the right ventricle cavity is enlarged.

As much as 75% of venous blood flowing into the right atrium passes directly from the right ventricle into the aorta without becoming oxygenated[28].

Obstructive lesions. Obstructive lesions may be either valvular stenosis or vascular bands, which cause decreased output and pressure overload of the corresponding ventricle. Progressive heart failure is a consistent finding is this group of anomalies. Obstructions to left ventricular outflow in the infant are often more devastating than in the adult because of their severity, poor myocardial tolerance and difficulty of surgical repair[35,36]. Examples of obstructive lesions are coarctation of the aorta, aortic stenosis and mitral stenosis.

Complex shunts. In complex shunts venous and arterial blood is mixed before being ejected from the heart, and an obstruction to flow may or may not be present. Blood ejected from the heart has a 'mixed' oxygen saturation (70% to 80%)[35]. An example of a complex shunt is transposition of the great arteries. In this defect, the pulmonary artery and aorta are 'switched', so that the right ventricle ejects into the aorta, and the left ventricle ejects into the pulmonary artery. This malformation is only compatible with extrauterine life when a ventricular septal defect or other similar cardiac abnormalities are present, to allow for mixing of oxygenated and deoxygenated blood. This is one of the most common congenital heart diseases in the newborn and is a frequent cause of death among the unoperated patients[35,36].

Medical educational simulation

Simulation, in its many forms, is widespread in several fields of human endeavor, and its history stretches back over the centuries. The military have been long-term users of simulation, and hold one of its earliest and most famous examples: the chess game, thought to have been developed during the 6th century[37]. In aviation, the first flight simulator appeared in 1928 through the work of Edwin Link. He believed that learning rudimentary piloting skills would be much easier and inexpensive using a ground aviation trainer[38]. The modern aviation industry has put enormous effort into the development of high-fidelity flight simulation and contributed to the improvement of teams training through crew resource management programs. Similarly, the space industry has made extensive use of simulation for training and testing[39].

In Medicine, some primitive forms of simulation have been in use since the 16th century[40]. The earliest known simulators are obstetrical manikins, introduced towards 1700 by father and son Grégoire of Paris, and intended for the practical instruction of midwives[41].

Physical models of anatomy and disease were constructed long before the advent of modern plastic or computers[37]. Nevertheless, when compared to other high-technology, high-risk professions, in which sophisticated technical and behavioral skills are also necessary (as in aviation), medical simulation has somewhat lagged behind[42]. The reasons for this delay include financial constraints, the complexity of human pathophysiology, demands for rigorous scientific evidence of effectiveness, and the resistance to change consequent to a strong professional culture[40].

Prompted by technological innovation and reform in medical education[39], a more receptive atmosphere for the use of simulators started to emerge in the 1990s. Pressures arising from the limited receptivity of patients to be involved in training, limited instruction time, increasingly complex technical procedures, and ethical issues raised by the patient safety movement also contributed to these changes[41,43]. The increased awareness of medical error and the need to implement risk reduction strategies[44,45] also highlighted simulation as an important tool for improving patient safety.

In response to the expanding interest in this field, two societies were established: the Society in Europe for Simulation Applied to Medicine (SESAM), founded in August 1994, and the Society for Simulation in Healthcare (SSH), established in January 2004. The inaugural issue of Simulation in Healthcare (the official journal of the SSH) was published in January 2006, and represents the first scientific publication entirely devoted to medical simulation.

Medical simulation tools

Medical simulation comprises a wide spectrum of tools and methods. Modern medical simulation can be classified into five main categories[46] that include standardized patients, as well as the new generation of part or complex task trainers, screen-based simulators and, high-fidelity simulators.

Standardized patients. The process of using patient actors in medical education is thought to have begun in 1963[37]. Standardized patients are actors trained to role-play patients with certain types of diseases, for training and assessment of history taking, physical examination, and communication skills[46]. This methodology is widely used in the United States of America, where in 1993, it was already adopted in more than three fourths of medical schools. Its dissemination throughout Europe has been much more limited.

Part-task trainers. These simulators are intended to represent a part of the body and often consist of a limb, or other body part or structure. They are usually intended to aid the acquisition of technical, procedural or psychomotor skills, such as venepuncture,

ophthalmoscopy or bladder catheterization. Some provide feedback (visual, auditory or printed) to the learner on the quality of their performance (e.g. a sound to represent the adequate depth of chest compression during cardiopulmonary resuscitation) [39]. Resusci® Annie is one of the first trainers in the history of medical simulation. Introduced in 1960, it was initially designed for the practice of mouth-to-mouth breathing. Nowadays, the updated version is commercialized by the Laerdal Medical Company and is used to teach cardiopulmonary resuscitation[47]. Although not the original purpose of part-task trainers, they can be used along with standardized patients to provide learners with clinical scenarios in which the practice of both technical and communication skills are combined[39].

Complex task trainers. These tools combine static models with audiovisual and touch/feel interactive cues. Some also include software for teaching, learning, and assessment[46]. An example is the Harvey Cardiology Patient Simulator[48] which presents several cardiovascular conditions for training of auscultation, and supports a comprehensive curriculum. A new generation of complex task trainers using virtual reality was introduced in the beginning of this century. These trainers use computer generated images to recreate environments or objects in a clinical setting. Currently available products support medical training of vascular catheterization, endoscopy and laparoscopy[39].

Screen-based simulators. These simulators began proliferating in medical education during the 1980s, with the introduction of personal computers. They have become increasingly used for training and assessment of clinical knowledge and decision making. In 1998, 34% of American medical schools reported using such softwares in basic science courses. Screen-based simulators offer a learning experience that is less dependent on external educators[46]. They can be simple self-tutorials[46] or more sophisticated tools, including scripts or models of human pathophysiology and pharmacology, reacting appropriately to the trainee actions, and providing feedback on decisions and actions. Examples of the latter are: BodySim[49], a multi-compartment modeling tool of human physiology and pharmacology initially developed at the University of California; RELAX[50], a multicompartment model of neuromuscular blockade; The Virtual Anesthesia Machine[51,52], an interactive, web-based, educational program depicting an anesthesia machine. The last two were developed at the University of Florida.

High-fidelity patient simulators. These usually consist of a full-body manikin, a computer workstation, and interface devices that activate manikin signs and drive emulated or actual monitors[46]. The first full-body human patient simulator (Sim-One) was constructed at the University of Southern California in 1966, and was used for anesthesia training[53]. Two decades later, with the advances in computer technology and bioengineering, other high-

fidelity simulators were developed in the academic environment[54,55]. Some of these went on to be commercial products. One such example is the Gainesville Anesthesia Simulator (GAS), developed at the University of Florida, the precursor of the Human Patient Simulator (HPS®) and many subsequent products currently commercialized by Medical Education Technologies, Inc. (METI). Many of these exhibit clinical signs (such as pulses and heart sounds, chest movement, blinking eyes, etc), and generate a number of monitored signals (such as an electrocardiogram, invasive and non-invasive blood pressures, pulse oximeter signal, etc). Therapeutic interventions range from ventilation and fluid resuscitation, to pharmacological interventions. A number of advanced life support techniques can be applied, such as relieve of a tension pneumothorax or cardiac tamponade, and the placement of chest drains. The simulation engine of such simulators may be automatically controlled through physiological and pharmacological models or via pre-programmed scripts (or a combination of both). An instructor-operator can interact with the simulation engine in real-time, controlling or overriding simulator responses[56]. Different patients can be created by changing variables such as weight, blood volume, and heart function indices[46]. These simulators are frequently used to train complex and high-risk clinical situations in a lifelike team training setting, and sometimes to assess performance[46].

Benefits of medical educational simulation

Simulation can provide a safe, supportive educational environment[57], allowing users at all levels of training to practice and develop skills without any risk to real patients. It encourages the acquisition of skills through experience, ideally in a realistic situation or environment, and can stimulate reflection on performance[39]. As opposed to the clinical setting, where errors must be prevented or repaired immediately to protect the patient, in a simulated environment errors may be allowed to progress, so as to demonstrate their implications to the trainee, or to enable a quick reaction to rectify them[46].

Simulation is a learner-centered educational experience rather than a patient-centered activity; in this context, learners' needs always receive the highest priority. With real patients, learning time is usually limited and the way the learning experience "fits" the trainee's needs and level of experience is often suboptimal. In simulation, on the other hand, trainees may receive exposure to a range of carefully designed clinical encounters, providing the opportunity for the educator to standardize the content, difficulty, and sequence of the curriculum[46].

Simulation also supports trainees in the acquisition of a range of basic clinical skills such, as history taking, physical examination, and communicating with the patient. Teamwork and inter-professional learning can similarly be undertaken[39].

Objectives and thesis outline

The work presented in this thesis fits within the general framework of model-driven medical simulator design. Its ultimate goals are to contribute to medical training and patient safety. The specific purpose of this study was to provide a consistent set of mathematical models for educational simulation of cardiovascular pathophysiology.

This thesis is presented in eight chapters. The current chapter presented a brief introduction to selected necessary background information for subsequent chapters. Chapters 2 to 7 represent the core content of this thesis and are briefly outlined below. The closing chapter places the presented research in its context, and lists the main conclusions and suggestions for future work.

Chapter 2 - Development of foetal and neonatal simulators at the University of Porto. The perinatal acute care context and several considerations on simulator design are introduced. Preliminary models for perinatal acute care simulators are presented.

Chapter 3 - A model for educational simulation of infant cardiovascular physiology. An existing cardiovascular model is described and adapted to reflect pediatric cardiovascular physiology. The goal is to obtain model parameters that allow the cardiovascular vital signs to reflect target data in normal and pathologic conditions, and that react appropriately to critical incidents and therapeutic interventions. The basic critical incident selected is moderate acute blood loss. Aortic stenosis is chosen to evaluate the capacity of the model to reflect changes observed in a pathological condition.

Chapter 4 - A model for educational simulation of neonatal cardiovascular pathophysiology. The first objective of this study is to find a new set of parameters for an existing mathematical model of the adult cardiovascular system, such that simulations provide vital signs reflecting target data observed in normal conditions, and react appropriately to critical incidents and therapeutic interventions. To achieve this, the same model and essentially the same parameter estimation method from the previous study are used. The second objective is to extend this model to reflect four congenital heart defects: patent ductus arteriosus, tetralogy of Fallot, coarctation of the aorta, and transposition of the great arteries. Unlike the previous study, achieving the second objective involves changes in model structure, as well as in model parameters.

Chapter 5 - Corrected and improved model for educational simulation of neonatal cardiovascular pathophysiology. Errors in the software implementation of the previous model are identified and corrected. One of the errors masked a modeling inaccuracy, which stimulated further investigation, especially of the baroreflex model.

Chapter 6 - A model for educational simulation of hemodynamic transitions at birth. The main objective of this study is to develop an essential component of a perinatal acute care simulator, namely a model for the educational simulation of normal hemodynamic transitions during and shortly after birth. To achieve this objective, we propose a fetal hemodynamic model controlled by a carefully designed time-and-event-based script.

Chapter 7 - Sensitivity analysis of a hemodynamic model to facilitate programming simulation patients. The recurring need for parameter estimation for new patients, and adaptation of existing ones, prompted a systematic sensitivity analysis of the adult hemodynamic model. We propose to apply sensitivity analyses at two levels: the basic physiological level, where 38 hemodynamic model parameters and 13 simulated monitored signals are examined, and the empirical level, where only 6 normalized hemodynamic factors (grouping selected parameters) and 5 of the most important monitored signals are considered.

References

1. Quarteroni, A. Modeling the Cardiovascular System - A Mathematical Adventure: Part I. SIAM News. 2001;34(5).

2. Acierno, LJ. The History of Cardiology. New York: The Parthenon Publishing Group. 1994.

3. Dunn PM. Galen (AD 129-200) of Pergamun: anatomist and experimental physiologist. Arch Dis Child Fetal Neonatal Ed. 2003; 88(5):F441-3.

4. Timmons WD. Cardiovascular models and control. In: Bronzino JD (ed) The biomedical engineering handbook. CRC press, USA, 1995.

5. Hales S. Statistical Essays: Containing Haemastaticks (vol 2). Innys and Manby, London, 1733.

6. Peterson LH. Analogs, models and equations. Circ Res. 1958;6(6):675-7.

7. Guyton AC. Determination of cardiac output by equating venous return curves with cardiac response curves. Physiol Rev. 1955;35(1):123-9.

8. Guyton AC, Lindsey AW, Kaufmann BN. Effect of mean circulatory filling pressure and other peripheral circulatory factors on cardiac output. Am J Physiol. 1955;180(3):463-8.

9. Grodins FS. Integrative cardiovascular physiology: a mathematical synthesis of cardiac and blood vessel hemodynamics. Q Rev Biol. 1959;34(2):93-116.

10. Warner HR. The use of an analog computer for analysis of control mechanisms in the circulation. Proceedings of the IRE. 1959; 47(11): 1913-16.

11. Vadot L. [Examination of hemodynamic problems by means of an electrical analogy. Special application to cardiac abnormalities.] Pathol Biol (Paris). 1962;10:1499-509.

12. Defares JG, Osborn JJ, Hara HH. On the theory of the cardiovascular system. Bull Math Biophys. 1965;27:Suppl:71-83.

13. Beneken JEW. A mathematical approach to cardiovascular function. The uncontrolled human system [PhD Thesis]. University of Utrecht, The Netherlands. 1965.

14. Beneken JEW, DeWit B. A physical approach to hemodynamic aspects of the human cardiovascular system. In: Reeve EB, Guyton AC (eds) Physical bases of circulatory transport: Regulation and exchange. W.B. Saunders, Philadelphia, 1967.

15. McLeod J. PHYSBE - A physiological simulation benchmark experiment. Simulation. 1966; 7:324-9.

16. McLeod J. PHYSBE - A year later. Simulation. 1968; 10:37-45.

17. Mathworks. Physbe. Web site. Available at: http://www.mathworks.com/products/demos/simulink/physbe/. Accessed April, 2009.

18. Huikeshoven F, Coleman TG, Jongsma HW. Mathematical model of the fetal cardiovascular system: the uncontrolled case. Am J Physiol. 1980; 239(3):R317-25.

19. Huikeshoven FJ, Hope ID, Power GG, Gilbert RD, Longo LD. Mathematical model of fetal circulation and oxygen delivery. Am J Physiol. 1985; 249(2 Pt 2):R192-202.

20. Pennati G, Bellotti M, Fumero R. Mathematical modeling of the human foetal cardiovascular system based on Doppler ultrasound data. Med Eng Phys. 1997; 19:327-35.

21. Euliano TY, Caton D, van Meurs W, Good ML. Modeling obstetric cardiovascular physiology on a full-scale patient simulator. J Clin Monit. 1997; 13(5):293-7.

22. Grigioni M, Carotti A, Daniele C, D'Avenio G, Morbiducci U, Di Benedetto G, Albanese S, Di Donato R, Barbaro V. A mathematical model of the fetal cardiovascular system based on genetic algorithms as identification technique. Int J Artif Organs. 2001;24(5):286-96.

23. Barnea O, Santamore WP, Rossi A, Salloum E, Chien S, Austin EH. Estimation of oxygen delivery in newborns with a univentricular circulation. Circulation. 1998;98(14):1407-13.

24. Li X, Bai J, Cui S, Wang S. Simulation study of the cardiovascular functional status in hypertensive situation. Comput Biol Med. 2002;32(5):345-62.

25. Migliavacca F, Pennati G, Dubini G, Fumero R, Pietrabissa R, Urcelay G, Bove EL, Hsia TY, de Leval MR. Modeling of the Norwood circulation: effects of shunt size, vascular resistances, and heart rate. Am J Physiol Heart Circ Physiol. 2001;280(5):H2076-86.

26. Ursino M, Magosso E. Acute cardiovascular response to isocapnic hypoxia. I. A mathematical model. Am J Physiol Heart Circ Physiol. 2000;279(1):H149-65.

27. Levy MN. The cardiovascular system. In: Berne RM, Levy MN, Koeppen BM, Stanton BA (eds) Physiology (5th Edition). Mosby, Philadelphia, 2004.

28. Guyton AC. Textbook of medical physiology (8th Edition). W.B. Saunders Company, Philadelphia, 1991.

29. Friedman AH, Fahey JT. The transitions from fetal to neonatal circulation: Normal responses and implications for infants with heart disease. Semin Perinatol. 1993;17(2):106-121.

30. Brook MM, Heymann MA, Teitel DF. The heart. In: Klaus MH, Fanaroff AA (eds) Care of the high-risk (5th Edition). W.B. Saunders Company, Philadelphia, 2001.

31. Walthers FJ, Benders MJ, Leighton JO. Early changes in the neonatal circulatory transition. J Pediatr. 1993;123(4):625-632.

32. Shiota T, Harada K, Takada G. Left ventricular systolic and diastolic function during early neonatal period using transthoracic echocardiography. Tohoku J Exp Med. 1993;197(3):151-158.

33. Hiraishi S, Misawa H, Oguchi K, Kadoi N, Saito K, Fujino N, Hojo M, Horiguchi Y, Yashiro K. Two-dimensional Doppler echocardiographic assessment of closure of the ductus arteriosus in normal newborn infants. J Pediatr. 1987;111(5):755-760.

34. Kishkurno S, Takahashi Y, Harada K, Ishida A, Tamura M, Takada G. Postnatal changes in left ventricular volume and contractility in healthy term infants. Pediatr Cardiol. 1997; 18(2):91-95.

35. Bell C, Kain Z. The Pediatric anesthesia handbook (2nd Edition). Mosby Year Book, St. Louis, 1997.

36. Avery GB, Fletcher MA, MacDonald MG. Neonatology: Pathophysiology and management of the newborn (5th Edition), Lippincott Williams and Wilkins, Philadelphia, 1999.

37. Rosen KR. The history of medical simulation. J Crit Care. 2008;23(2):157-66.

38. The Link Trainer. Stark Ravings Web site. Available at: http://www.starksravings.com/linktrainer/linktrainer.htm. Accessed April, 2009.

39. Bradley P. The history of simulation in medical education and possible future directions. Med Educ. 2006;40(3):254-62.

40. Ziv A, Wolpe PR, Small SD, Glick S. Simulation-based medical education: an ethical imperative. Acad Med. 2003;78(8):783-8.

41. Buck GH. Development of simulators in medical education. Gesnerus. 1991;48 Pt 1:7–28.

42. Miller CO. System safety. In: Wiener EL, Nagel DC (eds). Human Factors in Aviation. San Diego CA: Academic Press, 1988.

43. Issenberg SB, McGaghie WC, Hart IR, Mayer JW, Felner JM, Petrusa ER, Waugh RA, Brown DD, Safford RR, Gessner IH, Gordon DL, Ewy GA. Simulation technology for health care professional skills training and assessment. JAMA. 1999;282(9):861-6.

44. Kohn, L, Corrigan J, Donaldson M (eds). To Err is Human: Building a Safer Health System. Committee on Quality in America. Institute of Medicine, Washington, DC: National Academy Press, 1999.

45. Berwick DM, Leape LL. Reducing errors in medicine. BMJ. 1999;319:136–7.

46. Ziv A, Small SD, Wolpe PR. Patient safety and simulation-based medical education. Medical Teacher. 2000;22(5):489-95.

47. Laerdal. Resusci® Anne Basic and SkillGuide™. Web site. Available at: http://www.laerdal.com/doc/7595233/Resusci-Anne-Basic-and-SkillGuide.html. Accessed April, 2009.

48. Health Sciences Library. Harvey Cardiac Patient Simulator.Web site. Available at: http://library.nymc.edu/HARVEY/harvey.cfm. Accessed April, 2009.

49. BodySim. Advanced Simulation Corporation Web site. Available at: http://www.advsim.com/biomedical/what_is_body_simulation.htm. Accessed April, 2009.

50. Ohrn MAK, van Oostrom JH, van Meurs WI. A comparison of traditional textbook and interactive computer teaching of neuromuscular block. Anesth Analg 1997;84:657-61.

51. Virtual Anesthesia Machine (VAM). Center for Simulation, Advanced Learning and Technology–University of Florida. Web site. Available at: http://vam.anest.ufl.edu/index.html. Accessed April, 2009.

52. Lampotang S, Dobbins W, Good MI, et al. Interactive, web-based, educational simulation of an anesthesia machine. Department of Anesthesiology–University of Florida. Web site. Available at: http://www.anest.ufl.edu/tds/semabstract.html; Accessed April, 2009.

53. Denson JS, Abrahamson S. A computer-controlled patient simulator. JAMA. 1969 21;208(3):504-8.

54. Gaba DM, DeAnda A. A comprehensive anesthesia simulation environment: re-creating the operating room for research and training. Anesthesiology. 1988;69(3):387-94.

55. Gravenstein JS. Training devices and simulators. Anesthesiology. 1988;69(3):295-7.

56. Van Meurs WL, Couto PM, Couto CD, Bernardes JF, Ayres-de-Campos D. Development of foetal and neonatal simulators at the University of Porto. Med Educ. 2003;37 Suppl 1:29-33.

57. Gordon J, Wilkerson W, Shaffer D, Armstrong E. Practising medicine without risk: students' and educators' responses to high-fidelity patient simulation. Acad Med 2001;76:469–72.

Chapter 2

Development of foetal and neonatal simulators at the University of Porto

van Meurs WL, Sá Couto PM, Sá Couto CD, Bernardes JF, Ayres de Campos D

Med Educ 2003;37(Suppl. 1):29-33

Abstract

BACKGROUND: Human error can be expected to play a significant role in adverse outcomes in perinatal acute care. In acute care of the adult, simulator based training is recommended and used to improve patient safety.

AIMS: Our general goal is to develop model-driven foetal and neonatal educational simulators and curricula. The specific objectives of this paper are to introduce the reader to the perinatal acute care context and simulator design considerations, as well as to give initial results and describe ongoing developments. A brief description of adult simulators and simulation engines is followed by a more detailed description of a foetal distress simulator (FDS) and of models for a neonatal simulator developed at the University of Porto. Ongoing developments involve the modelling of foetal baroreflexes, the effect of uterine contractions, and an adapted method for estimating foetal heart rate variability parameters.

RESULTS: We present FDS simulation results reflecting the changes in oxygen supply to the foetus and the foetal heart rate in response to a reduction in uterine blood flow. We also present a structural diagram of a model for the educational simulation of congenital heart disease and preliminary simulation results reflecting a patent ductus arteriosus.

CONCLUSION: We expect that, after initial clinical and educational validation, the presented models and simulators will play a role in simulator-based educational programmes contributing to increased perinatal safety.

Keywords*: Education; medical; undergraduate/ *methods, *patient simulation; curriculum; clinical competence/ *standards/ economics; perinatal care/ *standards/ methods.*

Introduction

As an introductory example, consider the following case: following epidural analgesia, a patient in labour develops severe respiratory depression. The relatively inexperienced anaesthesiologist has difficulties intubating the patient. After various failed attempts, the mother's oxygen levels become critically low, and the attending obstetrician alerts the health care team that the foetal heart rate tracing manifests a prolonged deceleration, indicative of foetal distress. The patient is rushed to the operating room, where another anaesthesiologist finally succeeds with intubation and oxygenation, and the baby is delivered through caesarean section. This situation, risking the lives of both mother and foetus, and resulting in an unnecessary caesarean section and a neonate requiring resuscitation, could have been avoided by adequate training; in this particular case, training of the anaesthesiologist in difficult airway management. Given the risk to the patient and the relative rarity of such events, simulation is the only option for such training. We propose to develop a simulation technology and educational curricula required to address this and other issues in perinatal safety.

In the following sections we will highlight selected aspects of perinatal safety, and give a brief general description of educational simulators and simulation engines for acute care of the adult patient. The remainder of the paper describes two ongoing projects in educational simulation for perinatal acute care at the University of Porto. The general purpose of this paper is to introduce ongoing developments in the perinatal area and to provide background information which will facilitate the interactions between clinical instructors and simulator developers, giving shape to new medical educational simulator applications and technologies.

Key learning points

Distinguish the main components of a full-scale medical educational simulator.

Know what the main requirements for the simulation engine of a medical educational simulator are, and how they are evaluated.

Have examples of target applications for educational simulation in perinatal acute care training.

An understanding of some of the ongoing foetal and neonatal simulator developments and design challenges.

Perinatal safety

Examples of critical situations in obstetrics and in anaesthesia of the pregnant woman are: maternal hypotension following epidural anaesthesia, maternal hypoxia associated with ventilatory complications, and foetal hypoxia caused by umbilical cord compression. Babies born under these conditions often require intensive neonatal care. Other newborns require intensive care because of pathologies such as congenital heart diseases. An early recognition of pathologies and critical incidents and appropriate, timely, therapeutic interventions are important factors for survival and quality of life. As for the adult, human error can be expected to play a significant role in adverse outcomes[1]. Adequate training can help to reduce these risks. As for other fields of acute care medicine, the training of health care providers in the complex medical procedures involved in perinatal acute care is compounded by the risk to the patient and the relative rarity of the critical incidents.

Adult simulators and physiological models

Originally created as full-scale, manikin-based anaesthesia simulators[2-4], these state-of-the-art learning systems have evolved significantly over the past decade to become patient simulators[5-7]. Full-scale patient simulators help not only anaesthesiologists, but a wide variety of medical practitioners and students to learn the diagnosis and management of clinical problems without risk to real patients.

They consist of a manikin that exhibits vital signs, such as pulses and heart sounds, chest movement and blinking eyes, etc. A number of monitored signals are generated by the simulator, for example, an electrocardiogram, invasive and non-invasive blood pressures, a pulse oximeter signal, etc. Therapeutic interventions range from ventilation and fluid resuscitation, to pharmacological interventions. A number of advanced life support techniques can be applied, such as relieve of a tension pneumothorax or cardiac tamponade, and the placement of a chest drain. Defibrillation and external pacing are detected automatically.

The simulation engine is the component of the simulator that generates the physiological and pharmacological responses of the simulated patient to the therapeutic interventions. A good simulation engine provides life-like reactivity to the simulator. An automatic way of generating these responses is through a combination of time and event driven scripts, and models of human physiology and pharmacology[8,9]. An instructor-operator can interact with the simulation engine in real-time, initiating critical incidents directly in the physiological models, or via the control of preprogrammed scripts. Overrides of selected vital signs are available. Different patients and pathologies can be programmed by adjusting parameters of the physiological models. Figure 1 summarizes the run-time information flow

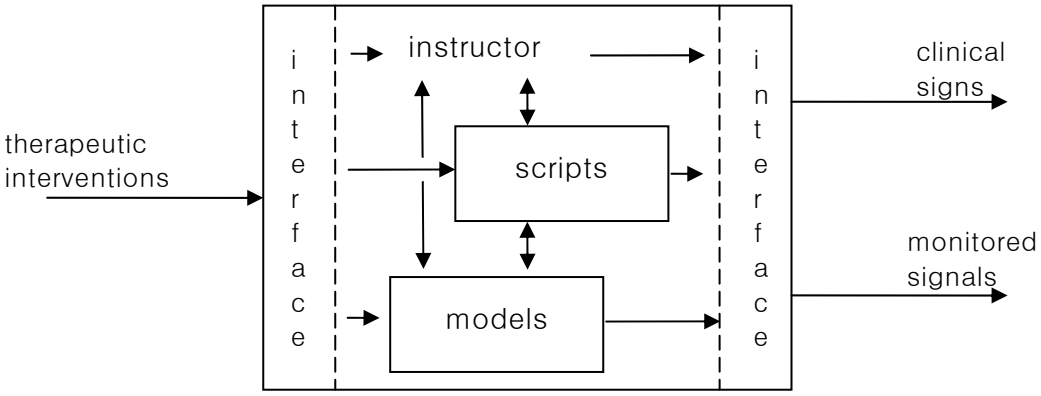

Figure 1. Information flow in a script-controlled model-driven medical simulator.

in a script-controlled model-driven medical simulator. Note that this figure does not contain the direct visual and verbal communication between instructor and trainee. High-quality simulation engines and interfaces are prerequisites to the "suspense of disbelief" and allow the instructor to focus in on the educational objectives of the ongoing simulator-based exercise. Various types of trainee interfaces have been presented and discussed by van Meurs et al[8]. There are a number of requirements for the, predominantly mathematical, models of physiology and pharmacology of the simulation engine of a medical educational simulator:

1. Realism of baseline vital signs and their responses to correct and incorrect therapeutic interventions is the most basic one;
2. Parameter data reflecting different patients and pathologies should be available in the scientific literature;
3. A clinical instructor should be able to manipulate the models to simulate a range of patients, pathologies, or incidents; and
4. Models of different aspects of physiology and pharmacology included in a simulation engine should interact appropriately.

While increasing model complexity usually helps meeting requirement 1, requirements 2 and 3 are, in general, more easily met using less complex models. Requirements 2 and 3 will be reflected in the selection of the model structures referred to or described in the remainder of the paper. Meeting the basic requirement 1 involves comparing model responses to animal or human data presented in the literature. A challenge in this context is that many situations that are interesting to simulate from an educational point of view involve extreme physiological states, and little to no data on controlled experiments with human subjects in such situations are available. Comparison of the model response to data

from animal experiments and evaluation of the response by clinical experts are the remaining options to assess the quality of a simulation engine. A next level of evaluation involves the quality of the whole simulator. For screen-based trainers, with a limited set of leaning objectives, trainee satisfaction and educational impact can be evaluated (see Öhrn et al.[10] for example). An evaluation of full-scale simulation environments involves measures and quality statements concerning the simulator, instructor and educational programme. The broad range of knowledge, skills and attitudes that can be transferred or trained in such an environment further compounds this analysis. This level of evaluation does not yet apply to the prototype simulators described in the remainder of this paper. Our joint goal is to develop the physiological models, the simulation technologies and the curricula for training and research and development in the area of perinatal safety. In this paper we describe ongoing work in this field at the Institute for Biomedical Engineering and at the University of Porto College of Medicine.

Foetal distress simulator

The target audience of a training programme using a foetal simulator consists of residents in obstetrics and gynaecology, midwives and nurses in training, residents in obstetric anaesthesia and medical students. Our general objective is to design an educational foetal distress simulator (FDS) for critical situations which can occur during labour. This simulator can either function in a stand-alone configuration on a personal computer, or can be integrated with a full-scale simulator representing the mother[11]. We have recently presented an original low order, yet realistic model for the educational simulation of oxygen delivery to the foetus[12]. Validation of model response was based on human data for the baseline arterial oxygen levels, and on animal data for the response to reductions in uterine perfusion pressure and maternal arterial oxygen levels. We have also presented a generator for the oxygen supply dependent foetal heart rate (FHR) signal[13]. Figure 2 shows the simulation of a reduction in uterine blood flow, as, for example, during maternal cardiac arrest and resuscitation, and its effect on foetal heart rate. The simulated foetal heart rate (FHR) shows a prolonged deceleration. Because of the limited duration of the absence of uterine perfusion, the state of the foetus does not become irreversibly pathologic. With the restoration of uterine perfusion, the partial pressure of oxygen returns to normal, and the FHR baseline and variability return to a pre-arrest value. In a preliminary evaluation experiment, we asked an experienced obstetrician to classify a number of simulated FHR tracings as “cannot be distinguished from real tracings”, or “are realistic enough for educational simulations”, or “are unrealistic”. The tracing in Figure 2 was considered realistic enough for educational simulation, with a specific comment on the unrealistically fast full return to normal variability after the incident. For

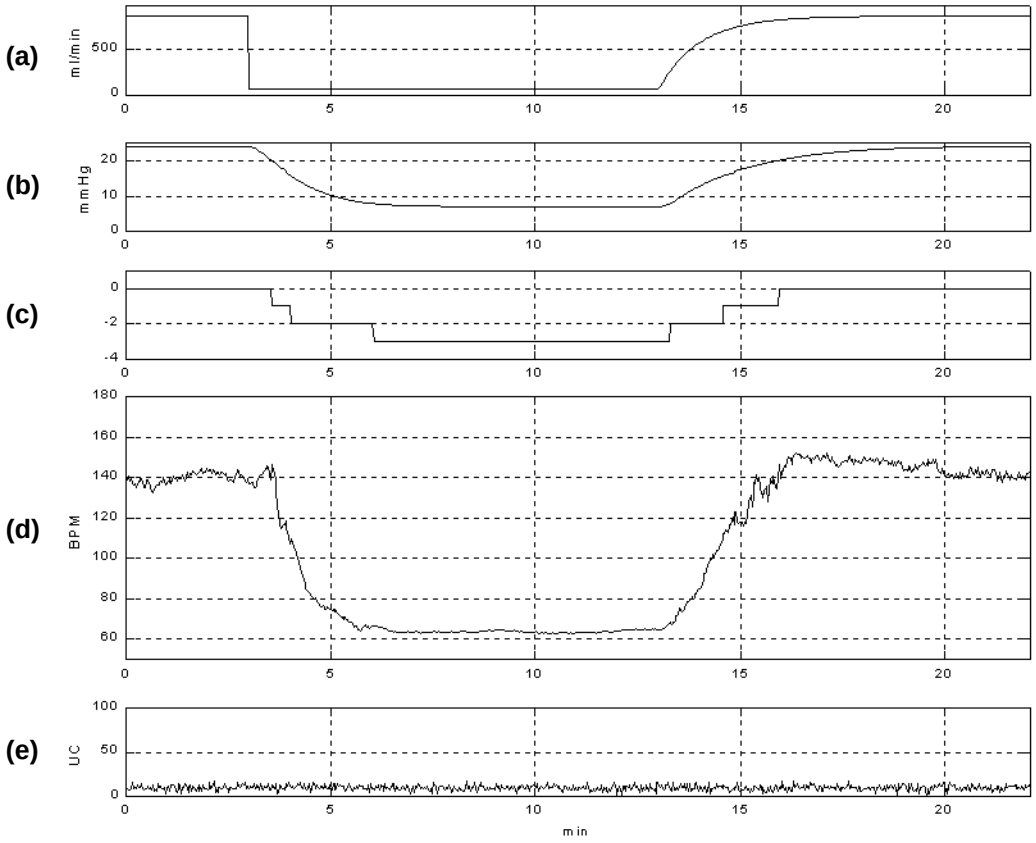

Figure 2. Simulation of a reduction in **(a)** uterine blood flow, and its effect on **(b)** the partial pressure of oxygen in the fetal arterial blood, **(c)** the pathologic state of the fetus (0: normal, -1: suspicious, increased variability, -2: suspicious, decreased variability, -3: pathologic, reversible, -4: pathologic, irreversible, -5: death), and on **(d)** fetal heart rate. The last signal **(e)** represents the uterine contractions, absent in the simulated pre-labor conditions.

training uses, the FHR and uterine contraction signals are presented via an emulation on a computer screen of standard cardiotocographic paper. In conjunction with a full-scale simulator representing the mother, the FDS can be used to train the recognition and treatment of these and other reductions in foetal oxygen supply, repeatedly, and without risk to real patients. The physiological models presented by Sá Couto et al. correctly simulated the effect of umbilical cord compression on the partial pressure of oxygen in foetal arterial blood[(12)]. However, the immediate effect that these compressions have on FHR, primarily mediated by baroreflexes, was not incorporated in the model. Data for the effect of umbilical cord compressions on foetal arterial blood pressure and FHR are available from studies in animals[(14)] and humans[(15,16)]. A model incorporating a more detailed representation of the foetal and placental circulations, as well as the foetal baroreflexes, is currently being developed at our institutions.

Hypertonic uterine contractions during labour can reduce foetal oxygen supply and cause foetal distress[17,18]. Based on the work presented by Butler et al.[19], in another ongoing study we are developing a physiological and pharmacological model that will allow us to simulate such situations.

A fractal model of short- and long-term FHR variability, presented by Felgueiras et al.[20] was used by Sá Couto et al. to generate this component of the signal for the FDS[13]. An ongoing study looks at how clinically and educationally relevant FHR variability features can be extracted from real signals, and incorporated into the signal generator of the FDS.

Evaluation of the clinical realism of the existing FDS prototype is ongoing, and takes a new phase every time new critical incidents or therapeutic interventions are included. After this evaluation, demonstrations and interactive training sessions will be incorporated into the obstetrics curriculum.

Models for a neonatal simulator

The aim of the work in this area is to represent congenital heart diseases graphically and mathematically for use in screen-based or full-scale educational simulations of the neonate and infant[21]. It is based on a previously published model for the adult cardiovascular system[22]. Structural elements representing a patent ductus arteriosus (PDA) and an open foramen ovale, presented in another study[23], were incorporated in this model. We also incorporated structural elements representing a ventricular septal defect, Figure 3. This model was initially simulated with parameters reflecting a 6-month-old infant (J.A. Goodwin et al., unpublished results). Table 1 shows preliminary simulation results with and without a moderate PDA. The relative pressure changes are similar to those reported for neonates[24].

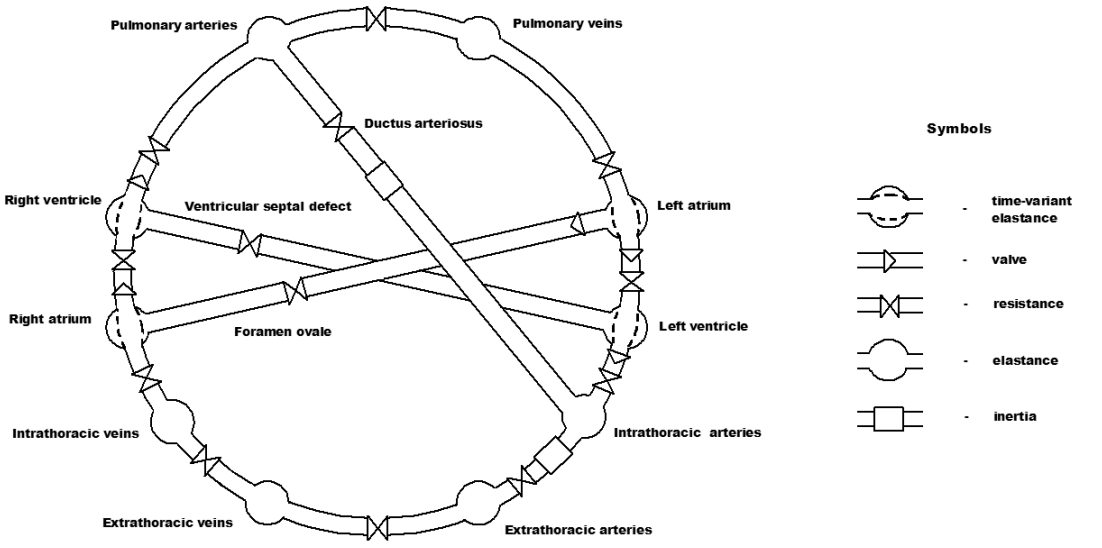

Figure 3. Hydraulic analog of the cardiovascular model reflecting congenital heart diseases[21].

Table 1 - Simulation results: Normal infant and an infant with a moderate PDA. RV– right ventricle, LV– left ventricle, PA – Pulmonary arteries, Ao – Aorta, PV – Pulmonary veins, Co – cardiac output (from RV).

	Pressures (mmHg)					**Co (l/m)**
	RV	**LV**	**PA**	**Ao**	**PV**	
Normal	19/3	90/3	15/6	84/55	6	1.7
PDA	29/4	82/3	25/14	73/25	10	1.1

Ongoing work on physiological models for educational simulation of the neonate will look into the cardiovascular system and oxygen transport.

Conclusion

We have presented the context and some results of the research and development, at the University of Porto, of educational simulators for training health care providers in foetal and neonatal acute care. We have demonstrated some of the complexity involved in the development of these models of foetal and neonatal physiology and of their role in the educational environment.

After initial clinical and educational validation of the presented models and simulators, we expect that they will play a role in simulator-based educational programmes and contribute to increased perinatal safety.

References

1. Kohn LT, Corrigan JM, Donaldson MS, eds. To Err Is Human, Building a Safer Health Care System. Washington, DC: National Academic Press; 2000.

2. Denson JS, Abrahamson S. A computer-controlled patient simulator. JAMA 1969;208:504–8.

3. Gaba DM, DeAnda A. A comprehensive anesthesia simulation environment. re-creating the operating room for research and training. Anesthesiology 1988;69:387–94.

4. Good ML, Gravenstein JS. Anesthesia simulators and training devices. Int Anesthesiol Clin 1989;27:161–8.

5. Gaba D, Howard S, Fish K, Smith B, Sowb Y. Simulation based training in anesthesia crisis resource management (ACRM): a decade of experience. Simulation Gaming 2001;32:175–93.

6. Gordon JA et al. 'Practicing' medicine without risk: students' and educators' responses to high-fidelity patient simulation. Acad Med 2001;76:469–72.

7. Olympio MA. Simulation saves lives. Newsletter of the American Society of Anesthesiologists. Park Ridge: American Society of Anesthesiologists; 2001.

8. Van Meurs WL, Good ML, Lampotang S. Functional anatomy of full-scale patient simulators. J Clin Monit 1997;13:317–24.

9. Van Meurs WL, Nikkelen E, Good ML. Pharmacokinetic-pharmacodynamic model for educational simulations. IEEE Trans Biomed Eng 1998;45:582–90.

10. Öhrn MAK, van Oostrom JH, van Meurs WL. A comparison of traditional textbook and interactive computer learning of neuromuscular block. Anesth Analg 1997;84:657–61.

11. Euliano TY, Caton D, van Meurs WL, Good ML. Modeling obstetric cardiovascular physiology on a full-scale patient simulator. J Clin Monit 1997;13:293–7.

12. Sá Couto PM, van Meurs WL, Bernardes JF, Marques de Sá JP, Goodwin JA. Mathematical model for educational simulation of the oxygen delivery to the fetus. Cont Eng Prac 2002;10:59–66.

13. Sá Couto PM, van Meurs WL, Bernardes JF. Marques de Sá JP, Goodwin JA. Combined model-driven and rule-based approach for educational simulation of fetal heart rate. In: Jan J, Kozumplík J, Provazník I, eds. BIOSIGNAL 2002. Proceedings of the 16th Biennial International Conference of the European Association for Speech, Signal and Image Processing (EURASIP), 26–28 June 2002, Brno, Czech Republic. Brnon: Vutium Press; 2002:400–2.

14. Itskovitz J, LaGamma EF, Rudolph AM. Heart rate and blood pressure responses to umbilical cord compression in fetal lambs with special references to the mechanism of variable deceleration. Am J Obstet Gynecol 1983;147: 451–7.

15. Lee ST, Hon EH. Fetal hemodynamic response to umbilical cord compression. J Obstet Gynecol 1963;22:553–62.

16. Goodlin RC, Lowe EW. A functional umbilical cord occlusion heart rate pattern – The significance of overshoot. Obstet Gynecol 1974;43:22–30.

17. Scheffs J, Vasicka A, Li C, Solomon N, Siler W. Uterine blood flow during labor. Obstet Gynecol 1971;38:15–24.

18. Brotanek V, Hendricks CH, Yoshida T. Importance of changes in uterine blood flow in initiation of labor. Am J Obstet Gynecol 1969;105:535–46.

19. Butler LA, Longo LD, Power GG. Placental blood flows and oxygen transfer during uterine contractions: a mathematical model. J Theor Biol 1976;61:81–95.

20. Felgueiras C, Marques de Sá JP, Bernardes J, Gama S. Classification of foetal heart rate sequences based on fractal features. Med Biol Eng Comput 1998;36:197–201.

21. Sá Couto CD, van Meurs WL, Goodwin JA. Graphical and mathematical representation of congenital heart disease. Proceedings of the SESAM Annual Meeting, 10–11 May 2002; Santander, Spain; 2002: 18.

22. Beneken JEW. A mathematical approach to cardiovascular function: The uncontrolled human system. PhD dissertation. Utrecht, The Netherlands: Rijksuniversiteit Utrecht; 1965.

23. Huikeshoven F, Coleman TG, Jongsma HW. Mathematical model of the fetal cardiovascular system: the uncontrolled case. Am J Physiol 1980;239:R317–25.

24. Klaus MH, Fanaroff AA. Care of the High-Risk Neonate, 5th ed. Philadelphia: WB Saunders; 2001.

Acknowledgements

The authors acknowledge the contributions to the presented work and the critical evaluation of this paper by J.P. Marques de Sá, J.A. Goodwin, M.H. Guimarães, G. Rocha, H. Alonso, V.M. Pinho and P.A. Vieira. A lecture on 'Development of foetal and neonatal simulators at the University of Porto' was presented by Willem van Meurs at the 'Seminário Ensino-Treino-Aprendizagem de Gestos Clínicos, dos fundamentos aos simuladores', University of Porto College of Medicine, 14 November 2002, and in the context of the 'Semana de Ciência e da Tecnologia 2002', at the University of Porto College of Engineering, 27 November 2002.

Funding

This work was funded in part by a grant from Medical Education Technologies Inc., Sarasota, Florida, USA.

Chapter 3

A model for educational simulation of infant cardiovascular physiology

Goodwin JA, van Meurs WL, Sá Couto CD, Beneken JEW, Graves SA

Anesth Analg 2004;99:1655–64

Abstract

Full-body patient simulators provide the technology and the environment necessary for excellent clinical education while eliminating risk to the patient. The extension of simulator-based training into management of basic and critical situations in complex patient populations is natural. We describe the derivation of an infant cardiovascular model through the redefinition of a complete set of parameters for an existing adult model. Specifically, we document a stepwise parameter estimation process, explicit simplifying assumptions, and sources for these parameters. The simulated vital signs are within the target hemodynamic variables, and the simulated systemic arterial pressure wave form and left ventricular pressure volume loop are realistic. The system reacts appropriately to blood loss, and incorporation of aortic stenosis is straightforward. This infant cardiovascular model can form the basis for screen-based educational simulations. The model is also an essential step in attaining a full-body, model-driven infant simulator.

Introduction

Traditional medical education relies on the clinical setting to teach students, residents, and other medical personnel. However, this is not an ideal learning environment because the learning experience may be limited by the critical condition of the patient. Full-body patient simulators provide the technology and the environment necessary for excellent clinical education while eliminating risk to the patient. Currently, more than 450 full-body model-driven simulators are being used throughout the world to teach basic skills[1], responses to complex problems[2], and crisis resource management[3] to a variety of personnel, including residents, medical students, and allied health care professionals.

The extension of simulator-based training into management of basic and critical situations in complex patient populations is natural. Complex models have been adapted to simulate the cardiovascular physiology of the obstetric patient[4]. A simulation-based training program in neonatal resuscitation has also been developed[5]. Obstetric patients, neonates, and children often present a management challenge in the acute care setting because of complex physiology and the need for swift therapeutic interventions. The modeling of pediatric cardiovascular physiology is an important step in attaining a full-body model-driven pediatric simulator that can be used for clinical education. The cardiovascular physiology of the neonate, infant, child, and adolescent all differ because of continuing development and maturation of the cardiovascular system. Although each pediatric patient may present a unique challenge to the acute care provider, we based the cardiovascular physiology of our simulated patient on that of an infant.

The cardiovascular system of an infant differs significantly from that of an adult, and, therefore, modeling the cardiovascular physiology requires the redefinition of a complete set of parameters. Our hypothesis was that the described model structure could adequately reflect pediatric cardiovascular physiology for educational simulation purposes. Our goal was to find model parameters such that the cardiovascular vital signs reflect target pediatric vital signs in normal and pathologic conditions and that they react appropriately to critical incidents and therapeutic interventions. The selected basic critical incident was moderate acute blood loss. To evaluate the capacity of our model to reflect pathology, we chose aortic stenosis.

Methods

In our study, we used the linearized, improved model of cardiovascular physiology presented by Beneken[6] (Figure 1) to represent the uncontrolled cardiovascular system. This model was also the basis for the model of cardiovascular physiology for the Human Patient Simulator (HPS™; developed at the University of Florida and commercially available from

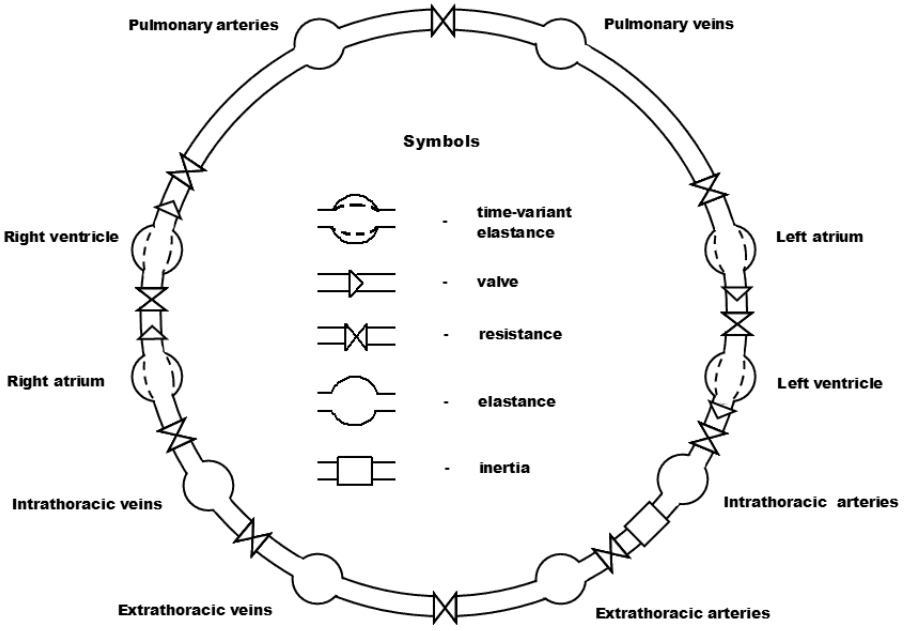

Figure 1. Hydraulic analog for the cardiovascular model.

Medical Education Technologies, Inc., Sarasota, FL). This uncontrolled model was selected because although it is of relatively reduced complexity, it could support a wide range of anticipated learning objectives. The model can generate pulsatile blood pressure wave forms and reacts appropriately to blood loss and volume administration, intrathoracic pressure, baroreflex control of circulation, and drug influences.

A physiologic interpretation of the model structure and parameter values is desirable for easy coupling of this model to other models and for adjustment of parameter values to reflect pathologies, critical incidents, or other patients. The interactive simulation application requires the model to run in real time. The 1965 model was used because some of the added detail in the later models[7] or in the HPS implementation was judged unnecessary for the present application. In our study, we used the baroreflex model presented by Wesseling and Settels[8]. Appendix 1 describes these models in detail. The interfacing of model input and output signals to the simulator mannequin and the monitors, as well as the interactions of the cardiovascular model with other physiologic models, is described elsewhere[9].

Adapting the above-described model to simulate the cardiovascular system of a pediatric patient involved several steps. First, target hemodynamic variables for the patient - specifically, a 6-mo-old infant - were defined by reviewing pediatric and pediatric anesthesia textbooks[10,11] and are listed together with the simulation results in Table 1 (second column).

Table 1. Simulated cardiovascular vital signs for a 6-month-old infant.

		Simulation results					
		Independent systems			**Full circulation**		
Variable	Target	Left/ systemic	Right/ pulmonary	Right/ pulmonary (2)	Baseline	50-mL Blood loss	Aortic stenosis
Heart rate (bpm)	115-145	129	129	129	129	135	140
Systemic systolic pressure (mmHg)	70-110	89	--	--	86	82	76
Systemic diastolic pressure (mmHg)	50-65	59	--	--	57	56	57
Central venous pressure (mmHg)	3-12	3	3	3	3	2	3
Pulmonary systolic pressure (mmHg)	12-28	--	21	16	16	14	20
Pulmonary diastolic pressure (mmHg)	4-12	--	7	6	6	5	12
Pulmonary capillary wedge pressure (mmHg)	NA	4	4	4	4	3	10
Cardiac output ($L.min^{-1}$)	1.2-2.0	1.8	2.6	1.8	1.8	1.6	1.5

NA - not available.
The second iteration for the right/pulmonary side and full circulation uses a reduced right heart contractility.

To further simplify the development process, we observed that opening the cardiovascular loop would allow us to work on the left/systemic and right/pulmonary sides of the cardiovascular system independently. The second step consisted of temporarily fixing the model parameters: pulmonary venous pressure to 4 mmHg and intrathoracic systemic venous pressure to 3 mmHg. This created a system that allowed independent manipulation of left heart and systemic vascular parameters and of right heart and pulmonary vascular parameters. In this phase, physiologic model parameters were derived from the literature and incorporated into the model. Once target values were achieved for each uncontrolled system half independently, the third step consisted of lifting the restrictions on the pulmonary and systemic venous pressure and combining the two systems to yield a full uncontrolled system. In the last step, the influence of the baroreflex was added, governing the system behavior when it receives a perturbation. The dynamic response to blood loss is evaluated in this controlled system. As a test of the capability of this model to reflect pathologies via the adjustment of model parameters, we obtained data for aortic valve stenosis and simulated this pathology.

Review of published literature provided clinical variables that describe the left ventricular function and global descriptions of the systemic and pulmonary circulation of an approximately 6-mo-old infant (Table 2). However, cardiovascular data for the healthy infant were not as plentiful as for the healthy adult. In addition, one cannot assume that animal data always correlate well with that for humans. With these facts in mind, certain model

Table 2. Clinical variables describing left ventricular function and global descriptions of the systemic and pulmonary circulation of an approximately 6-Month-Old Infant from the literature (assumed body-surface area, 0.4 m^2).

Variable	Absolute value	Normalized value	Reference
Heart			
LVEDV	17 mL	42 $mL.m^{-2}$	(12)
LVEDP	5 mmHg		(12)
LVESV	5 mL	13 $mL.m^{-2}$	(12)
LVESP	82 mmHg		(12)
Circulation			
SVR	25-50 $mmHg.L^{-1}.min$	10-20 $mmHg.L^{-1}.min.m^2$	(17)
PVR	2.5-7.5 $mmHg.L^{-1}.min$	1-3 $mmHg.L^{-1}.min.m^2$	(17)
Arterial compliance	0.46 $mL.mmHg^{-1}$	1.15 $mL.mmHg^{-1}.m^{-2}$	(19)

LVEDV - left ventricular end-diastolic volume; LVEDP - left ventricular end-diastolic pressure; LVESV - left ventricular end-systolic volume; LVESP - left ventricular end-systolic pressure; SVR - systemic vascular resistance; PVR - pulmonary vascular resistance.

parameters were obtained directly from the literature, some were derived through the use of well established formulas, and still others required that physiologically sound assumptions be made. We have explicitly documented these steps. Appendix 2 describes the parameter-estimation procedure and its assumptions.

The model simulation results that were validated first were normal heart rate, cardiac output, and systemic arterial, central venous, pulmonary arterial, and pulmonary capillary wedge pressures. We also showed the generated pulsatile arterial blood pressure wave form. We further presented simulation results on the model response to acute moderate blood loss and validated the simulated vital signs for aortic stenosis.

Congenital aortic stenosis may be caused by a spectrum of lesions that obstruct blood flow from the left ventricle to the aorta. Inclusion in an educational simulation is relevant for the training in recognition of and possible therapeutic interventions on an infant with this condition. Three parameter changes were made to the model. The aortic valve and intrathoracic artery resistance (Appendix 2) was increased from 0.016 to 0.8 $mmHg.mL^{-1}.s$. On the basis of a left ventricular pressure volume curve given by Graham and Jarmakani[12], we changed the left ventricular filling characteristics by increasing the diastolic elastance of the left ventricle from 0.55 to 1.5 $mmHg.mL^{-1}$ while reducing the unstressed volume from 2 to 0 mL. This is thought to reflect the reduced compliance and unstressed volume due to the increased cardiac muscle mass.

The model equations were numerically integrated by using the Euler forward method with a step size of 1 ms. All simulations were implemented in Microsoft Visual Java - Version 6.0 on a personal computer with an 1800-MHz Pentium™ 4 processor.

Results

Table 1 gives the target values and simulated vital signs. When the isolated halves were simulated (Appendix 2), the vital signs for the left/systemic side were within the target values. The pressures for the right/pulmonary side were within the target values, but the cardiac output was high. Moreover, it was higher than the cardiac output of the isolated left/ systemic side. The contractility of the right ventricle, as reflected in the *ERVMAX* (maximum systolic elastance of the right ventricle) parameter, was not directly derived from a measured pressure-volume loop, but rather through scaling from the left ventricle. We therefore adjusted this parameter and the corresponding right atrial parameter *ERAMAX* (maximum systolic elastance of the right atrium) to obtain a similar cardiac output for the right/pulmonary part of the circulation. A reduction of 40% was necessary. This second iteration is also reflected in Table 1. The "Baseline" column of this table demonstrates that combining the isolated halves into the full circulation did not significantly influence the simulated vital signs and that they were well within the ranges of the target vital signs. Results from the echocardiographic study of 30 infants performed by Wodey et al.[13] provided data for baseline heart rate, systolic blood pressure, cardiac index, and shortening fraction. Their results further substantiate the clinical appropriateness of our simulated vital signs. In this simulation experiment, we used a total blood volume of 685 mL, which is slightly more than the approximately 640 mL expected for an 8-kg infant.

The pulsatile nature of the model is highlighted by the simulation results in Figures 2 and 3. Figure 2 shows the systemic arterial blood pressure wave form. We consider this wave form realistic enough for the envisioned simulation application in acute care training. Figure 3 (normal case) shows the simulated left ventricular pressure-volume loop and the clinical

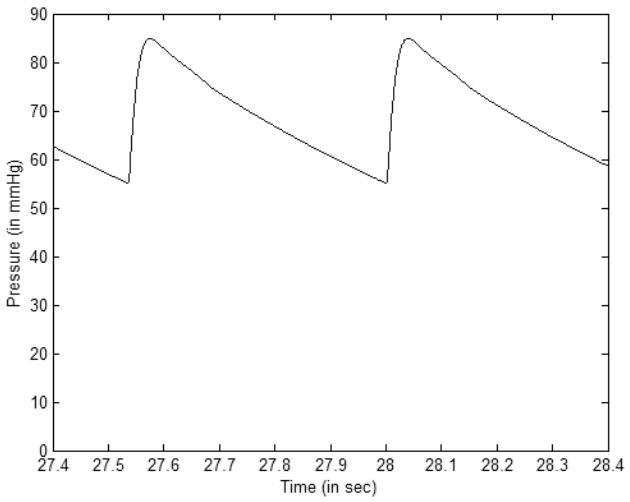

Figure 2. Simulated systemic arterial blood pressure.

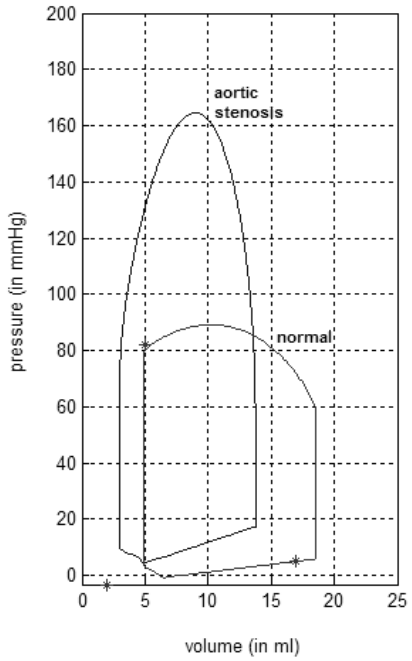

Figure 3. Simulated left ventricular pressure-volume loops with and without aortic stenosis. (*)Clinical variables and the assumed unstressed volume from which the model parameters were derived.

variables and the assumed value for the unstressed volume from which the left ventricle model parameters were calculated. The curve, simulated with a full circulation model, reproduces the clinical variables characterizing the end-diastolic and end-systolic situations in good approximation.

For our 6-mo-old infant, an acute blood loss of 50 mL corresponds to an approximately 7% loss in blood volume. The simulated vital signs demonstrate an appropriate clinical response (Table 1; “50-mL Blood loss” column). Note that the “Baseline” column in Table 1 represents the vital signs of the system with baroreflex control in its baseline operating point. These vital signs are identical, by design, to the vital signs of the uncontrolled full circulation.

Figure 3 also shows the simulated left ventricular pressure-volume loops with aortic stenosis. The changes are indeed very similar to the ones reported by Graham and Jarmakani[12]. Table 1 (final column) lists the effects on the monitored signals. From Figure 3 and the systemic systolic pressure in Table 1 we observed that the pressure difference across the stenotic valve was approximately 90 mmHg, corresponding to a severe stenotic situation. From the same figure and table, we note that for the simulated normal infant, there is no

apparent stenotic pressure decrease. With the indicated integration step size, programming language, and hardware, the cardiovascular model runs 300 times faster than real time.

Discussion

From the perspective of educational simulations of clinical scenarios, the main differences between the cardiovascular system of an infant and an adult are quantitative rather than qualitative. Therefore, modeling the cardiovascular physiology in this context does not require formulating a new model structure, but it does require the redefinition of a complete set of parameters. We describe an existing simulation model and the derivation of a new parameter set for the infant cardiovascular system. Several parameters were derived through proportionality constants or adjustments. The simulated vital signs were within the target hemodynamic variables, and the system reacts appropriately to blood loss. Arterial pressure wave forms and left ventricular pressure volume curves were, in our opinion, realistic enough for educational simulations. From the simulation of aortic stenosis, we concluded that through only a few simple and intuitive parameter changes, we can manipulate our model to realistically reflect essential aspects of aortic stenosis.

A simulation engine of a medical simulator typically includes many other models, and other simulator functionality requires further processing time. Our simulation results show that run time is not a limiting factor to the complexity of this model. However, increasing model complexity would further complicate the already extensive parameter-estimation procedure and make future manipulation by clinical instructors to simulate other patients, pathologies, and incidents virtually impossible.

Two fundamental physiologic aspects complicate both teaching and parameter estimation of the cardiovascular system. The first aspect is the circular nature of the system. A change in any part of the circulation will affect blood volumes, pressures, and flow rates in all parts. The second aspect is control by the baroreflex. This powerful control system also spreads out the effect of a local change to many parts of the circulation and masks the dependency of system variables on system parameters. We solved both problems by initially considering the left/systemic and right/pulmonary sides of the uncontrolled cardiovascular system independently. The ability to work on a smaller set of parameters, and without the circular effect of a parameter change, did facilitate identifying and adjusting a problem with the contractility of the right heart. After combining the two sides of the circulation, we then incorporated a model of basic aspects of the baroreflex.

This model can form the basis for a screen-based teaching tool. The model may be used to demonstrate the many clinically important differences between normal infant and adult cardiovascular physiology. Clinical scenarios may be created to demonstrate specific

learning objectives. In addition, this model may be used as the underlying model for the uptake and distribution of respiratory and anesthetic gases, as well as simulation of the effects of anesthetics. Models for the simulation of the myocardial oxygen balance and electrophysiologic phenomena can easily be coupled to it, with the ultimate goal of simulation of a six-month-old infant in full scale.

Appendix 1
A model for adult cardiovascular physiology

The uncontrolled cardiovascular model (Figure 1) accepts as inputs blood volume changes and intrathoracic pressure and generates as outputs systemic and pulmonary artery blood pressures, central venous and all pulmonary artery catheter blood pressures, and cardiac output. Note that in the 1965 model, the pressure decreases over the systemic and pulmonary beds are represented by a single resistance each; this model does not represent the accumulation of blood in tissue, nor does it reflect distinct parallel vascular beds.

For each model compartment, the variables blood pressure, inflow rate, and volume change are computed. The compartment equations are coupled because the inflow rate of a compartment also depends on the pressure of the upstream compartment, and the volume change results from the difference between inflow and outflow rates. The relationships between variables are governed by resistance, elastance, and unstressed volume. The elastances of the heart chambers vary and reflect the contraction. Transmural compartment pressure ($p(t)$) is a linear function of the difference between the compartment volume ($v(t)$) and the unstressed volume (UV) (for $v(t) > UV$). For selected compartments, average intrathoracic pressure is added to the transmural pressure to obtain the absolute pressure. The elastance (E) is the second parameter in the volume-pressure relationship:

$$p(t) = E(v(t) - UV) \tag{A1}$$

The elastances of the heart chambers are time varying, reflecting the contraction. Compartment inflow rate ($f(t)$) is a linear function of the pressure in the upstream compartment [$p_{in}(t)$ and $p(t)$]. The inflow resistance (R) governs this relationship:

$$f(t) = \frac{p_{in}(t) - p(t)}{R} \tag{A2}$$

The resistances of the atrial inflow tracts to backward flow are 10 times superior to the resistances to forward flow. The resistances of the heart valves are also nonlinear, reflecting the infinite cardiac valve resistance to back flow. The change of compartment volume is equal to the difference between $f(t)$ and the compartment outflow rate ($f_{out}(t)$):

$$\frac{dv(t)}{dt} = f(t) - f_{out}(t) \tag{A3}$$

A single differential equation governs the inertial behavior of the blood in the arteries by using a similar notation as in Table 3, formally introduced in Appendix 2:

$$\frac{df_{etha}(t)}{dt} = \frac{p_{itha}(t) + PTH - RETHA\, f_{etha}(t) - p_{etha}(t)}{LETHA} \tag{A4}$$

Beneken[6] derived the parameter values that represent a normal adult in the supine position for the uncontrolled model from a combination of clinical data and computation based on physics (Table 3).

The description of the heart is critical for the estimation of the infant parameters and will be given in detail. Figure 4A shows a typical ventricular pressure-volume loop and the clinical variables that are used to characterize it. Such a loop can be generated by a time-varying elastance model of the ventricle[7]:

$$p(t) = e(t)\left[v(t) - UV\right] \tag{A5}$$

where *p(t)* is the ventricular pressure and *v(t)* the ventricular volume as a function of time. The relationship between these variables is determined by the unstressed volume (*UV*) and the elastance time profile (*e(t)*). Suga et al.[14] verified this model in dogs and showed that *e(t)*, which is characterized by its maximum value and the time of this maximum, reflects the ventricular contractility. We parameterized the ventricular elastance curve as follows:

$$e(t) = \begin{cases} EMIN + (EMAX - EMIN)\dfrac{1}{K_n}\dfrac{t-(T_{as}+T_{av})}{T_{vs}}\sin\left(\pi\dfrac{t-(T_{as}+T_{av})}{T_{vs}}\right) \\ \qquad\qquad if \quad (T_{as}+T_{av} \le t < T_{as}+T_{av}+T_{vs}) \\ EMIN \qquad\qquad otherwise \end{cases} \tag{A6}$$

The minimum and maximum elastances are *EMIN* and *EMAX*, respectively. T_{as}, T_{av}, and T_{vs} are the durations of atrial systole, atrioventricular delay, and ventricular systole, respectively. K_n is a normalization constant equal to the maximum of the time function

$$\frac{\left(t-\left(T_{as}+T_{av}\right)\right)}{T_{vs}}\sin\left(\pi\frac{\left(t-\left(T_{as}+T_{av}\right)\right)}{T_{vs}}\right)$$

Table 3. Cardiovascular parameters for the adult and infant.

Part of circulation	Compartment	Parameter description	Parameter name	Parameter values	
				Adult	Infant
Total circulation	All	Initial total blood volume	VTOTAL	4740	685
Heart	Atria and ventricles	Heart rate	HR	72.0	129
Intrathoracic	All intrathoracic	Average intrathoracic pressure	PTH	-4.00	-3.25
Left heart	Left atrium	Resistance to forward flow of the inflow tract	RLAIN	0.00300	0.00600
		Mitral valve resistance	RLAOUT	0.00300	0.00600
		Diastolic elastance	ELAMIN	0.120	0.733
		Maximum systolic elastance	ELAMAX	0.280	1.99
		Unstressed volume	VLAU	30.0	1.00
	Left ventricle	Aortic valve and intrathoracic artery resistance	RLV	0.00800	0.01600
		Diastolic elastance	ELVMIN	0.0900	0.550
		Maximum systolic elastance	ELVMAX	4.00	28.4
		Unstressed volume	VLVU	60.0	2.00
Systemic circulation	Intrathoracic arteries	Elastance	EITHA	1.43	7.76
		Unstressed volume	VITHAU	140	18.2
	Extrathoracic arteries	Blood flow inertia	LETHA	0.000700	0.000200
		Resistance	RETHA	0.0600	0.120
		Elastance	EETHA	0.556	3.02
		Unstressed volume	VETHAU	370	48.1
	Peripheral vessels	Resistance	RSP	1.00	2.00
	Extrathoracic veins	Resistance (to forward flow)	RETHV	0.0900	0.180
		Elastance	EETHV	0.0169	0.0918
		Unstressed volume	VETHVU	1000	130
	Intrathoracic veins	Elastance	EITHV	0.0182	0.0989
		Unstressed volume	VITHVU	1190	155
Right heart	Right atrium	Resistance to forward flow of the inflow tract	RRAIN	0.00300	0.00600
		Tricuspid valve resistance	RRAOUT	0.00300	0.00600
		Diastolic elastance	ERAMIN	0.0500	0.317
		Maximum systolic elastance	ERAMAX	0.150	0.630
		Unstressed volume	VRAU	30.0	1.50
	Right ventricle	Pulmonic valve and pulmonary artery resistance	RRV	0.00300	0.00600
		Diastolic elastance	ERVMIN	0.0570	0.348
		Maximum systolic elastance	ERVMAX	0.490	2.09
		Unstressed volume	VRVU	40.0	3.00
Pulmonary circulation	Pulmonary arteries	Elastance	EPA	0.233	1.27
		Unstressed volume	VPAU	50.0	6.50
	Peripheral vessels	Resistance	RPP	0.110	0.220
	Pulmonary veins	Elastance	EPV	0.0455	0.247
		Unstressed volume	VPVU	350	45.5

Units are as follows: heart rates, bpm; resistances, $mmHg.mL^{-1}.s$; elastances, $mmHg.mL^{-1}$; volumes, mL; inertia, $mmHg.mL^{-1}.s^2$

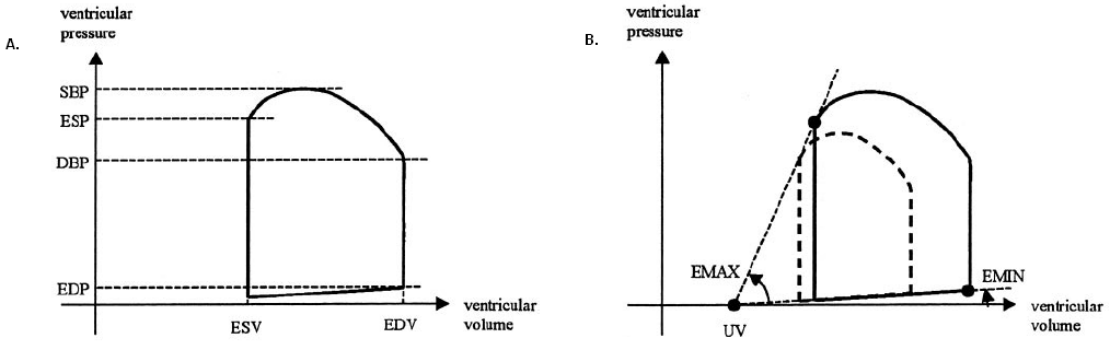

Figure 4. Ventricular pressure-volume curve. **A.** Clinical variables: end-systolic (ESV), end-diastolic volume (EDV), and end-systolic (ESP) and end-diastolic pressures (EDP). SBP- systolic blood pressure; DBP - diastolic blood pressure. **B.** Model parameters: minimum and maximum elastances (EMIN and EMAX) and unstressed volume (UV). The dashed curve represents a situation with identical parameters but reduced preload.

part of equation (A6). It can be observed that this curve is a reasonable approximation of the curve for the left ventricle calculated from measured data by Suga et al.[14]. Figure 4B shows the same pressure-volume loop as in Figure 4A, now with the model parameters *UV*, *EMIN*, and *EMAX*. This figure also shows a second curve that is obtained under different preload conditions, but with the same model parameters. The model parameters can be derived directly when a number of measured curves are available. If only clinical descriptors, such as in Figure 4A, are available, and provided that we have an estimate for the unstressed volume *UV*, *EMIN* and *EMAX* can be calculated as follows:

$$EMIN = \frac{EDP - PTH}{EDV - UV} \tag{A7}$$

$$EMAX = \frac{ESP - PTH}{ESV - UV} \tag{A8}$$

Note that in the calculation of these slopes, we use the (average) intrathoracic pressure (*PTH*) as a reference, rather than 0 (atmospheric pressure). This can be made plausible by observing that the unstressed volume occurs at a zero transmural pressure across the ventricular wall, which requires a ventricular pressure equal to the intrathoracic pressure. The atrial elastance curves are identical to those proposed by Beneken[6] and are parameterized as follows:

$$e(t) = \begin{cases} EMIN + (EMAX - EMIN)\ \sin\left(\pi \dfrac{t}{T_{as}}\right) & (0 \le t < T_{as}) \\ EMIN \quad (otherwise) \end{cases} \tag{A9}$$

The minimum and maximum elastances are *EMIN* and *EMAX*, respectively, and T_{as} is the duration of the atrium systole. The ventricle systole starts at time T_{as} + T_{av} after the initiation of the atrium systole, where T_{av} represents the atrioventricular delay.

Beneken gives the duration of atrium and ventricle systole as a function of heart period (*HP*) and a numerical value for the atrioventricular delay (in seconds):

$$\begin{aligned} T_{as} &= 0.03 + 0.09HP \\ T_{av} &= 0.01 \\ T_{vs} &= 0.16 + 0.20HP \end{aligned} \tag{A10}$$

The resistances and unstressed volumes of selected compartments depend on the baroreflex. The baroreflex also affects heart rate and contractility (maximum heart chamber elastance).

The single receptor of the Wesseling and Settels model for the baroreflex[8] is represented by a sigmoid function of mean arterial blood pressure, with a threshold of 50 mmHg, saturation of 180 mmHg, and maximum sensitivity around the “resting pressure” of 100 mmHg. The baroreflex part of the model has four effector variables: heart rate, contractility, total peripheral resistance (TPR), and venous unstressed volume. Parameter data for response gain, delay, and time constant are presented by Ten Voorde[15].

For our study, we implemented a variant of this model. To facilitate parameter estimation and manipulation, we replaced the receptor function with a piecewise linear function with a slope of 1 at the mean arterial blood pressure in equilibrium. The slope is dimensionless, resulting in an output of the receptor function in millimeters of mercury. We maintained the four effector variables, substituting heart period for heart rate. Because our objective was to obtain a realistic simulated response to phenomena such as blood loss and pharmacologic interventions, but not to study beat-to-beat heart rate variability, we maintained the gains but did not include delays or the time constants of the response. Table 4 gives the numerical values for the adult for the baseline baroreflex effectors from Beneken[6], the absolute baroreflex gains of the Wesseling and Settels model in the units specified by Ten Voorde[15], and, for later reference, the derived relative gains in percentage per millimeter of mercury.

Table 4. Numerical values for the adult baroreflex effectors and gains.

Baroreflex effector	**Baseline value**	**Absolute gain**	**Relative gain**
Heart period	833 ms	16.6 ms.mmHg^{-1}	1.99 %.mmHg^{-1}
Maximum elastance of the left ventricle	4.00 mmHg.mL^{-1}	-0.0160 mL^{-1}	-0.40 %.mmHg^{-1}
Total peripheral resistance	1.15 mmHg.mL^{-1} s	-0.0270 s.mL^{-1}	-2.35 %.mmHg^{-1}
Venous unstressed volume	2190 mL	27.0 mL.mmHg^{-1}	1.23 %.mmHg^{-1}

In our model, the relative gain for the maximum elastance of the left ventricle is applied to the output of the receptor function, thus affecting the maximum elastance of all four heart chambers. The baroreflex-mediated change in the RSP (resistance of the systemic peripheral vessels) parameter of the Beneken model (Table 3) is such that the total peripheral resistance change is equal to the relative gain. The relative gain for the (total) unstressed volume affects the unstressed volumes of both intrathoracic and extrathoracic compartments.

Appendix 2
Parameter estimation for infant cardiovascular physiology

The following provides explicit documentation of the steps taken for derivation of specific model parameters for the infant.

Left Heart. From the clinical variables describing the left ventricle (Table 2), assuming a left ventricular unstressed volume of 2.0 mL and an average intrathoracic pressure of -3.25 mmHg[16], the model parameters for the left ventricle diastolic and maximum systolic elastances were derived by using Equations (A7) and (A8). The assumed and calculated parameter values are listed in Table 3. Aortic valve resistance, mitral valve resistance, and left atrial inflow tract resistance were each doubled with respect to the adult values. Left atrial unstressed volume was decreased proportionally from the adult value by comparison to the left ventricle. The left atrial minimum and maximum elastances were proportionally increased from adult values by comparison to the left ventricle, because no data concerning the infant atria were available.

Systemic Circulation. Systemic vascular resistance was a calculated value and for an infant was equal to 10–20 $mmHg.L^{-1}.min.m^2$ [17]. This value is a function of body-surface area and was similar in infants and adults[18]. Because of the infant's smaller body-surface area, its absolute value for systemic vascular resistance was approximately twice that of an adult. Accordingly, the infant parameters resistance of the extrathoracic arteries and veins and of the systemic peripheral vessels were obtained by multiplying adult parameters by 2.

The literature provided a value of 0.46 $mL.mmHg^{-1}$ for the arterial compliance in infants[19]. The adult systemic arterial compliance in the Beneken model is equal to (1/EITHA)+(1/EETHA)=2.5 $mL.mmHg^{-1}$, where *EITHA* and *EETHA* are the elastances of the intrathoracic and extrathoracic arteries, respectively. The ratio between pediatric and adult systemic arterial elastance is therefore equal to 2.5/0.46 ≅ 5.43. Infant *EITHA* and *EETHA* were derived by proportionally increasing these values from those of the adult by using this ratio. The same ratio was used to derive the elastance of the intrathoracic and extrathoracic veins. Arterial and venous unstressed volumes were each proportionally decreased from those of the adult model on the basis of comparison of total blood volumes for that of an infant (80 $mL.kg^{-1}$) versus an adult (70 $mL.kg^{-1}$)[20]. For an 8-kg infant and a 70-kg adult, this leads to a proportionality constant of approximately 0.13. Note that this assumes a similar distribution of blood between arterial and venous circulations in adults and infants.

The above-mentioned parameters were then incorporated in the model software to yield the first iteration of vital signs for the uncontrolled left heart and systemic loop of the infant cardiovascular system. The blood flow inertia parameter was adjusted to optimize the

pressure wave form in the intrathoracic artery compartment. Note that when this parameter is used in such an empirical fashion, it should no longer be referred to in terms of underlying physics.

Right Heart. In the infant, the end-diastolic volume (*EDV*) of the right ventricle is approximately 1.5 times the *EDV* of the left ventricle[21]. We applied this ratio to the unstressed volume going from the left to right ventricle and did the same going from the left to the right atrium. Right atrial and ventricle minimum and maximum elastances were derived by scaling the right heart from adult to infant in the same way as the left heart. As for the left heart, all right heart resistances were multiplied by 2.

Pulmonary Circulation. We used a pulmonary peripheral vascular resistance of 3.7 $mmHg.L^{-1}.min$ = 0.22 $mmHg\text{-}mL^{-1}.s$, which is within the published range of 2.5–7.5 $mmHg.L^{-1}.min$ for pediatric patients[17]. This value is two times the adult value in the Beneken model (1.83 $mmHg.L^{-1}.min$ = 0.11 $mmHg.mL^{-1}.s$) and is therefore also consistent with changes made to the systemic circulation. Elastance of the pulmonary arteries and pulmonary veins were both derived by increasing these values from those of the adult, proportional to the increase in systemic arterial elastance. Similarly, pulmonary arterial and pulmonary venous unstressed volumes were both proportionally decreased from that of the adult model on the basis of comparison of total blood volume for an infant versus an adult. Note that with more numerical data on changes in pulmonary vascular tone in infancy, the value of this parameter may change.

The right heart and pulmonary circulation parameters were then incorporated in the model software to yield the first iteration of vital signs for the uncontrolled right heart and pulmonary loop of the infant cardiovascular system. Two parameter changes were made to correct a difference in right and left cardiac output. Table 3 contains the corrected parameters. Subsequently, we combined the two halves of the circulation and simulated the full uncontrolled infant system with the parameters summarized in Table 3. Throughout the simulations, we maintained a constant intrathoracic pressure of -3.25 mmHg.

Baroreflex. There are no published data for the baroreflex of a 6-mo-old infant. The parameters for the baroreflex were therefore derived from published data concerning the neonate[22]. Drouin et al.[22] observed a spontaneous baroreflex sensitivity in full-term neonates of 10.23 $ms.mmHg^{-1}$ to changes in systolic blood pressure. At a heart period of 465 ms (heart rate of 129 bpm), this corresponds to a relative baroreflex gain for the heart period of 2.2%.$mmHg^{-1}$. This relative change is similar to that of the adult (Table 4). We used the same relative gains as in the adult for all baroreflex control effectors: heart period, contractility, peripheral resistance, and venous unstressed volume.

References

1. Good ML, Gravenstein JS. Training for safety in an anesthesia simulator. Semin Anesth 1993;12:235–50.

2. Gaba DM, DeAnda A. The response of anesthesia trainees to simulated critical incidents. Anesth Analg 1989;68:444 –51.

3. Howard SK, Gaba DM, Fish KJ, et al. Anesthesia crisis resource management training: teaching anesthesiologists to handle critical incidents. Aviat Space Environ Med 1992;63:763–70.

4. Euliano TY, Caton D, van Meurs W, Good ML. Modeling obstetric cardiovascular physiology on a full-scale patient simulator. J Clin Monit 1997;13:293–7.

5. Halamek LP, Kaegi DM, Gaba DM, et al. Time for a new paradigm in pediatric medical education: teaching neonatal resuscitation in a simulated delivery room environment. Pediatrics 2000;106:E45.

6. Beneken JEW. A mathematical approach to cardiovascular function: the uncontrolled human system [PhD thesis]. Medisch Fysisch Institut TNO, Utrecht, The Netherlands: 1965.

7. Beneken JEW, DeWit B. A physical approach to hemodynamic aspects of the human cardiovascular system. In: Reeve EB, Guyton AC, eds. Physical bases of circulatory transport: regulation and exchange. Philadelphia: Saunders, 1967;1– 45.

8. Wesseling KH, Settels JJ. Baromodulation explains short-term blood pressure variability. In: Orlebeke JF, Mulder G, van Doornen LJP, eds. Psychophysiology of cardiovascular control. New York: Plenum Press, 1985;69 –97.

9. Van Meurs WL, Good ML, Lampotang S. Functional anatomy of full-scale patient simulators. J Clin Monit 1997;13:317–24.

10. Pruitt AW, Gersony WM. The cardiovascular system. In: Behrman RE, ed. Nelson textbook of pediatrics. 14th ed. Philadelphia: Saunders, 1992;1125–227.

11. Gregory GA. Monitoring during surgery. In: Gregory GA, ed. Pediatric anesthesia. New York: Churchill Livingstone, 1994; 261–79.

12. Graham TP Jr, Jarmakani MM. Evaluation of ventricular function in infants and children. Pediatr Clin North Am 1971;18: 1109–32.

13. Wodey E, Plady P, Copin C, et al. Comparative hemodynamic depression of sevoflurane versus halothane in infants. Anesthesiology 1997;87:795– 800.

14. Suga H, Sagawa K, Shoukas AA. Load independence of the instantaneous pressure-volume ratio of the canine left ventricle and effects of epinephrine and heart rate on the ratio. Circ Res 1973;2:314 –22.

15. Ten Voorde B. Modeling the baroreflex: a system analysis approach [PhD thesis]. Vakgroep Medische Fysica, Amsterdam, The Netherlands: 1992.

16. Cunningham MD. Bedside pulmonary function testing of infants. In: Levin DL, Morriss FC, eds. Essentials of pediatric intensive care. St. Louis: Quality Medical, 1990;878–83.

17. Strafford MA. Cardiovascular physiology. In: Motoyama EK, Davis PJ, eds. Smith's anesthesia for infants and children. St. Louis: Mosby, 1996;69 –104.

18. Lake CL. Cardiovascular anatomy and physiology. In: Barash PG, Cullen BF, Stoelting RK, eds. Clinical anesthesia. Philadelphia: Lippincott, 1992;989 –1020.

19. Hsieh K, Chen P, Fu S. A simple, noninvasive method to investigate vascular characteristics in children. Angiology 1996;47: 361–7.

20. Stoelting RK, Miller RD. Basics of anesthesia. Philadelphia: Churchill Livingstone, 2000;364 –75.

21. Thilenius OG, Argilla RA. Angiographic right and left ventricular volume determination in normal infants and children. Pediatr Res 1974;8:67–74.

22. Drouin E, Gournay V, Calamel J, et al. Assessment of spontaneous baroreflex sensitivity in neonates. Arch Dis Child Fetal Neonatal Ed 1997;76:F108 –12.

Acknowledgements

J. S. Gravenstein and M. L. Good provided encouraging and guiding comments for this study.

Funding

Funded by the Department of Anesthesiology, University of Florida College of Medicine, Gainesville, FL, USA, and Medical Educational Technologies, Inc., Sarasota, FL, USA.

Chapter 4

A model for educational simulation of neonatal cardiovascular pathophysiology

Sá Couto CD, van Meurs WL, Goodwin JA, Andriessen P

Simul Healthc 2006;1 Spec no.:4-9

Abstract

Full-body patient simulators provide a technological basis for clinical education without risk to real patients. In a previous study, we described a model for educational simulation of infant cardiovascular physiology. Using essentially the same methodology, we derive a mathematical model for the cardiovascular system of a healthy 1-week-old neonate. Computer simulations of this model result in vital signs that are close to target hemodynamic variables. Simulated systemic arterial pressure waveform and left ventricular pressure-volume loop are realistic, and the system reacts appropriately to blood loss. We also adapt the model structure and change its parameters to reflect the congenital heart defects: patent ductus arteriosus, tetralogy of Fallot, complex coarctation of the aorta with patent foramen ovale, and transposition of the great arteries. Simulated vital signs are again close to target hemodynamic variables. The resulting model for neonatal cardiovascular pathophysiology is an essential step in attaining a full-body, model-driven neonatal acute care simulator.

Keywords*: Mathematical model, Simulation, Medical education, Neonate, Cardiovascular physiology, Congenital heart defect.*

Introduction

Because of their complex physiology and need for swift therapeutic interventions, neonates present considerable management challenges in the acute care setting. The first studies on the use of simulator based training for this patient population are encouraging, but also mention anatomic and physiological limitations of currently available neonatal simulator technology[1]. In a previous study, we described a model for educational simulation of infant cardiovascular physiology[2]. The first objective of the present study is to find a new set of parameters for an existing mathematical model of the adult cardiovascular system such that computer simulations of this model result in vital signs that reflect target neonatal vital signs in normal conditions, and that they react appropriately to critical incidents and therapeutic interventions. To achieve this objective, we will use the same model and essentially the same parameter estimation method as in our previous study. Our second objective is to extend this model to reflect four congenital heart defects: patent ductus arteriosus, tetralogy of Fallot, coarctation of the aorta, and transposition of the great arteries. Inclusion of these pathologies in a model for educational simulations is relevant for training recognition and treatment of complications resulting from these conditions. Unlike our previous study, achieving this second objective will involve changes in model structure, as well as in model parameters.

Methods

As in our previous study on infant cardiovascular physiology[2], we used the linearized, improved model of cardiovascular physiology, presented by Beneken[3] to represent the uncontrolled cardiovascular system (Figure 1). (This model was also the basis for the model of cardiovascular physiology for the Human Patient Simulator (HPS) developed at the University of Florida, and commercially available from Medical Education Technologies, Sarasota, Fl, USA.) This model was selected because, although of relatively reduced complexity, it could support a wide range of anticipated learning objectives. It can generate pulsatile blood pressure waveforms, and reacts appropriately to blood loss and volume administration, intrathoracic pressure, baroreflex control of circulation, and drug influences. A physiologic interpretation of the model structure and parameter values is desirable for easy coupling of this model to other models, and for the adjustment of model structure and parameter values to reflect pathologies, critical incidents, or other patients. In our study, we used the baroreflex model presented by Wesseling and Settels[4]. Appendix 1 of Goodwin et al.[2] describes these models in detail.

As in Goodwin et al.[2], contractile activity of atria and ventricles is represented by time-varying elastances[5,6]. In this study, we use a slightly different parameterization of the

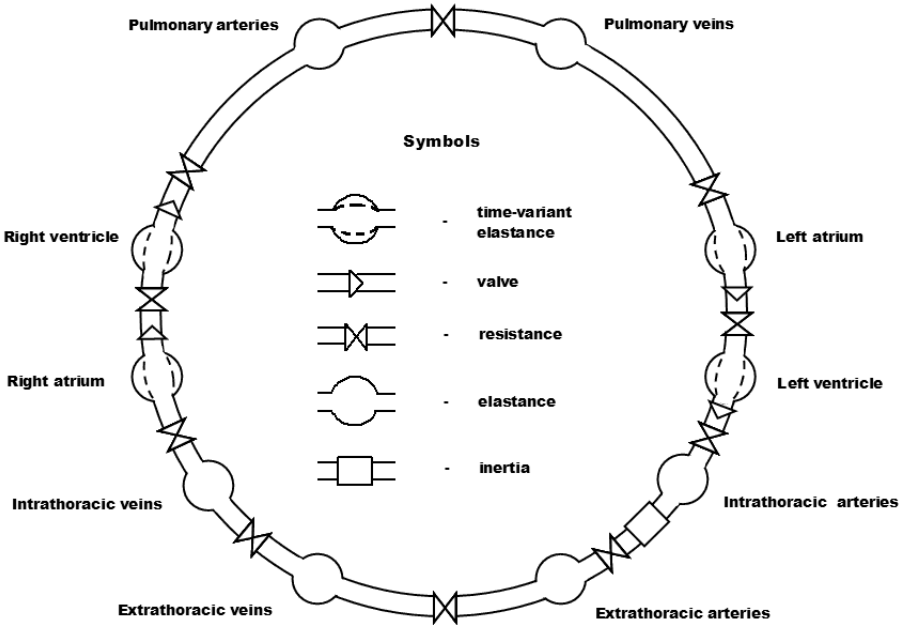

Figure 1. Hydraulic analog for the cardiovascular model. (Reprinted with permission from Goodwin et al.[2])

ventricular elastance curve, based on the activation curves for a full-term fetus presented by Pennati et al.[7]:

$$e(t) = \begin{cases} EMIN + (EMAX - EMIN)\left(\sin\left(\pi \dfrac{t - \Delta T}{T_{vs}}\right)\right)^2 & if \quad \Delta T \le t < \Delta T + T_{vs}) \\ EMIN \quad (otherwise) \end{cases} \qquad (1)$$

The minimum and maximum elastances are *EMIN* and *EMAX*, respectively. ΔT and T_{vs} are the delay in initiation of ventricle activation and the duration of ventricular systole, respectively. The atrial elastance curves are similar to the ones used for the ventricles, and are parameterized as follows:

$$e(t) = \begin{cases} EMIN + (EMAX - EMIN)\left(\sin\left(\pi \dfrac{t}{T_{as}}\right)\right)^2 & (0 \le t < T_{as}) \\ EMIN \quad (otherwise) \end{cases} \qquad (2)$$

T_{as} is the duration of atrium systole. Pennati et al.[7] give the duration of atrium and ventricle systole and the ventricular delay as a function of heart period (*HP*), in seconds:

$$T_{as} = 0.3HP\,, \quad \Delta T = 0.02HP\,, \quad T_{vs} = 0.16 + 0.3HP \tag{3}$$

Target hemodynamic variables for an approximately 1-week-old, full-term, healthy, sleeping neonate[8-10] are listed in the second column of Table 1. Experiments underlying simulation results, which are included in the same table to facilitate comparison, will be introduced later. For a normal 1-week-old, the transition from fetal to neonatal circulation is complete, including functional closing of the "ductus arteriosus." The literature also provided clinical variables describing left and right ventricular function and global descriptions of the systemic and pulmonary circulation[11-13]. An addendum to this paper provides a detailed listing of these data. Based on these and additional data[14-16], we derived model parameters for the normal neonate. The addendum explicitly documents the parameter estimation and its assumptions. Resulting numerical values for model parameters are listed in the Appendix, and together with adult parameters in the addendum. Simulation of baseline vital signs used this model and parameter set.

For simulation of the dynamic response to blood loss, we included a baroreflex model described in detail in Goodwin et al.[2] with neonatal baroreflex parameters derived from data presented by Ten Voorde[17] and Andriessen et al.[18]. The addendum explicitly documents estimation of neonatal parameters and underlying assumptions. Resulting numerical values for neonatal model parameters are listed in the Appendix.

We modeled four congenital heart defects: patent ductus arteriosus, tetralogy of Fallot, coarctation of the aorta, and transposition of the great arteries with atrial and

Table 1. Target data and simulated cardiovascular vital signs for an approximately 1-week-old neonate.

Variable	**Target** (Mean±SD)	**Reference**	**Simulation results**	
			Baseline	**30% blood loss**
Heart rate (min^{-1})	135±20	(8)	130	175
Systemic systolic pressure (mmHg)	73±11	(8)	68	43
Systemic diastolic pressure (mmHg)	45±12	(8)	40	31
Pulmonary systolic pressure (mmHg)	38.5±5.8	(9)	29	12
Pulmonary diastolic pressure (mmHg)	13±6	(9)	10	3
Cardiac output ($mL.min^{-1}$)	500±165	(10)	455	252

Table 2. Target data and simulated cardiovascular vital signs for selected congenital heart diseases.

Variable	Patent ductus arteriosus		Tetralogy of Fallot		Coarctation of the aorta		Transposition of the great arteries	
	Target data[12]	Simulation results	Target data[19]	Simulation results	Target data[20]	Simulation results	Target data[21]	Simulation results
Heart rate (beats/min)	NA	130	NA	130	NA	130	NA	130
Left ventricular systolic pressure (mmHg)	70	72	85	85	NA	70	88±23 *	74
Left ventricular diastolic pressure (mmHg)	7	4	4	3	NA	7	8	4
Systemic systolic pressure (mmHg)	70	70	83	85	60	57	76± 19 *	74
Systemic diastolic pressure (mmHg)	30	20	48	47	30	20	45±16 *	40
Mean systemic pressure (mmHg)	42	40	--	65	24±5 *, †	26 †	--	54
Right ventricular systolic pressure (mmHg)	50	52	85	85	51±21 *	56	88±15 *	75
Right ventricular diastolic pressure (mmHg)	4	3	5	3	0±0 *	0	4	1
Pulmonary systolic pressure (mmHg)	50	51	20	18	48±7 *	55	47±6 *	44
Pulmonary diastolic pressure (mmHg)	28	18	6	7	24±12 *	16	16±6 *	9
Mean pulmonary pressure (mmHg)	35	33	NA	15	NA	32	NA	24
Cardiac output – Systemic (mL/min)	NA	316	NA	548	NA	264	NA	900
Cardiac output – Pulmonary (mL/min)	NA	1125	NA	360	NA	1186	NA	450

*Mean ±SD. †Measured in the descending aorta.
NA, not available.

ventricular septal defects. Target hemodynamic variables for these defects[12,19-21] are listed in Table 2. The structural diagram for the standard hydraulic analog of the cardiovascular system is shown in Figure 1. The modifications to the structure needed to represent the four defects are shown in Figure 2. Numerical values for most model parameters were derived empirically by comparing simulation results with target data. The Appendix lists pathology specific new parameters and pathology specific changes in numerical values of other model parameters.

Patent Ductus Arteriosus. The ductus arteriosus is a large vessel that connects the main pulmonary trunk with the descending aorta. It normally closes quickly after birth. If a full-term baby has a patent ductus arteriosus (PDA) the outcome depends on the size of the channel, reflected by a resistance (Figure 2A). The model also includes a component representing blood inertia in the PDA[22]. With the decrease of pulmonary vascular resistance, the fetal right-to-left shunt becomes a left-to-right shunt, resulting in excessive pulmonary blood flow and left ventricular dilatation. This structural change is also represented in Figure 2A. To represent PDA mathematically, a new state variable was included: flow rate through the ductus arteriosus. Its governing equation is similar to equation (A4) in Goodwin et al.[2] without the term representing intrathoracic pressure. The state equations for intrathoracic arterial volume and pulmonary arterial volume were modified to include flow rate through the

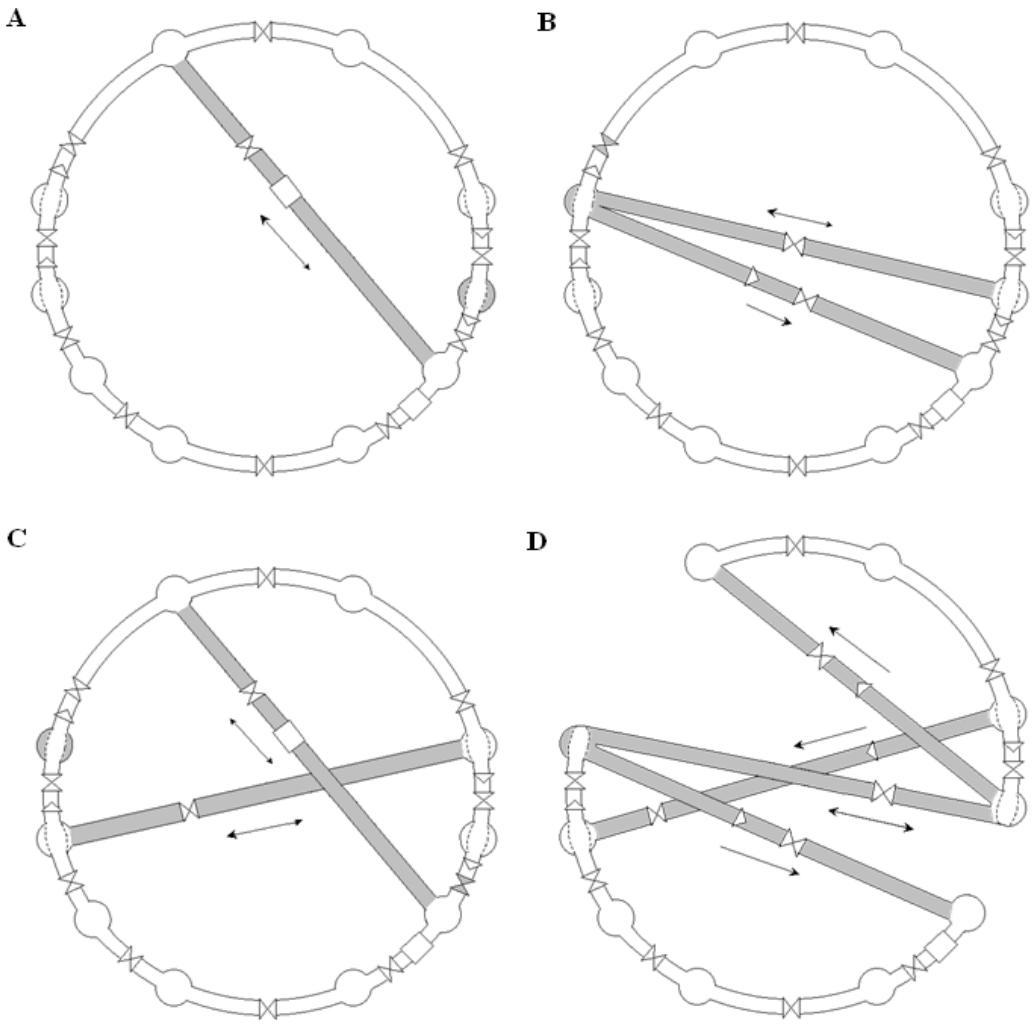

Figure 2. Hydraulic analog of the selected pathologies. **A**. Patent ductus arteriosus. **B**. Tetralogy of Fallot. **C**.Coarctation of the aorta with patent foramen ovale and a small patency of the ductus arteriosus. **D**. Transposition of the great arteries with septal defects. Arrows, possible directions of flow rate; gray ventricles, dilatation or hypertrophy; gray resistances, pulmonary stenosis (**B**) or coarctation (**C**).

ductus. The new parameters, *RDA* and *LDA*, reflect resistance to blood flow in the patent ductus arteriosus, and inertia, respectively. Left ventricular dilation affects the diastolic pressure-volume characteristics and contractility. The parameters governing the piecewise linear representation of left ventricular pressure-volume characteristics during diastole are unstressed volume, *VLVU*, and diastolic elastance, characteristic, with an important effect on ejection fraction, but hardly any effect on simulated vital signs. This parameter was left unchanged. *ELVMIN*, however, affecting diastolic filling, has a large effect on simulated vital signs. The effect of dilation on the diastolic pressure-volume characteristic is therefore

represented by a decrease in *ELVMIN*. The concomitant increase in contractility is represented by an increase in the maximum elastance of the left ventricle, *ELVMAX*.

Tetralogy of Fallot. Tetralogy of Fallot (Figure 2B) is characterized by four anomalies: pulmonary stenosis, ventricular septal defect, overriding aorta, and right ventricular hypertrophy. The degree of right ventricular outflow obstruction is inversely proportional to pulmonary blood flow. The state equations for intrathoracic arterial, right ventricular, and left ventricular volumes were modified to include the new flow rates. Flow through the ventricular septal defect is bidirectional, whereas direction of flow through the overriding aorta is fixed by a valve. Flow rates through the pathologic shunts are represented mathematically by pressure differences divided by linear resistances. The new parameters *RVSD* and *ROA* reflect resistance to blood flow through the ventricular septum, and the overriding aorta, respectively. The effect of right ventricular dilation on diastolic pressure-volume characteristics is represented by a decrease in *ERVMIN*, and its effect on contractility by an increase in *ERVMAX*. A significant increase in right ventricular outflow resistance (*RRV*) reflects pulmonary stenosis.

Coarctation of the Aorta. Coarctation of the aorta is a vascular obstruction which causes decreased perfusion and pressure overload of the left ventricle. In the case of associated anomalies, such as a patent foramen ovale (PFO), the pressure overload will be transferred to the right ventricle, producing ventricular dilatation. A structural diagram representing this cardiac anomaly is shown in Figure 2C. The state equations of intrathoracic arterial, pulmonary arterial, right atrial, and left atrial volumes were modified to include the new flow rates through the PFO and PDA. Flow rate through the PFO is represented mathematically by a pressure differences divided by a linear resistance *RFO*. Flow rate through the PDA is represented mathematically as described above, with the new parameters *RDA* and *LDA*. Left ventricular obstruction is created by increasing *RLV*, and right ventricular dilation by a decrease in *ERVMIN* and an increase in *ERVMAX*.

Transposition of the Great Arteries. With transposition of the great arteries, the aorta arises from the right ventricle and the pulmonary artery from the left ventricle. This is one of the most common congenital heart lesions in the newborn and a frequent cause of death. Transposition often occurs along with other cardiac abnormalities, including septal defects, patent ductus arteriosus, and coarctation. Figure 2D shows the structural diagram of a transposition of the great arteries with a ventricular septal defect and patent foramen ovale. Because of the high flow entering in the right ventricle it develops dilatation and hypertrophy. In the model, flow rates from the left ventricle to the aorta and from the right ventricle to the

pulmonary arteries are eliminated. The state equations of intrathoracic arterial, pulmonary arterial, right and left atrial, and right and left ventricular volumes were modified to include new flow rates through the foramen ovale and the ventricular septal defect, and from the left ventricle to the pulmonary artery and the right ventricle to the aorta. Flow rates through the foramen ovale and the ventricular septal defect are represented mathematically by pressure differences over the linear resistances *RFO* and *RVSD*, respectively. The parameters *RTPA* and *RTA* represent the resistance to flow into the transposed vessels. Right ventricular dilation is created by changes in *ERVMIN* and *ERVMAX*.

Running the Model. Model equations were numerically integrated using the Euler forward method with a step size of 1 millisecond. All simulations were implemented in Microsoft Visual Java++ V6.0 on a personal computer with an 1800 MHz Pentium 4 processor. With the indicated integration step size, programming language, and hardware, the cardiovascular model runs 300 times faster than real-time.

The first model simulation results that we validated were systemic and pulmonary arterial systolic and diastolic blood pressures and cardiac output, at a heart rate fixed at 130 bpm. We also examined the model's pulsatile systemic arterial blood pressure waveform and a left ventricular pressure-volume loop. We then assessed the simulation model, including the model for the baroreflex, by reproducing an experiment which reduces total blood volume by 30% (corresponding to 93 mL)[23]. We also validated the simulated vital signs for the selected congenital defects. Our model of the baroreflex is formulated with respect to deviations of arterial blood pressure from equilibrium (see Appendix 1 of Goodwin et al.[2]). For simulation of the defects, a new operating point for the baroreflex was first established.

Results

Table 1 gives the target values and simulated neonatal vital signs. The standard deviation on the target vital signs represents deviation from the mean in measurements on a number of neonates. The baseline column of this table demonstrates that all simulated vital signs are within a standard deviation of the target vital signs, with the exception of the systolic pulmonary artery pressure (*SPAP*). Because simulated *SPAP* is close enough to the target values, and to avoid moving away from data from the literature underlying parameter values and consistency between other vital signs and targets, no attempt was made to change parameter values further to make *SPAP* match more closely. The pulsatile nature of the model is highlighted by the simulation results in Figure 3 (arterial blood pressure waveform) and Figure 4 (left ventricular pressure-volume loop).

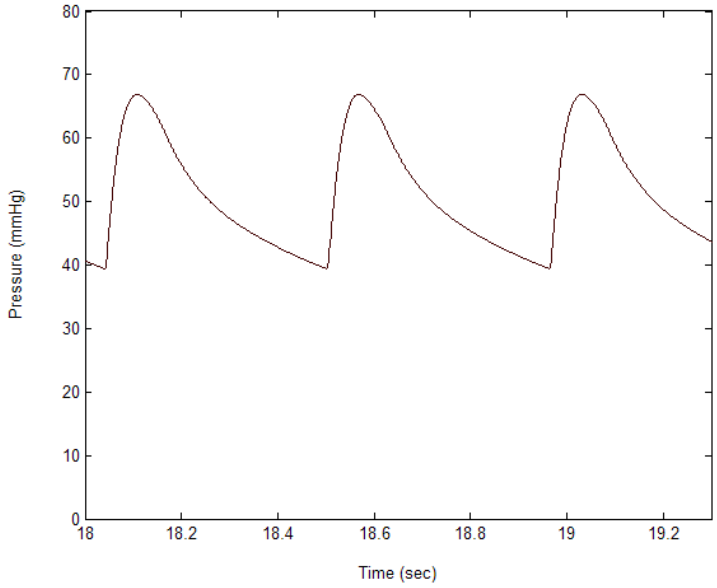

Figure 3. Simulated systemic arterial blood pressure.

Wallgren et al. observed that in their experiments, heart rate rose in a compensatory fashion from a mean of 130 to 170 bpm, and the systemic pressure dropped to dangerously low values, approximately half of normal[23]. As the last column in Table 1 shows, the simulated heart rate response to blood loss is realistic, albeit a little stronger than expected, and the simulated decrease in blood pressure is somewhat smaller than expected. Both observations correspond to a stronger than expected effect of the baroreflex. We maintained the referenced gain for reasons elaborated upon in the discussion.

Table 2 shows simulation results and target data for the selected pathologies. The model provided an overall realistic simulation of these abnormalities. The imbalance of systemic and pulmonary flow rates indicates the type of the shunt: left-to-right or right-to-left. The relatively low systemic and pulmonary diastolic pressures in the simulated PDA cannot be rejected based on a single reference patient, especially in view of realistic simulated mean pressures. The model correctly reflects that the majority of aortic blood flows through the ductus into the pulmonary artery and then through the lungs. A similar observation holds for the systemic diastolic pressure in the simulation of the coarctation with septal defects.

Discussion

We describe an existing simulation model and the derivation of a new parameter set representing the cardiovascular system of a normal 1-week-old neonate after term delivery.

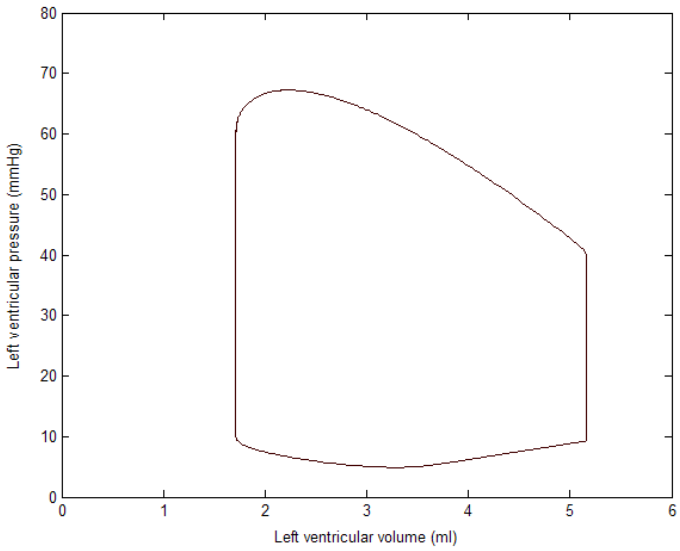

Figure 4. Simulated left ventricular pressure-volume loop.

All simplifying assumptions are explicitly described, making it possible to revisit selected empirical parameter estimation steps if more measured target and parameter data become available. Simulated vital signs were close to hemodynamic target values, and the system reacted appropriately to blood loss. A small discrepancy in systolic pulmonary artery pressure was noted. We do not believe this reflects a fundamental - even if minor - limitation to the model, but rather a small inconsistency in parameter data from different sources. The arterial pressure waveform and left ventricular pressure-volume curve are, in our opinion, realistic enough for educational simulations.

Our simulation of blood loss constitutes a deliberate, large amplitude disturbance, similar to pharmacological pressor-depressor evaluation studies of the baroreflex. The baroreflex gain we used was derived from spontaneous small variations. We maintained this gain for correct simulation of smaller perturbations. However, our simulation data suggest it may be necessary to include nonlinear saturations on baroreflex function to weaken it for larger amplitude disturbances.

Unlike in our previous study on the infant[(2)], simulation of the selected pathologies required sometimes extensive changes to model structure, mathematical formulation, and governing parameters. The anatomic model structure made it possible to implement these changes in a relatively intuitive and time-efficient manner. Simulation results for four congenital heart defects - patent ductus arteriosus, tetralogy of Fallot, coarctation of the aorta, and transposition of the great arteries with atrial and ventricular septal defects - compare favorably to target data and are considered realistic enough for educational simulations.

Our study forms a basis for model-driven educational simulation of neonatal cardiovascular pathophysiology. Expansion of this model with transport of oxygen and other respiratory gases should be relatively straightforward and might further enhance its potential educational impact. Linking the cardiovascular models with those for lung mechanics and pulmonary gas exchange could lead to a full-body, model-driven simulator[24] that would make possible fully immersive simulation of important aspects of challenging situations in neonatal intensive care or anesthesia.

Appendix
Numerical values for neonatal cardiovascular parameters

To facilitate reproducing simulation results by other investigators, this appendix provides in a compact format all neonatal model parameters and their numerical values. The web addendum to this paper provides a more extensive listing of these parameters. Symbols are as introduced in the main text or in Table 3 of Goodwin et al.[(2)]. Units are: resistances in $mmHg.mL^{-1}.s$, unstressed volumes in mL, elastances in $mmHg.mL^{-1}$, inertia in $mmHg.mL^{-1}.s^2$.

Cardiovascular model parameters for the baseline one week-old neonate: VTOTAL 310, HR 130, PTH -3.0, RLAIN 0.015, RLAOUT 0.06, ELAMIN 3.5, ELAMAX 3.72, VLAU 0.25, RLV 0.018, ELVMIN 2.63, ELVMAX 53.1, VLVU 0.5, EITHA 13.64, VITHAU 9.16, LETHA 0.0018, RETHA 1.5, EETHA 5.8, VETHAU 24.20, RSP 4.2, RETHV 0.21, EETHV 0.25, VETHVU 65.4, EITHV 0.5, VITHVU 77.83, RRAIN 0.015, RRAOUT 0.06, ERAMIN 2.26, ERAMAX 10.1, VRAU 0.25, RRV 0.018, ERVMIN 2.62, ERVMAX 34.38, VRVU 0.33, EPA 10.95, VPAU 3.27, RPP 0.85, EPV 0.48, VPVU 22.89.

Relative gains for simulation of the neonatal baroreflex: heart period: $3.2\%.mmHg^{-1}$, contractility: $-0.64\%.mmHg^{-1}$, total peripheral resistance: $-3.78\%.mmHg^{-1}$, venous unstressed volume: $1.98\%.mmHg^{-1}$.

Pathology specific parameters. For patent ductus arteriosus: ELVMAX 106, ELVMIN 1.75, RDA 0.5, and LDA 0.0018. For tetralogy of Fallot: ERVMAX 51.6, ERVMIN 1.75, RRV 3.6, RVSD 0.5, ROA 0.05. For coarctation of the aorta: RLV 0.36, RDA 0.9, LDA 0.0018, RFO 0.5, ERVMAX 114, ERVMIN 1.31. For transposition of the great arteries: RTPA 0.5, RTA 0.05, RVSD 0.1, RFO 0.5, ERVMAX 85.95, ERVMIN 1.31.

Addendum
Parameter estimation for neonatal cardiovascular physiology

Heart chambers. No data could be found in the literature for the unstressed volumes of the heart chambers in the neonate. The unstressed volume of the left ventricle (*VLVU*) was set to 0.5 mL, an arbitrary value between zero and the end systolic volume (*ESV*) of 1.73 mL, Table Ad1. Unstressed volumes for the right ventricle, and left and right atria (*VRVU*, *VLAU*, and *VRAU*, respectively) were proportionally reduced from adult values by comparison to the left ventricle. The average intrathoracic pressure was assumed equal to -3.0 mmHg, similar to the infant value[14]. Using these values, end-systolic and end-diastolic pressures from Table Ad1, and equations (A7) and (A8) in Goodwin et al.[2], the minimum and maximum elastances for the left and right ventricles (*ELVMIN*, *ELVMAX*, *ERVMIN*, and *ERVMAX*, respectively) were calculated. Minimum and maximum elastances for the left and right atria (*ELAMIN*, *ELAMAX*, *ERAMIN*, and *ERAMAX*, respectively) were proportionally increased from the adult values by comparison to the ventricles. All parameter values are listed in Table Ad2.

Blood volumes. Neonatal unstressed volumes of the intra- and extrathoracic arteries and veins, and pulmonary arteries and veins (*VITHAU*, *VETHAU*, *VETHVU*, *VITHVU*, *VPAU*, and *VPVU*) respectively were proportionally decreased from adult values, considering a total neonatal blood volume of 88.4 $mL.kg^{-1}$[15] and a neonatal weight of 3500 g.

Resistances. Total systemic resistance (SVR), with a value taken from the range indicated in Table Ad1, was distributed over extrathoracic arteries, peripheral vessels,

Table Ad1. Clinical variables describing left and right ventricular function and global descriptions of the systemic and pulmonary circulation of an approximately 1-week-old neonate.

			Value	Reference
Heart	Left ventricle	EDV	3.54 mL	(11)
		EDP	5 mmHg	(12)
		ESV	1.73 mL	(11)
		ESP	62.3 mmHg	(11)
	Right ventricle	EDV	2.62 mL	(13)
		EDP	3 mmHg	(12)
		ESV	1.29 mL	(13)
		ESP	30 mmHg	(12)
Circulation		SVR	4.5-6 $mmHg.mL^{-1}.s$	(12)
		PVR	0.75-0.9 $mmHg.mL^{-1}.s$	(12)

EDV, end diastolic volume; EDP, end diastolic pressure; ESV, end systolic volume; ESP, end systolic pressure; SVR, systemic vascular resistance; PVR, pulmonary vascular resistance.

Table Ad2. Cardiovascular parameters for adult and neonate.

Part of circulation	Compartment	Parameter description	Parameter name	Parameter values	
				Adult	Neonate
Total circulation	All	Initial total blood volume	VTOTAL	4740	310
Heart	Atria and ventricles	Heart rate	HR	72.0	130
Intrathoracic	All intrathoracic	Average intrathoracic pressure	PTH	-4.00	-3.0
Left heart	Left atrium	Resistance to forward flow	RLAIN	0.00300	0.01500
		Mitral valve resistance	RLAOUT	0.00300	0.0600
		Diastolic elastance	ELAMIN	0.120	3.50
		Maximum systolic elastance	ELAMAX	0.280	3.72
		Unstressed volume	VLAU	30.0	0.250
	Left ventricle	Aortic valve and intrathoracic artery resistance	RLV	0.00800	0.0180
		Diastolic elastance	ELVMIN	0.0900	2.63
		Maximum systolic elastance	ELVMAX	4.00	53.1
		Unstressed volume	VLVU	60.0	0.500
Systemic circulation	Intrathoracic arteries	Elastance	EITHA	1.43	13.6
		Unstressed volume	VITHAU	140	9.16
	Extrathoracic arteries	Blood flow inertia	LETHA	0.000700	0.00180
		Resistance	RETHA	0.0600	1.50
		Elastance	EETHA	0.556	5.80
		Unstressed volume	VETHAU	370	24.2
	Peripheral vessels	Resistance	RSP	1.00	4.20
	Extrathoracic veins	Resistance (to forward flow)	RETHV	0.0900	0.210
		Elastance	EETHV	0.0169	0.250
		Unstressed volume	VETHVU	1000	65.4
	Intrathoracic veins	Elastance	EITHV	0.0182	0.500
		Unstressed volume	VITHVU	1190	77.8
Right heart	Right atrium	Resistance to forward flow	RRAIN	0.00300	0.0150
		Tricuspid valve resistance	RRAOUT	0.00300	0.0600
		Diastolic elastance	ERAMIN	0.0500	2.26
		Maximum systolic elastance	ERAMAX	0.150	10.1
		Unstressed volume	VRAU	30.0	0.250
	Right ventricle	Pulmonary artery resistance	RRV	0.00300	0.0180
		Diastolic elastance	ERVMIN	0.0570	2.62
		Maximum systolic elastance	ERVMAX	0.490	34.4
		Unstressed volume	VRVU	40.0	0.330
Pulmonary circulation	Pulmonary arteries	Elastance	EPA	0.233	10.9
		Unstressed volume	VPAU	50.0	3.27
	Peripheral vessels	Resistance	RPP	0.110	0.850
	Pulmonary veins	Elastance	EPV	0.0455	0.480
		Unstressed volume	VPVU	350	22.9

Units: heart rate, min^{-1}; resistances, $mmHg.mL^{-1}.s$; elastances, $mmHg.mL^{-1}$; volumes, mL; inertia, $mmHg.mL^{-1}.s^2$

extrathoracic veins, and right atrium inflow (*RETHA*, *RSP*, *RETHV*, and *RRAIN*, respectively) in such way that a realistically shaped arterial pressure waveform was obtained. Total

pulmonary resistance (PVR), also with a value taken from the range indicated in Table Ad1, was distributed over peripheral vessels and left atrium inflow (*RPP*, and *RLAIN*, respectively) considering *RLAIN=RRAIN*. Heart valve resistances (*RLAOUT*, *RLV*, *RRAOUT*, and *RRV*, respectively) are assumed equal to those of a full-term fetus as used by Huikenshoven et al.[16].

Elastances and inertia. Elastances of the extra- and intrathoracic veins (*EETHV* and *EITHV*, respectively) are again assumed equal to those of a full-term fetus[16]. Intrathoracic systemic arterial (*EITHA*) and pulmonary arterial and venous elastances (*EPA*, and *EPV*, respectively) were calculated using the pressure-volume relationship, equation (A5) in Goodwin et al.[2] based on pressure values reported in literature[12], (stressed) compartment volumes which are proportionally decreased from adult values, and the unstressed volumes calculated before. Extrathoracic arterial elastance (*EETHA*) was proportionally increased from the adult value by comparison to *EITHA*. The inertia value used by Huikeshoven et al. refers to the ductus arteriosus[16]. We use this value for the inertia of blood in the extrathoracic arteries (*LETHA*).

Table Ad3. New parameters for selected congenital heart defects.

Disease	Part of circulation	Parameter description	Parameter name	Parameter value
Patent ductus arteriosus	Left ventricle	Maximum systolic elastance	ELVMAX	106
		Diastolic elastance	ELVMIN	1.75
	Patent ductus arteriosus	Resistance	RDA	0.5
		Inertia	LDA	0.0018
Tetralogy of Fallot	Right ventricle	Maximum systolic elastance	ERVMAX	51.6
		Diastolic elastance	ERVMIN	1.75
		Outflow resistance	RRV	3.6
	Ventricular septal defect	Resistance	RVSD	0.5
	Overriding aorta	Resistance	ROA	0.05
Coarctation of the aorta	Left ventricle	Resistance	RLV	0.36
	Patent ductus arteriosus	Resistance	RDA	0.9
		Inertia	LDA	0.0018
	Foramen ovale	Resistance	RFO	0.5
	Right ventricle	Maximum systolic elastance	ERVMAX	114
		Diastolic elastance	ERVMIN	1.31
Transposition of the great arteries	Transposition of the pulmonary artery	Resistance	RTPA	0.5
	Transposition of the aorta	Resistance	RTA	0.05
	Ventricular septal defect	Resistance	RVSD	0.1
	Foramen ovale	Resistance	RFO	0.5
	Right ventricle	Maximum systolic elastance	ERVMAX	85.9
		Diastolic elastance	ERVMIN	1.31

Units: resistances, $mmHg.mL^{-1}.s$; elastances, $mmHg.mL^{-1}$; inertia, $mmHg.ml^{-1}.s^{2}$.

Baroreflex. The parameters for the baroreflex were derived from published data presented by Andriessen et al.[18]. They observed a spontaneous baroreflex sensitivity in term neonates of 15 ms.mmHg^{-1}. At a heart period of 462 ms (heart rate of 130 bpm) this corresponds to a relative baroreflex gain for heart period of 3.2 %.mmHg^{-1}. Table 4 in Goodwin et al.[2] presents relative gains for the adult baroreflex, computed from baseline values of the Beneken model[3] and data presented by Ten Voorde[17]. With respect to the adult value, 3.2 %.mmHg^{-1} represents an increase of a factor of 1.61. The other relative gains for the neonatal baroreflex were proportionally increased from adult values by comparison to the heart period gain, leading to -0.64 %.mmHg^{-1} for the maximum elastance of the left ventricle (contractility), -3.78 %.mmHg^{-1} for total peripheral resistance, and 1.98 %.mmHg^{-1} for venous unstressed volume.

Congenital heart defects. Table Ad3 lists the new parameters for selected congenital heart defects. Derivation of these parameter values is described in the main text.

References

1. Halamek LP, Kaegi DM, Gaba DM, et al. Time for a new paradigm in pediatric medical education: teaching neonatal resuscitation in a simulated delivery room environment. Pediatrics. 2000; 106:E45.

2. Goodwin JA, van Meurs WL, Sá Couto, CD, Beneken JEW, Graves SA. A model for educational simulation of infant cardiovascular physiology. Anesth Analg. 2004; 99:1655-1664.

3. Beneken JEW. A mathematical approach to cardiovascular function. The uncontrolled human system [thesis]. The Netherlands: University of Utrecht, 1965.

4. Wesseling KH, Settels JJ. Baromodulation explains short-term blood pressure variability. In Orlebeke JF, Mulder G, van Doornen LJP (eds). Psychophysiology of Cardiovascular Control. New York: Plenum Press, 1985.

5. Beneken JEW, DeWit B. A physical approach to hemodynamic aspects of the human cardiovascular system. In Reeve EB, Guyton AC (eds). Physical Bases of Circulatory Transport: Regulation and Exchange. Philadelphia: Saunders, 1967.

6. Suga H, Sagawa K, Shoukas AA. Load independence of the instantaneous pressure-volume ratio of the canine left ventricle and effects of epinephrine and heart rate on the ratio. Circ Res. 1973;2:314–322.

7. Pennati G, Bellotti M, Fumero R. Mathematical modeling of the human foetal cardiovascular system based on Dopler ultrasound data. Med Eng Phys. 1997;19:327–335.

8. Tan KL. Blood pressure in full-term healthy neonates, Clin Pediatr. 1987;26:21–24.

9. Emmanouilides GC, Moss AJ, Duffie ER, Adams FH. Pulmonary arterial pressure changes in human newborn infants from birth to 3 days of age. J Pediatr. 1964;65:327–333.

10. Prec KJ, Cassels DE. Dye dilution curves and cardiac output in newborn infants. Circulation. 1955; 11:789–798.

11. Takahashi Y, Harada K, Ishida A, et al. Changes in left ventricular volume and systolic function before and after the closure of ductus arteriosus in full-term infants. Early Hum Dev. 1996; 44:77–85.

12. Klaus MH, Fanaroff AA. Care of the High-Risk. 5th Ed. Philadelphia: W.B. Saunders, 2001.

13. Tamura M, Harada K, Ito T, et al. Changes in right ventricular volume in early human neonates. Early Hum Dev. 1997; 48:1–9.

14. Cunningham MD. Bedside pulmonary function testing of infants. In Levin DL, Morriss FC (eds). Essentials of Pediatric Intensive Care. St. Louis: Churchill Livingstone, 1990.

15. Rawlings JS, Pettett G, Wiswell TE, Clapper J. Estimated blood volume in polycythemic neonates as a function of birth weight. J Pediatr. 1982; 101:594–599.

16. Huikeshoven F, Coleman TG, Jongsma HW. Mathematical model of the fetal cardiovascular system: the uncontrolled case. Am J Physiol. 1980; 239:R317–R325.

17. Ten Voorde B. Modeling the baroreflex, a system analysis approach [thesis]. The Netherlands: Free University of Amsterdam, 1992.

18. Andriessen P, Bambang Oetomo S, Peters C, et al. Baroreceptor reflex sensitivity in human neonates: the effect of postmenstrual age. J Physiol. 2005;568:333–341.

19. Avery GB, Fletcher MA, MacDonald MG. Neonatology: Pathophysiology and Management of the Newborn. 5th Ed. Philadelphia: Lippincott Williams & Wilkins, 1999.

20. Hartman AF Jr., Goldring D, Staple TW. Coarctation of the aorta in infancy: Hemodynamic studies. J Pediatr. 1967;70:95–104.

21. Shaher RM. The haemodynamics of complete transposition of the great vessels. Br Heart J. 1964;26:343–353.

22. Huikeshoven F, Jongsma HW. Cardiovascular changes due to premature closure of the ductus arteriosus: a mathematical model. Eur J Obstet Gynec Reprod Biol. 1985;20:305–310.

23. Wallgren G, Hanson JS, Tabakin BS, et al. Quantitative studies of the human neonatal circulation – V - Hemodynamic findings in premature infants with and without respiratory distress. Acta Paediatr Scand Suppl. 1967;179:71.

24. Van Meurs WL, Good ML, Lampotang S. Functional anatomy of full-scale patient simulators. J Clin Monit. 1997;13:317–324.

Acknowledgements

Comments by reviewers lead to improved simulation results for tetralogy of Fallot. By the time of first submission of this manuscript, Beatriz Sá Couto was a healthy 1-week old.

Chapter 5

Corrected and improved model for educational simulation of neonatal cardiovascular pathophysiology

Zijlmans M, Sá Couto CD, van Meurs WL, Goodwin JA, Andriessen P

Simul Healthc 2009;4(1):49-53

Abstract

We identified errors in the software implementation of the mathematical model presented in: Sá Couto CD, van Meurs WL, Goodwin JA, Andriessen P. A model for educational simulation of neonatal cardiovascular pathophysiology. Simul Healthcare 2006;1:4-12. Simulation results obtained with corrected code are presented for future reference. All but one of the simulation results do not differ by more than 9% from the previously published results. The heart rate response to acute loss of 30% of blood volume, simulated with corrected code is stronger than published target data. This modeling error was masked by errors in code implementation. We improved this response and the model by adjusting the gains and adding thresholds and saturations in the baroreflex model. General considerations on identification of model and code errors and model validity are presented.

Keywords*: Erratum, Verification, Validation, Mathematical model, Simulation, Neonate, Cardiovascular physiology, Baroreflex, Congenital heart defect.*

Introduction

In Sá Couto et al.[1] we presented a conceptual and corresponding mathematical model of the cardiovascular system of a healthy 1-week-old neonate and adapted this model to reflect selected congenital heart defects. Simulation results were obtained with a software implementation in Microsoft Java++ V6.0.

Recently we had the opportunity to double check the model derivation and simulation results when re-implementing the model. No errors were found in model equations, but we identified and corrected the following errors in the software implementation used by Sá Couto et al.[1]:

- The wrong variable was used for the pressure input to the baroreflex model.
- The heart period (HP) gain of the baroreflex was used to update heart rate.

Moreover, in code used for the simulation of the pathologies, we found the following errors:

- Transmural vascular pressure was reported, rather than absolute pressure.
- The numerical value of one of the contractility parameters was incorrect.
- The model allowed for unidirectional rather than bidirectional flow in two of the pathologies.

Simulation results obtained with corrected code match target data, with the exception of the response to acute loss of 30% of blood volume. This stimulated us to further investigate and adapt the model. The proposed changes to the model are:

- A small change in baseline heart rate.
- A lower baroreflex gain.
- Inclusion of thresholds and saturations on HP and other baroreflex control effectors.

Corresponding changes were included in the code implementation. Comparison of simulation results with target data will allow us to determine if the model is improved. In the next two sections, we describe code errors and corrections and model changes and validation in detail. In the discussion section, we elaborate on the broader questions raised by the detection and correction of these errors.

Corrections

Baroreflex. In the original software implementation, the mean arterial pressure (MAP) input to the baroreflex model was taken from the extrathoracic arteries compartment,

rather than from the intrathoracic arteries compartment. Despite compartment names suggesting anatomic interpretability, this is inconsistent with our interpretation that the underlying Beneken model[2,3] represents the arterial tree with two compartments, generating a single arterial pressure variable represented by the pressure in the intrathoracic compartment. In the discussion section we will elaborate on this choice.

The addendum to Sá Couto et al.[1] lists relative gains for HP and other baroreflex control effectors (in $\%.mmHg^{-1}$) in the operating point. In the original software implementation the HP gain was used to update heart rate. Because of the relative nature of the gains, this second error does not result in a difference when staying close to the pressure-heart rate operating point, but it is expected to affect simulation results for larger disturbances to the system, such as the simulated loss of 30% of blood volume.

Table 1 lists simulated neonatal vital signs at baseline and following loss of 30% of blood volume, comparing the previously obtained values to those obtained with the corrected software implementation. As expected, simulated baseline vital signs are the same as in Table 1 of Sá Couto et al.[1]. The code correction has considerable effect on the simulated heart rate response to the loss of blood volume. With the original code we obtained an increase of 45 beats per minute (bpm) from the 130 bpm baseline and with the corrected code an increase of 73 bpm. We also observe a moderate increase in systemic arterial pressure (4 mmHg) and a small increase in pulmonary arterial diastolic pressure (1 mmHg) between software implementations. Simulated cardiac output increases from 252 to 281 $mL.min^{-1}$. In this table as in the next, our purpose is to evaluate the effect of code corrections on simulation results. In the next section we will compare the obtained response to loss of blood volume to target data and describe an improvement of this response.

Pathologies. Table 2 of Sá Couto et al.[1] presents simulated vital signs for selected congenital heart defects. For all pathologies the output variables mean systemic and pulmonary pressures were calculated based on transmural rather than absolute pressures. This

Table 1. Simulated cardiovascular vital signs for an approximately 1-week-old neonate.

	Previous Simulation Results		**Corrected Simulation Results**	
Variable	Baseline	Loss of 30% of blood volume	Baseline	Loss of 30% of blood volume
Heart rate (min^{-1})	130	175	130	203
Systemic systolic pressure (mmHg)	68	43	68	47
Systemic diastolic pressure (mmHg)	40	31	40	35
Pulmonary systolic pressure (mmHg)	29	12	29	12
Pulmonary diastolic pressure (mmHg)	10	3	10	4
Cardiac output ($mL.min^{-1}$)	455	252	455	281

was corrected by adding the intrathoracic pressure (*PTH=-3 mmHg*) to the output variables.

Furthermore, for Tetralogy of Fallot the parameter that governs contractility of the right ventricle, the maximum systolic elastance *ERVMAX*, was assigned the value 34.4 $mmHg.mL^{-1}$, rather than the published 51.6 $mmHg.mL^{-1}$. Coarctation of the aorta was simulated with unidirectional rather than bidirectional flow in the patent ductus arteriosus and in the foramen ovale. Note that for this pathology, for consistency with the target data, the reported mean systemic pressure refers to the extrathoracic compartment.

Table 2 presents simulation results obtained with a corrected code implementation. The corrected blood pressures differ at most 6mmHg from the previously published results. See the original article for a comparison of those results to referenced target data. Although these corrections are not expected to have clinical educational impact, we include them here for future reference, especially for those investigators trying to reproduce our simulation results.

Table 2. Simulated cardiovascular vital signs for selected congenital heart diseases.

	Patent Ductus Arteriosus		**Tetralogy of Fallot**		**Coarctation of the Aorta**		**Transposition of the Great Arteries**	
Variable	Previous simulation results	Corrected simulation results	Previous simulation results	Corrected simulation results	Previous simulation results	Corrected simulation results	Previous simulation results	Corrected simulation results
Heart rate (min^{-1})	130	130	130	130	130	130	130	130
Left ventricular systolic pressure (mmHg)	72	72	85	87	70	76	74	74
Left ventricular diastolic pressure (mmHg)	4	4	3	3	7	7	4	4
Systemic systolic pressure (mmHg)	70	70	85	87	57	59	74	74
Systemic diastolic pressure (mmHg)	20	20	47	49	20	20	40	40
Mean systemic pressure (mmHg)	40	37	65	64	26*	27*	54	52
Right ventricular systolic pressure (mmHg)	52	52	85	87	56	53	75	75
Right ventricular diastolic pressure (mmHg)	3	3	3	2	0	0	1	1
Pulmonary systolic pressure (mmHg)	51	51	18	19	55	52	44	44
Pulmonary diastolic pressure (mmHg)	18	18	7	7	16	16	9	9
Mean pulmonary pressure (mmHg)	33	30	15	12	32	29	24	21
Cardiac output - systemic ($mL.min^{-1}$)	316	316	548	571	264	277	900	903
Cardiac output - pulmonary ($mL.min^{-1}$)	1125	1123	360	370	1186	1168	450	451

* Refers to pressure in the extrathoracic compartment.

Improvements

Baseline Heart Rate. Table 1 of Sá Couto et al.[1] presents a mean target heart rate of 135 bpm at baseline, but a heart rate of 130 bpm is used in the unperturbed system simulations. Because the baroreflex is modeled as perturbations around an operating point, we can set this parameter independently.

Setting the baseline heart rate to 135 bpm results in simulated vital signs that are identical to previous results or slightly closer to the target data. The effect of the small heart rate increase at baseline on simulated pressures for the pathologies is of the order of 1 mmHg or less.

Baroreflex Model. The baroreflex model governs the effect of MAP on HP, contractility, total peripheral resistance, and venous unstressed volume. In our discussion below, we will focus on the MAP-HP relationship, and refer to Goodwin et al.[2] and the addendum to Sá Couto et al.[1] for a more detailed discussion of the other control effectors. The model of the MAP-HP characteristic is a linear segment going through the operating point $(MAP_0, HP_0)=(51.7\ mmHg, 462\ ms)$ with a slope equal to the MAP-HP gain. For this gain, we used the upper limit of the range of 10–15 $ms.mmHg^{-1}$ as specified by Andriessen et al.[4]. As presented above, the code corrections significantly increase the simulated heart rate response to loss of blood volume (Table 1, last column). Setting baseline heart rate to 135 bpm results in a new operating point $(MAP_0, HP_0) = (53.0\ mmHg, 444\ ms)$. Table 3 presents

Table 3. Target data and simulation results at baseline and after loss of 30% of blood volume in a 1-week-old neonate.

Variable	Target data Wallgren et al.[6]	Simulation results		
		Corrected code and HR_0=135	+ Lower Gains	+ MAP threshold and saturation
Heart rate (min^{-1})	130 → 169♦ (+30 %)	135 → 214 (+59 %)	135 → 203 (+50 %)	135 → 177 (+31 %)
Systemic systolic pressure (mmHg)	79 → 38† (-52 %)	69 → 48 (-30 %)	69 → 44 (-36 %)	69 → 33 (-52 %)
Systemic diastolic pressure (mmHg)	54 → 23† (-57 %)	41 → 37 (-10 %)	41 → 33 (-20 %)	41 → 23 (-44 %)
Pulmonary systolic pressure (mmHg)	--	--	--	29 → 9
Pulmonary diastolic pressure (mmHg)	--	--	--	10 → 2
Cardiac output ($mL.min^{-1}$)	--	--	--	469 → 216

* Values obtained from 12 cases
† Values obtained from 3 cases

target data and corrected simulation results with a baseline heart rate of 135 bpm. Comparing the second column of Table 3 with the last column of Table 1 shows that changing the baseline heart rate does not have a significant additional effect on the heart rate response to loss of blood volume. Comparing these simulation results to the target data confirms that the simulated heart rate and systemic arterial blood pressure responses to loss of blood volume require adjustment.

To improve the simulation results, we first set the gain in the operating point to the lower limit of the range specified by Andriessen et al.[4] (10 ms.mmHg^{-1}), which corresponds to a relative HP gain of 2.25 %.mmHg^{-1}. The relative gains for the other control effectors were rescaled proportionally to: -0.45 %.mmHg^{-1} for contractility, -2.66 %.mmHg^{-1} for total peripheral resistance, and 1.39 %.mmHg^{-1} for venous unstressed volume. The simulation results (Table 3, third column) improve after lowering the gains, but are not yet considered satisfactory.

To further improve the response to loss of blood volume, basic nonlinear aspects of the MAP-control effector characteristic are included in the model. Figure 1 shows a piece-wise linear approximation of the MAP-HP characteristic. Values for the MAP threshold and saturation are determined as follows. Segar et al.[5] report MAP-HR characteristics for 11 day old newborn lambs. The curve reported by these authors can also be approximated by a piece-wise linear function. When the slope of this approximation is made equal to the baroreflex HR gain in the operating point, and the minimum and maximum heart rates are maintained, we obtain a piece-wise linear approximation with a mean arterial pressure threshold (MAP_{thr}) of 60 mmHg and a mean arterial pressure saturation (MAP_{sat}) of 92 mmHg. Note that threshold and saturation also apply to the MAP-HP characteristic. MAP_{thr} and MAP_{sat} are then scaled to

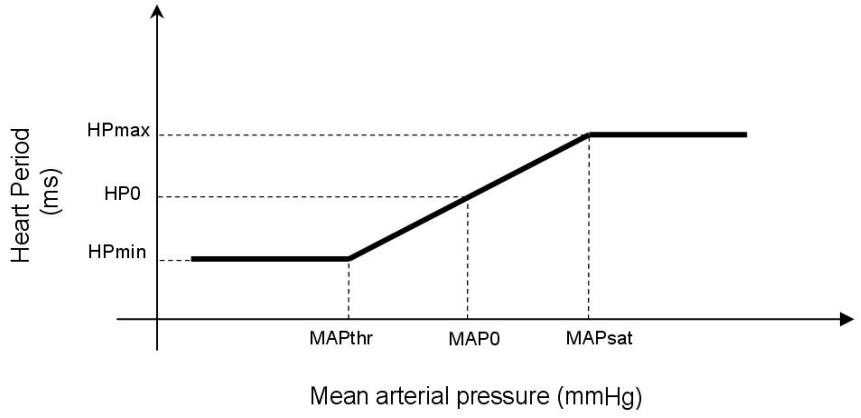

Figure 1. Piece-wise linear model of mean arterial pressure (MAP) - heart period (HP) characteristics.

human neonates by multiplication with $MAP_0human/MAP_0lamb=53/75$, resulting in MAP_{thr}= *42.4 mmHg* and MAP_{sat}*=65.0 mmHg*. The corresponding HP_{min} and HP_{max} are 338 and 564 ms, respectively. The same MAP threshold and saturation were applied to the other MAP – control effector characteristics. The last column in Table 3 presents simulation results after including a MAP threshold and saturation. The simulated heart rate and blood pressure responses to loss of 30% of blood volume closely match the target data, especially when considering relative changes. For future reference, we also include simulation results for pulmonary pressure and cardiac output of the resulting model.

Discussion

Corrections. Neither Sá Couto et al.[1] nor Goodwin et al.[2] explicitly state if the MAP input to the baroreflex model is taken from the intrathoracic or extrathoracic arteries compartment. Both model code implementations used the pressure from the extrathoracic compartment. This is consistent with the anatomic observation that the main baroreceptors are located in the carotid bodies, hence extrathoracically. However, it is inconsistent with our interpretation that the Beneken model[2,3] represents the arterial tree with two compartments, generating a single arterial pressure output represented by the pressure in the "intrathoracic arteries" compartment. This interpretation underlies the absence of explicit reference to intrathoracic or extrathoracic compartment for the choice of pressure input to the baroreflex model. It also underlies the comment in Goodwin et al.[2] (p1663) that: "The blood flow inertia parameter was adjusted to optimize the pressure wave form in the intrathoracic arteries compartment. Note that when this parameter is used in such an empirical fashion, it should no longer be referred to in terms of underlying physics." In all but one of the simulation experiments presented here, systemic arterial pressure, as a monitored signal or as an output to the baroreflex, was taken from the intrathoracic compartment. The single exception is the mean systemic pressure of Coarctation of the aorta, which for consistency with the original article and the target data was taken in the extrathoracic compartment. More in-depth consideration of modeling of the aorta and arterial tree could further complement this discussion, but is considered beyond the scope of this technical report.

The correction with the biggest quantitative effect on simulation results was the use of the baroreflex gain to change HP rather than heart rate. This change in the baroreflex model did not affect simulation results in the operating point (baseline simulations and pathology simulations). Simulation results did confirm the considerable effect on the response to loss of 30% of blood volume (Table 1) stimulating further analysis and adaptation of the model.

Table 2 shows the corrected simulation results for the pathologies. Although the clinical impact of such corrections is marginal, we presented these results here for future reference.

Improvements. The first improvement was an increase in the baseline heart rate from 130 to 135 bpm. This minor change makes the baseline heart rate consistent with the (baseline) target data presented in Sá Couto et al.[1], and slightly improves simulated pressures and cardiac output. Note that the baseline of the target data for the response to loss of 30% of blood volume (again) has a heart rate of 130 bpm.

Taking the corrected code as a basis and including the baseline heart rate update, we then reduced the baroreflex gain to the minimum of a published range and included a carefully derived threshold and saturation on the effect of MAP on heart rate, contractility, peripheral resistance, and venous unstressed volume. For the combined adaptations, simulated heart rate and blood pressure responses to loss of blood volume closely match the target data presented by Wallgren et al.[6] (Table 3), especially when considering the relative changes.

Independent clinical experts expressed hesitation concerning the relative small increase in target heart rate and low target diastolic blood pressure after loss of blood volume. We note that the blood pressure data are based on three patients only. As human target data for such experiments are very rare, we decided to continue to refer to these limited available data.

Lessons learned. Prompted by constructive editorial and reviewer comments, we asked ourselves why this error happened, what its consequences could have been, had it slipped through undetected, and what authors can do to avoid such errors occurring in the future.

It is standard procedure in our physiologic modeling team for a second author to independently check the model and software used to obtain simulation results. Checks on the model focus on consistent derivation and formulation of mathematical equations and correct units and numerical values of model parameters. Checks on software implementation focus on correct implementation of model equations and verification of the numerical integration method. The author responsible for these checks on Sá Couto et al.[1] was Dr. van Meurs. In the case of Sá Couto et al.[1], this procedure was not fully applied for the following very particular reasons. As pointed to in our acknowledgments, the first author delivered her first child 1 week after completing the first submission. Dr. van Meurs, therefore, took over corresponding author responsibilities and did not take the necessary time to check the code written by the first author. We further note considerable time pressure to get this article ready for the very first issue of the journal. The error in software implementation was detected when

a new trainee in our team, and first author of this technical report: Mariken Zijlmans, programmed the model equations in a new implementation.

As model developers we frequently encounter errors and/or omissions in physiologic modeling publications, even those by well respected authors in high level journals. An error in model equations or units of parameter values can usually be detected, but often only after a considerable amount of experimentation and searching. In our experience, errors in numerical values or in software underlying simulation results are almost impossible to confirm with certainty, especially if the publications are older. A first consequence is therefore loss of time and sometimes rejection of an article as a reference for further modeling work. This constitutes a strong motivation to avoid such errors in our own articles. Other consequences of undetected modeling errors depend on the application area. The main purpose of models of human physiology and pharmacology in the simulation engine of a medical educational simulator is to provide real-time, automatic, realistic, and consistent evolution of clinical signs and monitored signals, and of their response to therapeutic interventions. A second purpose is to provide a representation of the (patho)physiology of the simulated patient that can be manipulated in a logical fashion to simulate pathologies or critical incidents. An unrealistic physiologic model response in an educational simulator may lead to reduced suspension of disbelief in the trainee or, worse, negative teaching: The trainee may come to expect real patients to behave as the simulated patient, and be confused if they do not. A minimum requirement for physiologic models for use in educational simulation is therefore that they reflect at least a plausible patient, within normal interpatient variability. Unrealistic model responses could also lead to less confidence in, and less use of, the automatic response of the simulation engine by the simulator facilitator, thereby reducing the time that can be dedicated to other aspects of the simulation process.

In our experience, the procedure as outlined above is adequate for detecting most modeling and software implementation errors. Specialized reviewers could possibly detect errors in mathematical equations but, in our opinion, authors remain responsible for checking correct code implementation.

A broader question that includes detecting errors in the mathematical formulation of a physiologic model and in its software implementation, but that at the same time surpasses these issues, is that of model validity. In the context of this technical report, we will only discuss this fundamental issue briefly. Models gain validity when assumptions underlying structure and parameter values are “reasonable” and when simulated model responses match target data for the same condition. We contribute to the first type of validity by explicitly stating all assumptions on model structure and derivation of numerical values of parameters. Concerning target data, developers of physiologic models for educational simulation face the

paradox that the highly critical situations that are most interesting to simulate from an educational point of view are also the least likely to have published studies on such events in controlled conditions in human patients. To find published data on significant loss of blood volume in human neonates we had to search far back in the literature. Alternative validation strategies involve obtaining animal data and rescaling to human patients, and submitting simulation results to expert opinion. How much should be done by model developers and how much by journal editors, educational simulator manufacturers, or simulator users is an open question. As model developers and authors, our goal is again to contribute to validity by carefully describing our assumptions, target data, and simulation experiments.

Conclusion

We made corrections to the code implementation of a model for educational simulation of neonatal cardiovascular pathophysiology and presented the effect on simulation results. One of the corrections led to a significant change in the simulated response to loss of blood volume. Based on further analysis we adapted the baroreflex model and demonstrated that this leads to a closer match between simulation results and target data. We believe that the consistent, explicit definition of the presented model facilitates reproduction and validation of simulation results, and thereby sustains the intended educational application.

References

1. Sá Couto CD, van Meurs WL, Goodwin JA, Andriessen P. A model for educational simulation of neonatal cardiovascular pathophysiology. Simul Healthc 2006;1:4 –12.

2. Goodwin JA, van Meurs WL, Sá Couto CD, Beneken JEW, Graves SA. A model for educational simulation of infant cardiovascular physiology. Anesth Analg 2004;99:1655–1664.

3. Beneken JEW. A mathematical approach to cardiovascular function. The uncontrolled human system [thesis]. The Netherlands: University of Utrecht, 1965.

4. Andriessen P, Bambang Oetomo S, Peters C, Vermeulen B, Wijn PFF, Blanco CE. Baroreceptor reflex sensitivity in human neonates: the effect of postmenstrual age. J Physiol 2005;568:333–341.

5. Segar JL, Roghair RD, Segar EM, Bailey MC, Scholz TD, Lamb FS. Early gestation dexamethasone alters baroreflex and vascular responses in newborn lambs before hypertension. Am J Physiol Regul Integr Comp Physiol 2006;291:R481–R488.

6. Wallgren G, Barr M, Rudhe U. Hemodynamic studies of induced acute hypo- and hypervolemia in the newborn infant. Acta Paediatr 1964;53: 1–12.

Acknowledgements

Discussions with Medical Education Technologies, Inc., physiologic modelers Hugo Azevedo and Nishant Gopalakrishnan contributed to the presented verification procedure.

Funding

This work was supported, in part, by NUFFIC (Netherlands organization for international cooperation in higher education), Den Haag, The Netherlands and the Instituto de Engenharia Biomédica, University of Porto, Porto, Portugal.

Chapter 6

A model for educational simulation of hemodynamic transitions at birth

Sá Couto CD, Andriessen P, van Meurs WL, Sá Couto PM, Ayres de Campos D

Submitted to Pediatr Res

Abstract

Birth is characterized by swift and complex transitions in hemodynamic and respiratory variables. Unrecognized pathologies or incidents may quickly become fatal or cause permanent damage. This paper introduces an essential component of an acute perinatal care simulator, namely a model for educational simulation of normal hemodynamic transitions seen during and shortly after birth.

We explicitly formulate educational objectives and adapt a pre-existing model for the simulation of neonatal cardiovascular physiology to include essential aspects of fetal hemodynamics. From the scientific literature, we obtain model parameters that characterize these aspects quantitatively. The fetal model is controlled by a time-and-event-based script of changes occurring at birth, such as onset of breathing and cord-clamping, and the transitory phase up to 24 hours after birth. Comparison of simulation results to published target data confirms that realistic simulated hemodynamic vital signs are achieved.

Keywords*: Models, Cardiovascular; Computer Simulation; Fetus; Infant, Newborn; Term Birth;*

Introduction

Perinatal acute care is associated with specific clinical demands and challenges. The relatively small number of acute care cases occurring in many institutions, together with the presence of senior staff assuming the responsibility for their management, may hinder the establishment of adequate training for less experienced individuals. In other areas of acute care medicine, realistic simulators contribute to training of healthcare professionals and to patient safety.

Clinically relevant learning objectives for medical staff in Neonatology include the recognition of cardiovascular signs and symptoms occurring in pathologies that manifest shortly after birth, such as persistent pulmonary hypertension, left ventricular overload by a patent ductus arteriosus, myocardial depression, and hemorrhage. It is our contention that identification and handling of these complex, highly dynamic situations can best be trained in an immersive simulation environment using a full-body model-driven simulator.

This paper introduces a fundamental component of such a simulator, namely a simulation engine for normal hemodynamic transitions from the fetal to the early neonatal period. A simulation engine can contribute to a life-like training environment by providing real-time, automatic evolution of clinical signs and monitored signals and of their response to therapeutic interventions. To be able to simulate normal physiology and provide a platform for future simulation of the above mentioned incidents and pathologies, it is necessary that the engine reflect essential aspects of fetal hemodynamics and its subsequent transition to the neonate. Among others, structures such as lungs, placenta, heart, systemic arterial circulation, and the various fetal shunts need to be included. The simulation engine should be able to simulate realistic blood pressures and flow rates in these structures during fetal, transitional, and neonatal periods.

Methods

The proposed simulation engine for normal hemodynamic transitions from the fetal to the early neonatal period consists of a fetal hemodynamic model controlled by a time-and-event-based script[(1)]. The script triggers events occurring at birth such as onset of breathing, cord-clamping, and the transitory phase up to 24 hours after birth, via changes to selected model parameters.

Fetal hemodynamic model

In this study we used an adaptation of a previously described model for educational simulation of the neonatal circulation[(2)]. The latter was based on the linearized, improved

model of cardiovascular physiology, originally presented by Beneken[3], which is also the basis for the model of cardiovascular physiology of the Human Patient Simulator (HPS™; developed at the University of Florida, and commercially available from Medical Education Technologies, Inc., Sarasota, FL), and for a recently published model of infant cardiovascular physiology[4]. In the discussion section we will come back to other fetal hemodynamic models.

To reflect the unique aspects of fetal circulation, the neonatal model was adapted as follows (Figure 1):

- the ductus arteriosus (DA) was included between the pulmonary arteries and the aorta (part of the intrathoracic arteries compartment),
- the foramen ovale (FO) was included between the atria with a valve-like flap, and,
- the placental circulation (including the ductus venosus) was placed in parallel with the systemic circulation, returning all flow to the intrathoracic veins compartment.

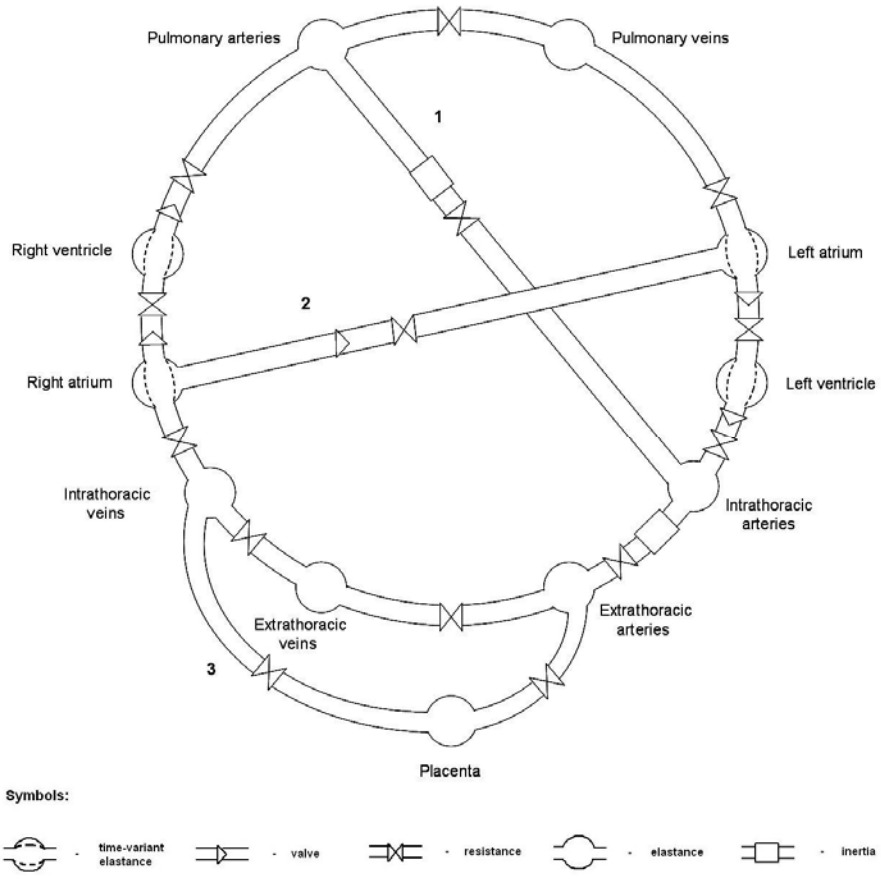

Figure 1. Hydraulic analog for the fetal cardiovascular model. Fetal shunts: 1 – Ductus arteriosus, 2 – Foramen Ovale, 3 – Ductus venosus.

The proposed fetal hemodynamic model consists of two major parts: The heart and seven vascular compartments. We refer to previous studies by our group for a detailed description of the mathematics associated with implementation of the model and similar extensions[2,4].

Numerical values for most model parameters were obtained directly from the scientific literature[5-14]. Numerical values for a few parameters that are specific to our model, needed to be derived, Appendix. Table 1 presents the complete parameter set for a full-term fetus with an assumed weight of 3 kg.

Scripted transitions at birth

Scripted transitions can be automatic or controlled by the simulation instructor. Twenty-four hours after birth, transitions are complete and the model structure (but not all parameter values) match the previously published model for a one-week old neonate. The following subsections describe the scripted model parameter changes in detail.

Intrathoracic pressure. During fetal life, the bronchoalveolar tract is filled with amniotic fluid, maintaining the lungs in a distended state, and an intrathoracic pressure of around 0 mmHg[13,14]. At birth, the fluid in the bronchoalveolar tract is replaced by air. In spontaneously breathing newborns, the diaphragm contracts during inspiration, thereby lowering the intrathoracic pressure (*PTH*) towards negative values of about -3 mmHg[14,15].

Pulmonary vascular resistance (PVR). Immediately after birth, concurrent with the onset of breathing, PVR decreases abruptly[16]. Following this period, there is a more gradual decline in resistance over the following days and weeks[16,17]. From the studies of Dawes et al.[18] in fetal lambs it was possible to estimate a reduction in PVR of 74% after the start of ventilation. A neonatal PVR value between 0.75 and 0.9 mmHg.ml-1.s was reported by Brook[19], and it was assumed that this is reached by the end of the first week of life. In our model, PVR is distributed over model parameters *RPP* and *RLAIN*, see Table 1 for abbreviations. An exponential was used to mimic the initial rapid decrease immediately after birth, and a linear function to reproduce the slower decrease thereafter, reported here only for the first 24 hours of life:

$$RPP(t) = \begin{cases} RPP_0\left(1 - 0.74\left(1 - e^{-6t}\right)\right) & for\ \ 0 \le t \le 2h \\ RPP_0\left(0.26 - 9.5\text{x}10^{-4}(t-2)\right) & for\ \ 2 < t \le 24h \end{cases} \quad (1)$$

Table 1. Fetal cardiovascular model parameters. Assumed weight: 3kg.

Part of circulation	Compartment	Parameter description	Parameter name	Parameter value
Total circulation	All, except placenta	Initial total blood volume	VTOTAL	234
	Placenta	Initial total blood volume	VPL	135
Heart	Atria and ventricles	Heart rate	HR	148
Intrathoracic	All intrathoracic	Average intrathoracic pressure	PTH	0.00
Left heart	Left atrium	Resistance to forward flow including pulmonary venous resistance	RLAIN	3.60
		Mitral valve resistance	RLAOUT	0.0600
		Diastolic elastance	ELAMIN	0.330
		Maximum systolic elastance	ELAMAX	1.00
		Unstressed volume	VLAU	0.00
	Left ventricle	Aortic valve and intrathoracic artery resistance	RLV	0.0180
		Diastolic elastance	ELVMIN	0.324
		Maximum systolic elastance	ELVMAX	12.0
		Unstressed volume	VLVU	-4.00
Systemic circulation	Intrathoracic arteries	Elastance	EITHA	7.69
		Unstressed volume	VITHAU	6.86
	Extrathoracic arteries	Blood flow inertia	LETHA	0.00200
		Resistance	RETHA	0.821
		Elastance	EETHA	6.25
		Unstressed volume	VETHAU	18.1
	Peripheral vessels	Resistance	RSP	2.30
	Extrathoracic veins	Resistance (to forward flow)	RETHV	0.336
		Elastance	EETHV	0.250
		Unstressed volume	VETHVU	47.5
	Intrathoracic veins	Elastance	EITHV	0.500
		Unstressed volume	VITHVU	56.5
	Ductus arteriosus	Resistance	RDA	0.120
		Inertia	LDA	0.0180
Placental circulation	Umbilical arteries	Resistance	RPLIN	3.18
	Placenta	Elastance	EPL	0.667
		Unstressed volume	VPLU	60.0
	Umbilical vein and ductus venousus	Resistance	RPLOUT	0.546
Right heart	Right atrium	Resistance to forward flow	RRAIN	0.0240
		Tricuspid valve resistance	RRAOUT	0.0600
		Diastolic elastance	ERAMIN	0.330
		Maximum systolic elastance	ERAMAX	1.00
		Unstressed volume	VRAU	0.00
	Right ventricle	Pulmonic valve and pulmonary artery resistance	RRV	0.0180
		Diastolic elastance	ERVMIN	0.324
		Maximum systolic elastance	ERVMAX	12.0
		Unstressed volume	VRVU	-4.00
	Foramen ovale	Resistance	RFO	0.214
Pulmonary circulation	Pulmonary arteries	Elastance	EPA	6.25
		Unstressed volume	VPAU	40.5
	Peripheral vessels	Resistance	RPP	7.82
	Pulmonary veins	Elastance	EPV	3.33
		Unstressed volume	VPVU	27.0

Units: heart rate, min^{-1}; resistances, $mmHg.mL^{-1}.s$; elastances, $mmHg.mL^{-1}$; volumes, mL; inertia, $mmHg.mL^{-1}.s^2$; pressures, mmHg.

where RPP_0 is the resistance in pulmonary peripheral vessels, for a normal term fetus. Similarly, for *RLAIN*:

$$RLAIN(t) = \begin{cases} RLAIN_0\left(1 - 0.74\left(1 - e^{-6t}\right)\right) & for\ \ 0 \le t \le 2h \\ RLAIN_0\left(0.26 - 9.5\text{x}10^{-4}(t-2)\right) & for\ \ 2 < t \le 24h \end{cases} \quad (2)$$

Systemic vascular resistance. With cord clamping, total systemic resistance (TSR) approximately doubles[20]. An initial rapid rise in TSR is followed by a slower, more sustained increase over time. The mechanisms behind this considerable increase are not fully understood, but it is thought that there are at least three contributing factors: removal of the low-resistance placental bed, catecholamine release[21,22], and a high sympathetic tone in the immediate postnatal period[23]. Measurements of TSR in full-term human neonates during the first 24 hours of life are available from several sources[24-26]. Based on these data, the following piecewise linear approximation was established:

$$TSR(t) = \begin{cases} 0.0846t + 3.45 & for\ \ 1/60 \le t \le 12h \\ 0.00420t + 4.42 & for\ \ 12 < t \le 24h \end{cases} \quad (3)$$

Cord clamping is assumed to take place at 1 minute. Only the peripheral vessel resistance (*RSP(t)*) is increased, while the resistances of extrathoracic arteries and veins (*RETHA* and *RETHV*) remain constant. TSR(t) corresponds to the sum of these three parameters.

Ductus arteriosus resistance. It is well known that the DA constricts rapidly after birth, with functional closure occurring within 12-36 hours in the majority of term infants. Experimental data for DA diameter changes in humans can be found in Rasanen et al.[11], for the full-term fetus, and in several other publications[25-28], for term neonates during the first 24 hours of life. To model DA closure we used a dynamic resistance that increases with neonatal age. The following curve of the diameter *DAD* in centimeters, as a function of age t in hours, was fitted to these data (Sá Couto, manuscript in preparation):

$$DAD(t) = 0.29\,e^{-0.43t} + 0.30\,e^{-0.054t} \quad (4)$$

Migliavacca et al.[29] present an application of Poiseuille's law to calculate ductus arteriosus resistance *DAR* as a function of its diameter:

$$DAR(t) = \frac{K}{DAD(t)^4} \quad (5)$$

where K is a proportionality constant in mmHg.s.cm. In our model K was set to 0.0145 mmHg.s.cm to match fetal ductus arteriosus resistance and *DAD(0)*.

Software implementation

Model equations were numerically integrated using the Euler forward method with a step size of 0.1 millisecond. All simulations were implemented in Matlab® V7.5(R2007b) (MathWorks, Inc.) on a personal computer with an 2.33-GHz Intel® Core™ Duo processor.

Results

To evaluate the realism of the described simulation engine, we compared simulation results to target data. This comparison was carried out at three physiologically and educationally relevant stages: Term fetus, ventilation and cord clamping, and the evolution during the first 24 hours of life.

Term fetus. Table 2 presents target data and simulation results for the term fetus. Note that to facilitate comparison across species, all flow rates are normalized to fetal weight. All but one of the simulated flow rates fall within one standard deviation of the mean target data obtained in the term fetal lamb[30,31]. Pulmonary blood flow rate is the exception, but like the other flow rates, matches human target data[11]. Combined ventricular stroke volume (CVSV) and output (CVO) also match human target data[8]. Simulated arterial blood pressures are within one standard deviation of animal target data[30,31]. This comparison demonstrates that the fetal model has clinically appropriate ventricular outputs, flow rates and pressures at baseline.

Ventilation and cord clamping. Table 3 presents target data[30] and simulation results for newborn ventilation and ventilation with cord clamping. Comments concerning the target data are included in the discussion section. The ventilation column shows that all simulated output variables are within one standard deviation of the target data, with the exception of arterial pressures that are within two standard deviations. Ventilation with cord occlusion results in a correct reversal of DA flow, from a predominantly right-to-left to a predominantly left-to-right shunt, and in increased left ventricular output. All simulated output variables are

Table 2. Target data[8, 11, 30, 31] and simulation results for the term fetus.

		Target data				Simulation results
		Mielke	Rasanen	Teitel	Anderson	
CVSV (mL.kg^{-1})		3	4	--	--	3
CVO (mL.min $^{-1}$.kg^{-1})		425	608	392±75	462±194	421
Flow rates (% of CVO)	Right ventricle	59	60	66±18	60±27	60
	Left ventricle	41	40	34±11	40±28	40
	DA	46	39	~57	54±29	42
	Pulmonary	11	21	8±5	6±5	18
	FO	33	19	26±12	34±27	22
	Placenta	--	--	35±12	--	34
Mean pressures (mmHg)	Central venous	--	--	3±3	--	5
	Right atrium	--	--	--	2.4±0.6	6
	Left atrium	--	--	3±3	2.9±1.0	5
	Systemic arterial	--	--	52±6	45.4±5.7	46
	Pulmonary arterial	--	--	53±8	47.8±6.0	47

(--) data not available; (~) data read from graph. CVSC, combined ventricular stroke volume; CVO, combined ventricular output.
Target data:
Mielke[8]: values expressed as median, measurements in 222 human fetuses (13-41 weeks);
Rasanen[11]: values expressed as mean, measurements in 63 human fetuses (mean gestational age: 38 weeks)
Teitel[30]: values expressed as mean ± SD, measurements in 16 term fetal lambs;
Anderson[31]: values expressed as mean ± SD, measurements in 12 near term fetal lambs;

within or at one standard deviation of target data. In the discussion section we will analyze the single exception, DA right-to-left flow.

Evolution during the first 24 hours of life. Table 4 presents target data[32,33] and simulation results for left ventricular stroke volume and output, from the term fetus until the 24-hour old neonate. With one exception, all simulation results are within one standard deviation of target data. Left ventricular output at 12 hours is one standard deviation removed from the target data.

Table 5 presents target data[34,35] and simulation results for arterial and atrial pressures 24 hours after birth. All but one of the simulation results are within one standard deviation of target data. Pulmonary arterial diastolic pressure is at one standard deviation.

Figure 2 shows target data[36] and simulation results for the evolution of the mean aortic-pulmonary pressure difference during the first 24 hours of life. These results demonstrate a plausible evolution of the simulated variable.

The pulsatile nature of the model is illustrated in Figure 3, depicting the evolution of systemic and pulmonary arterial pressures in the fetus and at 2, 12, and 24 hours after birth.

Table 3. Target data[30] and simulation results for transitions shortly after birth.

		Ventilation		Ventilation with cord clamping	
		Target data¶ (Teitel)	Simulation results*	Target data§ (Teitel)	Simulation results*
CVSV (ml.kg^{-1})		--	3	--	3
CVO (ml.min $^{-1}$.kg^{-1})		436±147	438	359±92	443
Flow rates (% of CVO)	Right ventricle	52±16	55	40±10	48
	Left ventricle	48±20	45	60±18	52
	DA	22±13 (R to L) 4± 7(L to R)	22 (R to L) 0 (L to R)	2±3 (R to L) 18± 12(L to R)	11 (R to L) 11 (L to R)
	Pulmonary	33±22	33	~55	52
	FO	15±9	11	3±4	0
	Placenta	31±17	28	3±5	0
Mean pressures (mmHg)	Central venous	4±3	7	3±3	6
	Right atrium	--	7	--	7
	Left atrium	7±4	7	10±4	7
	Systemic arterial	53±6	41	58±16	43
	Pulmonary arterial	55±9	42	48±16	43

(--) data not available; (~) data read from graph; CVSC, combined ventricular stroke volume; CVO, combined ventricular output; (R to L), right to left shunt; (L to R), left to right shunt.
Target data:
Teitel[30]: values expressed as mean ± SD; measurements in 16 term fetal lambs.
¶Artificial ventilation of the lungs for 15 min, with a gas mixture of 3% O_2, 5% CO_2 and 92% N_2 (mimicking fetal life); umbilical cord remained intact.
§Cord clamping after 30 min of artificial ventilation (initial 15 minutes with the gas mixture described above and last 15 minutes with 100% O_2) followed by another 15 minutes of artificial ventilation (with 100% O_2).
*Simulation times corresponding to target data. Mean intrathoracic pressure assumed to be +2 mmHg to mimic the effect of artificial ventilation; DA resistance only starts to increase at minute 15, to mimic DA sensitivity to oxygen levels.

Figure 4 provides an overview of all simulated phenomena, by presenting the scripted model parameters and the evolution of modeled flow rates and pressures from the fetus until the 24-hour old neonate. These results will be analyzed in the discussion section.

Table 4. Target data [32, 33] (mean±SD) and simulation results of the left ventricle performance from before birth to 24 hours after birth.

	Before birth		1h		2h		12h		24h	
	Target data (Agata)	Simulation results	Target data (Agata)	Simulation results	Target data (Harada)	Simulation results	Target data (Harada)	Simulation results	Target data (Agata, Harada)	Simulation results
Left ventricular stroke volume (mL.kg^{-1})	1.21±0.33	1.14	2.25±0.37	1.94	2.19±0.52	1.95	1.76±0.39	1.78	2.02±0.42 1.80±0.39	1.73
Left ventricular output (mL.min $^{-1}$.kg^{-1})	170±46	169	327±66	287	291±72	289	225±36	264	245±56 222±52	257

Target data:
Agata[32]: measurements in 39 normal full-term fetuses and neonates from before birth until 24 hours after birth;
Harada[33]: measurements in 22 normal term neonates from 2 until 24 hours after birth.

Table 5. Target data[34, 35] (mean±SD) and simulation results of blood pressures at 24 hours after birth.

Pressures (mmHg)		Target data		Simulation results
		Moss	Emmanouilides	
Atria	Right	--	2.3±1.2	2.5
	Left	--	4.5±1.4	3.5
Systemic arterial	Systolic	73.7±5.4	73.3±7.5	73.8
	Diastolic	52.2±4.3	49.6±5.2	48.9
	Mean	61.9±4.4	59.6±6.4	59.8
Pulmonary arterial	Systolic	56.5±7.4	--	50.4
	Diastolic	21.7±5.2	--	27.1
	Mean	38.3±6.1	--	38.6

(--) data not available.
Target data:
Moss[34]: 24 measurements in 12 normal full-term neonates with mean age of 18 hours (2-27h);
Emmanouilides[35]: measurements in 23 normal full-term neonates with mean age of 26 hours (6-35h).

Discussion

We present a combination of a mathematical model and a time-and-event-based script for educational simulation of fetal to early neonatal hemodynamic transitions. The pulsatile cardiovascular model presented by Beneken[3] was selected as a basis for this work because of its proven track record in simulating adult, infant, and neonatal cardiovascular physiology for educational simulation[1,2,4]. Inclusion of the DA, FO, and placental flow was relatively

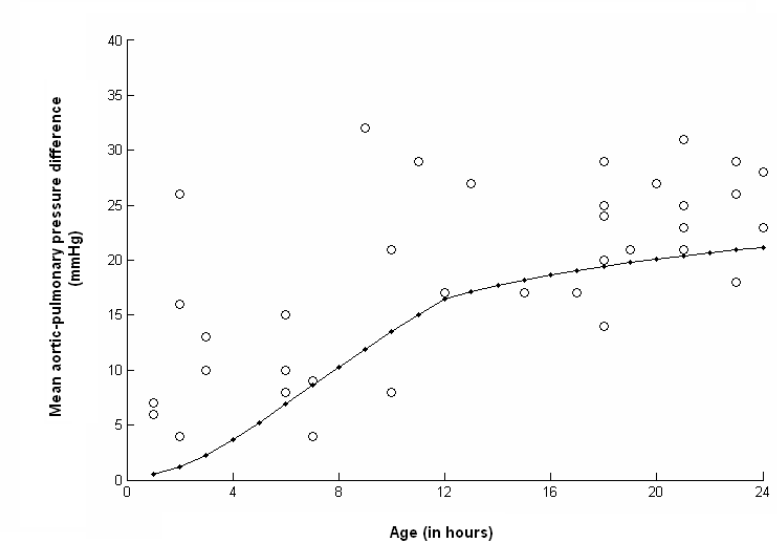

Figure 2. Mean aortic-pulmonary pressure difference in the first 24 hours after birth. Open circles: Target data[36] from 39 normal term human infants; Close dots and line: Simulation results.

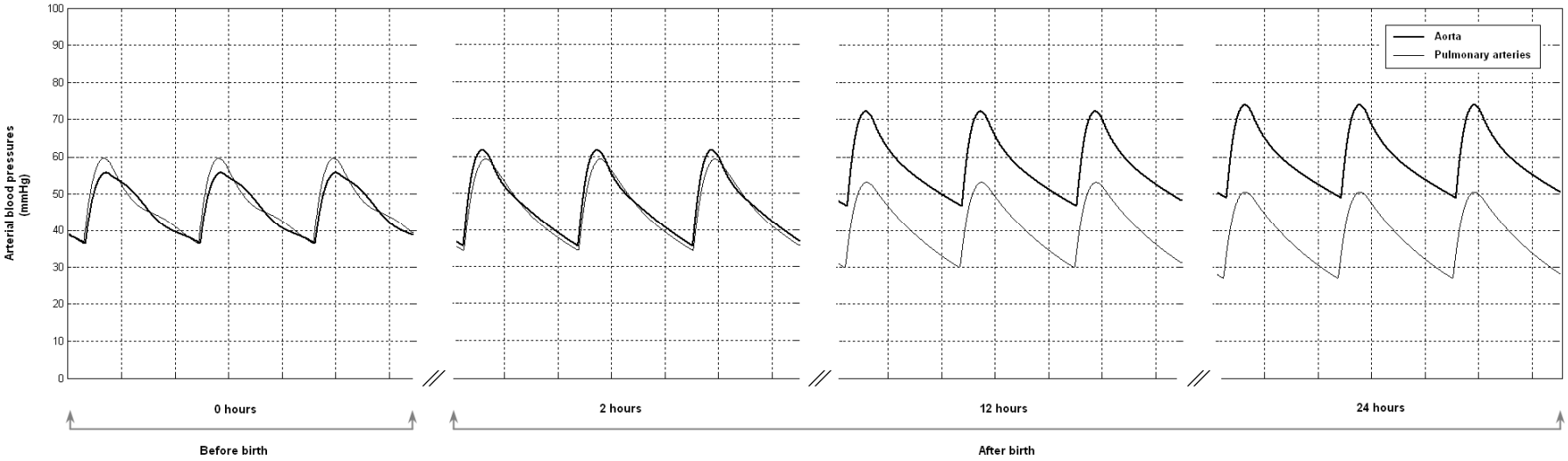

Figure 3. Simulated systemic (dark line) and pulmonary (grey line) arterial blood pressure before birth and at 2, 12, and 24 hours after birth.

straightforward. Other models of fetal cardiovascular physiology have been described in the past[6,10], but because of their complexity and large parameter sets, were judged to be difficult to apply in our envisioned educational application, which involves repeated parameter estimation and manipulation to represent different patients, pathologies, and critical situations. The relatively simple circulation model presented by Huikeshoven et al.[7] has a complex heart model. The structure of the presented model for a 24-hour old neonate is identical to that of a previously described one-week old neonate[2], but parameters differ considerably. This should in principle be exclusively due to the age difference, but an evaluation of the evolution from 24 hours to one week is needed to confirm this statement.

Simulations results demonstrate that, in general, the model is capable of correctly representing fetal hemodynamics and its evolution during the first 24 hours of life. The validation of events occurring shortly after birth (ventilation and cord clamping) is limited by the available experimental data, which do not completely represent normal physiological conditions. Target data used for this purpose includes three sequential events: ventilation, oxygenation and umbilical cord occlusion. Each event was continued for 15 minutes, as described in the footnote of Table 3. To reproduce these conditions, a few adaptations in scripted parameters were needed: 1) matching to reported timeline; 2) representation of artificial ventilation with a positive average intrathoracic pressure of +2 mmHg (instead of -3 mmHg). Intrathoracic pressure is positive throughout inspiration and remains slightly positive, whenever positive end-expiratory pressure is applied[15,37]; 3) delayed rise in DA resistance, corresponding to the initiation of ventilation with 100% oxygen. In these conditions, simulation results match the target data. The only exception is right-to-left DA flow during ventilation with cord clamping, which is higher than in target data. This may be explained by differences between species. Flow through the DA after birth, may not be the same in the human neonate and in the newborn lamb. In the latter, the pulmonary vascular resistance apparently falls sharply within minutes after the onset of respiration, and the fetal direction of flow suddenly becomes reversed[38].

Figures 3 and 4 illustrate potential educational applications of the model and show its integrated response. Evolution of aortic and pulmonary artery pressures can be simulated in accelerated time, providing students with a unique experience of these important yet complex phenomena. Figure 4 shows that, with the onset of breathing, intrathoracic pressure decreases abruptly to negative values, as observed in spontaneously breathing newborns. In addition, pulmonary vascular resistance decreases considerably in the first minutes after birth (bottom panel). As a consequence, arterial pressures increase and atrial pressures decrease (middle panel), but no relevant changes are observed in flow rates (top panel). An immediate result of cord clamping is the sudden increase in systemic resistance (bottom panel), causing an increase in systemic arterial blood pressure (middle panel), and the cessation of placental blood flow (top panel). Flow rate in the DA and pulmonary blood flow (top panel), are deeply affected by cord clamping. The continuous decrease of pulmonary resistance (bottom panel) further increases pulmonary blood flow (top panel). The increase in systemic resistance (bottom panel), and subsequent increase in left atrial pressure (middle panel) causes - at near constant right atrial pressure (middle panel) - a decrease in flow across the FO (top panel). The combination of increased left atrial pressure, due to higher pulmonary venous return, and diminished inferior vena cava return to the right atria, results in a reversal of the left and right atrial pressures (middle panel), functionally closing the FO, as can be observed around minute

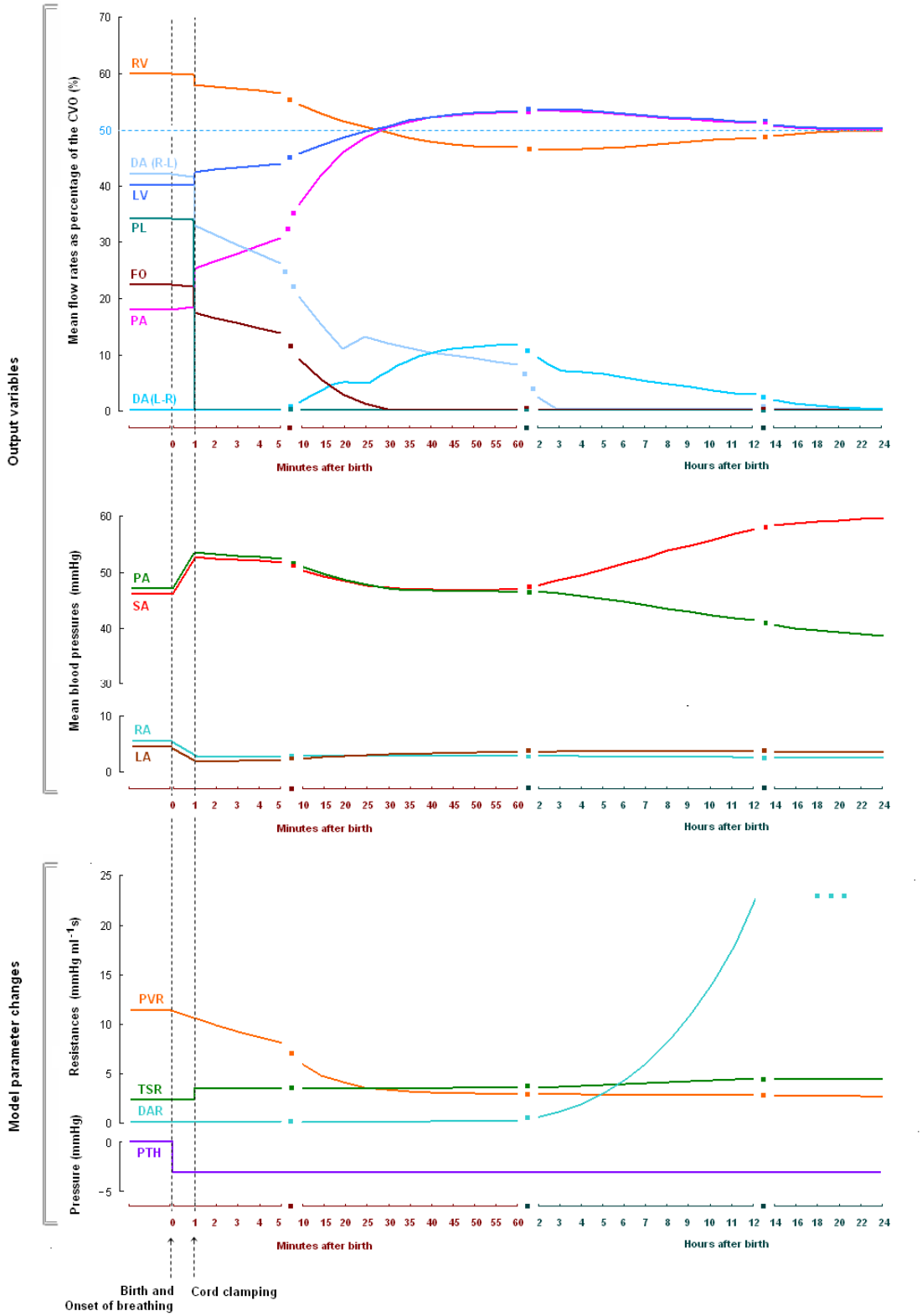

Figure 4. Simulated model parameter changes and output variables in the first 24 hours after birth. Right ventricle, RV; Ductus arteriosus, right to left flow, DA (R-L); Left ventricle, LV; Placenta, PL; Foramen ovale, FO; Pulmonary arterial, PA; Ductus arteriosus, left to right flow, DA (L-R); Systemic arterial, SA; Right atrium, RA; Left atrium, LA; Pulmonary vascular resistance, PVR; Total systemic resistance, TSR; Ductus arteriosus resistance, DAR; Mean intrathoracic pressure, PTH.

30 (top panel). From this time on, pulmonary inflow matches left ventricle flow rate (top panel). As pulmonary vascular resistance falls below systemic vascular resistance (bottom panel), the bidirectional DA flow decreases significantly, changing to a continuous left-to-right flow at the third hour of life (top panel). These changes in DA flow cause the left ventricle to pump more blood than the right ventricle. As DA resistance increases over time (bottom panel), flow through the ventricles and lungs converge (top panel). Another consequence of changes in DA flow is the increasing difference between mean systemic and pulmonary arterial pressures, which can be observed between the second and 24th hour after birth (middle panel).

In conclusion, we present an original model for educational simulation of fetal to early neonatal hemodynamic transitions. Fetal and neonatal end-points show realistic simulated hemodynamic variables. The transitions at birth and during the first 24h of life are also represented realistically. This model constitutes an essential component of educational simulators for perinatal acute care. It can also be used to demonstrate the complex hemodynamic transitions at birth.

Appendix
Parameter estimation for the fetal cardiovascular system

The following provides explicit documentation of how numerical values for specific fetal model parameters, listed in Table 1, were obtained.

Heart chambers. Ménigault et al.[5] present parameter values for the maximum (systolic) elastance and unstressed volume of the left and right ventricles (*ELVMAX*, *ERVMAX*, *VLVU*, and *VRVU*). These authors also present an end-diastolic cardiac volume of 10.5 ml and an end-diastolic pressure of 3 mmHg, obtained in human fetuses. Assuming both ventricles have the same end-diastolic volume, we can calculate the minimum (diastolic) elastance of the left and right ventricles (*ELVMIN* and *ERVMIN*) using equation (A7) from Goodwin et al.[4]. Note that the average intrathoracic pressure (*PTH*) was assumed to be 0 mmHg (assumed value further explained below).

Numerical values for atrial parameters are not as easily encountered as for the ventricles. Pennati et al.[6] and Huikeshoven et al.[7] present values for fixed atrial elastances (ranging between 0.33 $mmHg.mL^{-1}$ and 1 $mmHg.mL^{-1}$). We set the atrial diastolic elastances (*ELAMIN* and *ERAMIN*) to the lowest value and the maximum atrial elastances (*ELAMAX* and *ERAMAX*) to the highest value. The unstressed volumes (*VLAU* and *VRAU*) were assumed to be zero.

For the resistances of the heart valves (*RLAOUT, RLV, RRAOUT* and *RRV*) we used the values proposed by Huikeshoven et al.[7].

Heart rate (*HR*) is set to the mean value presented by Mielke and Benda[8] for term human fetus.

Blood volumes. Total fetal-placental blood volume for a term fetus is approximately 125 $ml.kg^{-1}$ [9]. The blood volume in the fetal body accounts for an average of 78 $ml.kg^{-1}$ and in the placenta for an average of 45 $ml.kg^{-1}$[9]. These values were necessary for the model initialization.

Huikeshoven et al.[7] give values for the unstressed volumes of the vascular compartments. For the placenta (*VPLU*) and the pulmonary arteries and veins (*VPAU* and *VPVU*) we directly used the reported values. (Total) venous and arterial unstressed volumes were obtained from Huikeshoven et al.[7] and distributed over the intrathoracic and extrathoracic compartments of our model (*VITHAU*, *VETHAU*, *VETHVU*, and *VITHVU*) in the same proportion as the neonatal parameters presented in Sá Couto et al.[2].

Resistances. Huikeshoven et al.[7,10] present values for fetal hemodynamic resistances. For the resistances of the ductus arteriosus (*RDA*), placental inflow and outflow (*RPLIN* and

RPLOUT), foramen ovale (*RFO*), and the left atrium inflow rate (*RLAIN*), we directly used the proposed values. As for the unstressed volumes, the (total) arterial and venous systemic resistances were obtained from Huikeshoven et al.[7] and distributed over the arterial and venous systemic compartments of our model, in the same proportion as the neonatal parameters presented in Sá Couto et al.[2]. To obtain pulmonary peripheral resistance (*RPP*), we used the ratio *RPP/RSP* of 3.4 for term human fetuses, presented by Rasanen et al.[11]. The resulting *RPP* is in the same range as the one obtained by Assali et al.[12] in term fetal lambs.

Elastances, inertia and intrathoracic pressure. Huikeshoven et al.[7] present values for the elastances of the vascular compartments. We use these values for the venous elastances (*EETHV*, *EITHV*, *EPL* and *EPV*). The values for the arterial elastances proposed by Pennati et al.[6] were distributed over the systemic and pulmonary arterial compartments of our model (*EITHA*, *EETHA* and *EPA*).

A value for blood flow inertia in the ductus arteriosus (*LDA*) is presented by Huikeshoven et al.[7]. For the inertia in the systemic arteries (*LETHA*) we use the value proposed by Pennati et al.[6].

The average intrathoracic pressure (*PTH*) was set to 0 mmHg (for lungs filled with fluid)[13,14].

References

1. Van Meurs WL, Good ML, Lampotang S. Functional anatomy of full-scale patient simulators. J Clin Monit. 1997;13(5):317-324.

2. Sá Couto CD, van Meurs WL, Goodwin JA, Andriessen P. A model for educational simulation of neonatal cardiovascular pathophysiology. Simul Healthcare. 2006;1:4-12.

3. Beneken JEW. A mathematical approach to cardiovascular function. The uncontrolled human system [thesis]. The Netherlands: University of Utrecht, 1965.

4. Goodwin JA, van Meurs WL, Sá Couto, CD, Beneken JEW, Graves SA. A model for educational simulation of infant cardiovascular physiology. Anesth Analg. 2004;99:1655-1664.

5. Ménigault E, Vieyres P, Lepoivre B, Durand A, Pourcelot L, Berson M. Fetal heart modelling based on a pressure-volume relationship. Med Biol Eng Comput. 1997;35(6):715-721.

6. Pennati G, Bellotti M, Fumero R. Mathematical modeling of the human foetal cardiovascular system based on Doppler ultrasound data. Med Eng Phys. 1997;19: 327-335.

7. Huikeshoven F, Coleman TG, Jongsma HW. Mathematical model of the fetal cardiovascular system: the uncontrolled case. Am J Physiol. 1980;239(3):R317-325.

8. Mielke G, Benda N. Cardiac output and central distribution of blood flow in the human fetus. Circulation. 2001;103(12):1662-1668.

9. Cunningham G, Leveno K, MacDonald P, Gilstrap III L, Gant N, Hankins G, Clark S. The morphological and functional development of the fetus. In: Cunningham G, Leveno K, MacDonald P, Gilstrap III L, Gant N, Hankins G, Clark S (eds) Williams Obstetrics [20th Edition]. Appleton & Lange, Connecticut, 1997.

10. Huikeshoven FJ, Hope ID, Power GG, Gilbert RD, Longo LD. Mathematical model of fetal circulation and oxygen delivery. Am J Physiol. 1985;249(2 Pt 2):R192-202.

11. Rasanen J, Wood DC, Weiner S, Ludomirski A, Huhta JC. Role of the pulmonary circulation in the distribution of human fetal cardiac output during the second half of pregnancy. Circulation. 1996;94:1068-1073.

12. Assali NS, Morris JA, Beck R. Cardiovascular hemodynamics in the fetal lamb before and after lung expansion. Am J Physiol. 1965;208:122-129.

13. Vilos GA, Liggins GC. Intrathoracic pressures in fetal sheep. J Dev Physiol. 1982; 4(4):247-256.

14. Hooper SB, Wallace MJ. Role of the physicochemical environment in lung development. Clin Exp Pharmacol Physiol. 2006;33(3):273-279.

15. Greenspan JS, Shaffer TH, Fox WW, Spitzer AR. Assisted ventilation: Physiologic implications and complications. In: Polin RA, Fox WW (eds) Fetal and neonatal physiology [2nd Edition]. W.B. Saunders Company, Philadelphia, 1998.

16. Friedman AH, Fahey JT. The transitions from fetal to neonatal circulation: Normal responses and implications for infants with heart disease. Semin Perinatol. 1993;17(2):106-121.

17. Ghanayem NS, Gordon JB. Modulation of pulmonary vasomotor tone in the fetus and neonate. Respir Res. 2001; 2(3):139-144.

18. Dawes GS, Mott JC, Widdicombe JG, Wyatt DG. Changes in the lungs of the new-born lamb. J Physiol. 1953;121(1):141-162.

19. Brook MM, Heymann MA, Teitel DF. The heart. In: Klaus MH, Fanaroff AA (eds) Care of the high-risk [5th Edition]. W.B. Saunders Company, Philadelphia, 2001.

20. Gutyon AC. Fetal and neonatal physiology. In: Guyton AC (ed) Textbook of medical physiology [8th Edition]. W.B. Saunders Company, Philadelphia, 1991.

21. Lagercrantz H, Bistoletti P. Catecholamine release in the newborn infant at birth. Pediatr Res. 1977;11(8):889-893.

22. Padbury JF, Diakomanolis ES, Hobel CJ, Perelman A, Fisher DA. Neonatal adaptation: sympatho-adrenal response to umbilical cord cutting. Pediatr Res. 1981;15(12):1483-1487.

23. Minoura S, Gilbert RD. Postnatal change of cardiac function in lambs: effects of ganglionic block and afterload. J Dev Physiol. 1987;9(2):123-135.

24. Coskun S, Yüksel H, Bilgi Y, Lacin S, Tansug N, Onag A. Non-invasive evaluation of the adaptations of cardiac function in the neonatal period: a comparison of healthy infants delivered by vaginal route and caesarean section. Acta Med Okayama. 2001;55(4):213-218.

25. Kishkurno S, Takahashi Y, Harada K, Ishida A, Tamura M, Takada G. Postnatal changes in left ventricular volume and contractility in healthy term infants. Pediatr Cardiol. 1997;18(2):91-95.

26. Shiota T, Harada K, Takada G. Left ventricular systolic and diastolic function during early neonatal period using transthoracic echocardiography. Tohoku J Exp Med. 2002;197(3):151-158.

27. Walthers FJ, Benders MJ, Leighton JO. Early changes in the neonatal circulatory transition. J Pediatr. 1993;123(4):625-632.

28. Hiraishi S, Misawa H, Oguchi K, Kadoi N, Saito K, Fujino N, Hojo M, Horiguchi Y, Yashiro K. Two-dimensional Doppler echocardiographic assessment of closure of the ductus arteriosus in normal newborn infants. J Pediatr. 1987;111(5):755-760.

29. Migliavacca F, Dubini G, Pennati G, Pietrabissa R, Fumero R, Hsia TY, de Leval MR. Computational model of the fluid dynamics in systemic-to-pulmonary shunts. J Biomech. 2000;33(5):549-557.

30. Teitel DF, Iwamoto HS, Rudolph AM. Effects of birth-related events on central blood flow patterns. Pediatr Res. 1987;22(5):557-566.

31. Anderson DF, Bissonnette JM, Faber JJ, Thornburg KL. Central shunt flows and pressures in the mature fetal lamb. Am J Physiol. 1981;241(1):H60-66.

32. Agata Y, Hiraishi S, Oguchi K, Misawa H, Horiguchi Y, Fujino N, Yashiro K, Shimada N. Changes in left ventricular output from fetal to early neonatal life. J Pediatr. 1991;119(3):441-445.

33. Harada K, Shiota T, Takahashi Y, Tamura M, Takada G. Changes in the volume and performance of the left ventricle in the early neonatal period. Early Hum Dev. 1994;39(3):201-209.

34. Moss AJ, Emmanouilides GC, Adams FH, Chuang K. Response of ductus arteriosus and pulmonary and systemic arterial pressure to changes in oxygen environment in newborn infants. Pediatrics. 1964;33:937-944.

35. Emmanouilides GC, Moss AJ, Monset-Couchard M, Marcano BA, Rzeznic B. Cardiac output in newborn infants. Biol Neonate. 1970;15(34):186-197.

36. Emmanouilides GC, Moss AJ, Duffie ER Jr, Adams FH. Pulmonary arterial pressure changes in human newborn infants from birth to 3 days of age. J Pediatr. 1964;65:327-333.

37. Soni N, Williams P. Positive pressure ventilation: what is the real cost? Br J Anaesth. 2008;101(4):446-457.

38. Moss AJ, Emmanouilides GC, Duffie ER Jr. Closure of the ductus arteriosus in the newborn infant. Pediatrics. 1963;32:25-30.

Acknowledgements

At the time of submission of this manuscript, Matilde Sá Couto was a healthy term-fetus, about to accomplish the remarkable hemodynamic transitions at birth.

Funding

Funded in part by the Máxima Medical Center, Veldhoven, The Netherlands and the Instituto de Engenharia Biomédica, Porto, Portugal.

Chapter 7

Sensitivity analysis of a hemodynamic model to facilitate programming simulation patients

Sá Couto CD, van Meurs WL

Abstract

When adapting a patient on model-driven medical simulators to meet learning objectives which are not supported by the available patients, the instructor-developer is faced with a challenging parameter estimation problem. To facilitate meeting this challenge we propose a sensitivity analysis of a frequently used hemodynamic model. The sensitivity analysis is carried out at two levels: At the basic physiological level, all 38 hemodynamic model parameters and 13 simulated monitored signals are taken into account, whereas at the empirical level only 6 normalized hemodynamic factors, grouping selected parameters, and 5 of the most important monitored signals are taken into account.

Presented data for both analyses allow for a systematic approach to adapting hemodynamic parameters and monitored signals of this particular model. The basic physiological analysis reveals that several parameters have a rather isolated effect on specific monitored signals, while others affect the entire circulation. The empirical analysis demonstrates consistency with the basic physiological analysis and confirms that the selected factors are applied to parameters with a major impact on monitored signals.

We expect that these analyses will guide and facilitate future adaptation of simulated patients and play a role in the creation of new patients representing a sub-population, such as pediatric or geriatric patients, or patients with a specific pathology.

Introduction

Full-body model-driven simulators provide a technological basis for training healthcare providers in a realistic environment without risk to real patients. The main purpose of models of human physiology and pharmacology in the simulation engine of a medical educational simulator is to provide real-time, automatic, realistic, and consistent evolution of clinical signs and monitored signals, and of their response to therapeutic interventions. A second purpose is to provide a representation of the (patho)physiology of the simulated patient that can be manipulated in a logical fashion to simulate pathologies or critical incidents[1].

The hemodynamic model presented by Beneken[2,3] has been used in several previous studies[3-6]. This model was also the basis for the model of cardiovascular physiology of the Human Patient Simulator (HPS™), developed at the University of Florida, and commercially available from Medical Education Technologies, Inc., Sarasota, FL, USA. This model was selected because, while of relatively reduced complexity, it could support a wide range of anticipated learning objectives. A physiologic interpretation of the model structure and parameter values is desirable for easy coupling of this model to other models, and for the adjustment of model structure and parameter values to reflect pathologies, critical incidents, or other patients. The model includes four heart chambers and six vascular compartments, Figure 1. We refer to Appendix 1 of Goodwin[3] for a detailed mathematical description.

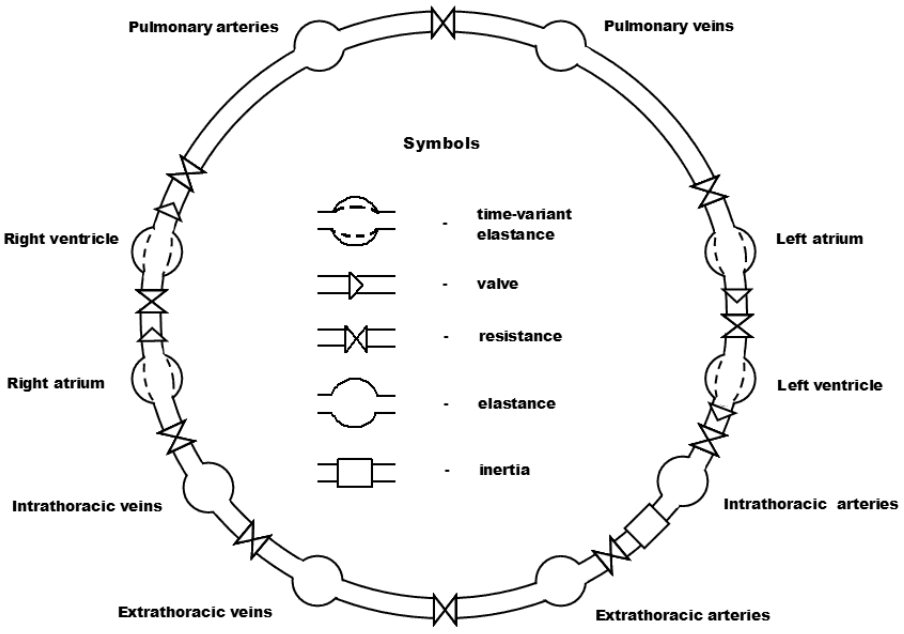

Figure 1. Hydraulic analog for the cardiovascular model (from Goodwin et al.[3]).

The 38 parameters that determine its response are listed in Table 1. The parameters of this model reflect a healthy, young, adult male.

Table 1. Complete set of parameters for the Beneken[2] hemodynamic model. Adapted from Goodwin et al.[3].

	Compartment	Parameter description	Parameter name	Parameter value
Total circulation	All	Initial total blood volume	VTOTAL	4740
Heart	Atria and ventricles	Heart rate	HR	72.0
Intrathoracic	All intrathoracic	Average intrathoracic pressure	PTH	-4.00
Left heart	Left atrium	Resistance to forward flow of the inflow tract	RLAIN	0.00300
		Mitral valve resistance	RLAOUT	0.00300
		Diastolic elastance	ELAMIN	0.120
		Maximum systolic elastance	ELAMAX	0.280
		Unstressed volume	VLAU	30.0
	Left ventricle	Aortic valve and intrathoracic artery resistance	RLV	0.00800
		Diastolic elastance	ELVMIN	0.0900
		Maximum systolic elastance	ELVMAX	4.00
		Unstressed volume	VLVU	60.0
Systemic circulation	Intrathoracic arteries	Elastance	EITHA	1.43
		Unstressed volume	VITHAU	140
	Extrathoracic arteries	Blood flow inertia	LETHA	0.000700
		Resistance	RETHA	0.0600
		Elastance	EETHA	0.556
		Unstressed volume	VETHAU	370
	Peripheral vessels	Resistance	RSP	1.00
	Extrathoracic veins	Resistance (to forward flow)	RETHV	0.0900
		Elastance	EETHV	0.0169
		Unstressed volume	VETHVU	1000
	Intrathoracic veins	Elastance	EITHV	0.0182
		Unstressed volume	VITHVU	1190
Right heart	Right atrium	Resistance to forward flow of the inflow tract	RRAIN	0.00300
		Tricuspid valve resistance	RRAOUT	0.00300
		Diastolic elastance	ERAMIN	0.0500
		Maximum systolic elastance	ERAMAX	0.150
		Unstressed volume	VRAU	30.0
	Right ventricle	Pulmonic valve and pulmonary artery resistance	RRV	0.00300
		Diastolic elastance	ERVMIN	0.0570
		Maximum systolic elastance	ERVMAX	0.490
		Unstressed volume	VRVU	40.0
Pulmonary circulation	Pulmonary arteries	Elastance	EPA	0.233
		Unstressed volume	VPAU	50.0
	Peripheral vessels	Resistance	RPP	0.110
	Pulmonary veins	Elastance	EPV	0.0455
		Unstressed volume	VPVU	350

Units are as follows: heart rates, bpm; resistances, $mmHg.mL^{-1}.s$; elastances, $mmHg.mL^{-1}$; volumes, mL; inertia, $mmHg.mL^{-1}.s^2$

Establishing a complete set of parameters for a new patient, such as an infant[3] or a neonate[5] involves in-depth physiologic research and careful adjustments of all 38 parameters. Adapting an existing baseline patient to reflect a specific physiology or pathology may be achieved via adjustment of a few carefully selected parameters[7]. Such adaptations may be difficult to accomplish by clinical instructors with limited physiologic modeling experience. In the context of the development of a simulator based hemodynamic monitoring class[8], HPS™ developers introduced 6 normalized hemodynamic "factors" grouping selected model parameters (see the methods section for a complete list). Euliano et al.[9] used these factors, and a few additional parameters, to define hemodynamic parameters of a parturient. In these projects no systematic analysis of the influence of parameters on simulated monitored signals was carried out.

Recently, classical sensitivity analysis has been applied to physiological models for parameter estimation[10,11] and other purposes: Reduction of model complexity[12], and evaluation of the relevance of a particular parameter for model response[13,14]. In this study, we present a sensitivity analysis of the Beneken model to facilitate programming hemodynamics of new patients and adapting existing ones. This analysis is applied at two levels: The basic physiological level, taking into account all 38 model parameters and 13 monitored signals, and the empirical level, taking into account the 6 factors and 5 of the most important monitored signals. Typically, a model developer will work at the basic physiological level and a clinical instructor at the empirical level.

The sensitivity analysis presented in this study applies most directly to patients simulated with a corresponding underlying hemodynamic model, such as Stan Vintage[4] for the HPS™. The analysis refers to the "uncontrolled model", i.e. in absence of baroreflex effects. Note that in the HPS™ the natural control mechanisms can and should be disabled before programming a new patient. Once a new operating point is established, the reflexes can be reactivated, also see Euliano et al.[9].

Methods

To perform the sensitivity analyses, parameters or factors were increased one-at-a-time by 1 %, and the relative impact on selected monitored signals was evaluated. The relative sensitivity matrix (SM) is given by:

$$SM_{i,j} = \frac{\frac{\Delta m_j}{m_{j,0}}}{\frac{\Delta p_i}{p_{i,0}}} \qquad (1)$$

where $p_{i,0}$ is the baseline value for parameter i and Δp_i its variation, $m_{j,0}$ is the baseline value of monitored signal j; and Δm_j its variation, caused by the variation in the parameter. The normalized, dimensionless elements of this matrix are easily interpreted and can be compared directly. As referred to above, $\Delta p_i/p_{i,0} = 0.01$.

At the basic physiological level, i corresponds to all 38 model parameters, and j to the 13 simulated monitored signals: end-diastolic and end-systolic left ventricular volumes, systolic, mean, and diastolic arterial blood pressures, central venous pressure, end-diastolic and end-systolic right ventricular volumes, systolic, mean, and diastolic pulmonary arterial pressures, pulmonary venous pressure (pulmonary capillary wedge pressure), and cardiac output.

At the empirical level, i corresponds to the 6 hemodynamic factors listed in Table 2, and j to the 5 monitored signals: Mean arterial blood pressure, central venous pressure, mean pulmonary arterial pressure, pulmonary venous pressure (pulmonary capillary wedge pressure), and cardiac output. Table 2 also presents how underlying model parameters are affected by hemodynamic factors.

A carefully verified software implementation of the Beneken model was used to simulate the monitored signals. The Euler forward method was used to integrate model equations with a step size of 1 millisecond. Parameters and factors were automatically changed one-at-a-time, and monitored variables were evaluated after 20 seconds of simulation time to allow for stabilization. The sensitivity matrixes were then generated using equation (1). All simulations were implemented in Matlab® V7.5(R2007b) (MathWorks, Inc.) on a personal computer with an 2.33-GHz Intel® Core™ Duo processor.

Table 2. Relationships between hemodynamic factors and model parameters. ":=" indicates the assignment of a new value to a parameter, based on its value listed in Table 1.

Factor	Relationship
Heart rate factor	HR := HR_factor*HR
Resistance factor (systemic)✧	RSP := (0.20 + 0.80*SVR_factor)*RSP
Resistance factor (pulmonary)✧	RPP := (0.20 + 0.80*PVR_factor)*RPP
Venous capacity factor	VITHVU := VUV_factor*VITHVU VETHVU := VUV_factor*VETHVU
Ventricular contractility factor (left)	ELVMAX := LV_CONT_factor*ELVMAX
Ventricle contractility factor (right)	ERVMAX := RV_CONT_factor*ERVMAX

✧SVR_factor and PVR_factor only affect the arteriolar part of systemic and pulmonary vascular resistance, respectively, which, at baseline, represents 80% of the total resistance. Note that in this description, perfusion of parallel tissue groups can be ignored.

Results

Figure 2 presents the SM at the basic physiological level for a +1% change in hemodynamic parameters. To facilitate interpretation of results, numerical values are represented using a color gradient. Numerical values are presented in the Appendix. In Figure 2, the parameters, as described in Table 1, are grouped by type: Heart rate, resistances, unstressed volumes, elastances, and "other". Parameters in the resistances, unstressed volumes, and elastances groups, are listed in anatomical order in the direction of blood flow. Monitored blood pressures are also ordered anatomically. The results demonstrate a high sensitivity to: 1) Heart rate (*HR*). An increase in *HR* produces increases in systemic arterial pressures and cardiac output. 2) Systemic peripheral resistance (*RSP*). An increase in *RSP* produces changes in systemic arterial pressures, which are similar to those caused by changes in *HR*, but with opposite changes in cardiac output. 3) Pulmonary peripheral resistance (*RPP*). *RPP* mostly affects the pulmonary arterial pressures. 4) Left ventricular unstressed volume (*VLVU*). An increase in *VLVU* produces rather isolated increases in both end-diastolic and end-systolic ventricular volumes, but without a net increase in stroke volume and cardiac output. These results indicate that the ventricular pressure-volume loop is shifted to the right. 5) Similar observations hold for the unstressed volume of the right ventricle (*VRVU*). 6) Venous unstressed volumes (*VETHVU* and *VITHVU*). These parameters influence the entire circulation in the same amount and direction. 7) Left atrial and ventricular minimum elastances (*ELAMIN* and *ELVMIN*). An increase in either parameter increases pulmonary venous pressure, and to a lesser extent, pulmonary arterial pressures, but does not affect any other part of the circulation. 8) Right atrial and ventricular minimum elastances (*ERAMIN* and *ERVMIN*). An increase in these parameters increases the "immediate upstream" central venous pressure, as for the left heart, and has a negative effect on the remainder of the circulation. 9) Right ventricular maximum elastance (*ERVMAX*). An increase in *ERVMAX* causes a decrease in end-systolic right ventricular volume, with a slight secondary increase in several other variables via an increase in cardiac output. 10) Total blood volume (*VTOTAL*). All monitored variables increase significantly following an increase in *VTOTAL*.

Figure 3 presents the SM at the empirical level for a +1% change in hemodynamic factors. As in Figure 2, numerical values are represented by a color gradient. Numerical values are again presented in the Appendix. These results demonstrate that: 1) The *VUV_factor* significantly affects all the monitored signals in the same direction. 2) *LV_CONT_factor*, *SVR_factor*, and *PVR_factor* produce relatively isolated changes in specific monitored signals: *PCWP*, *MAP*, and *MPAP*, respectively. Note that the dominant effect of an increase in *LV_CONT_factor* is a reduction in *PCWP*. 3) *HR_factor* and *RV_CONT_factor* affect all monitored signals, but with different magnitudes and directions.

Figure 2. Sensitivity matrix reflecting the relative variation of selected monitored signals to a 1% change in parameter values (one-at-a-time). Monitored signals: End-diastolic left ventricular volume, LVEDV; End-systolic left ventricular volume, LVESV; Systolic arterial blood pressure, SBAP; Mean arterial blood pressure, MAP; Diastolic arterial blood pressure, DBAP; Central venous pressure, CVP; End-diastolic right ventricular volume, RVEDV;, End-systolic right ventricular volume, RVESV;,Systolic pulmonary artery blood pressure, SPBP;,Mean pulmonary blood pressure, MPAP; Diastolic pulmonary artery blood pressure, DPBP; Pulmonary venous (wedge) pressure, PCWP; Cardiac output, CO. See Table 1 for the parameter definition.

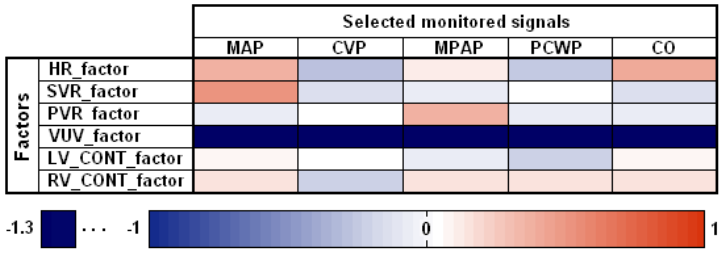

Figure 3. Sensitivity matrix reflecting the relative variation of selected monitored signals to a 1% change in factor values. See the legend of Figure 2 for monitored signals and Table 2 for definition of the factors.

Discussion

In this study, we present a sensitivity analysis of a hemodynamic model[2,3]. The sensitivity analysis is applied to the complete parameter set and 13 monitored signals (basic physiological level), and to hemodynamic factors and 5 monitored signals (empirical level). Note that the results and the discussion below apply most directly to this particular model, set of parameters, and operating point.

The basic physiological analysis reveals that several parameters have a rather isolated effect on specific monitored signals, while others affect the entire circulation. *VLVU* and *VRVU* can be used to manipulate left ventricular ejection fraction without significantly affecting any other hemodynamic variables. *ELAMIN* and *ELVMIN* have a rather isolated effect, unlike the corresponding parameters for the right heart which affect the whole circulation. We note that with the exception of *ERVMAX*, the maximum elastances have limited effect. The negligible effect of several parameters on monitored signals should be carefully interpreted. For example, resistances of heart valves (*RLAOUT*, *RLV*, *RRAOUT* and *RRV*) have low absolute values ($<10^{-2}$ mmHg.mL^{-1}.s). To simulate aortic stenosis in the infant, only a 50-fold increase resulted in the desired observable effect[3]. The blood inertia parameter (*LETHA*) does not seem to influence the monitored signals, but does have an effect on the shape of the simulated arterial blood pressure waveform.

The empirical analysis demonstrates consistency with the basic physiological analysis and confirms that the selected factors are applied to parameters with a major impact on monitored signals (cells with the highest sensitivities in Figure 2). A combination of changes in two parameters or factors may produce near-isolated changes in a specific monitored signal. For example, an increase in *HR_factor* and a matching decrease in *SVR_factor* produce a relatively isolated increase in cardiac output, with the effects on mean arterial pressure canceling out.

The results of the sensitivity analyses are mainly indicative; they can be used to find (combinations of) parameters that will change monitored variables in a particular direction. There may be multiple combinations of parameter changes that lead to the same change in monitored variables. The analyses do not determine if a chosen parameter change is also the most physiologically consistent one for the intended simulated condition.

Preliminary results indicate that the SM is essentially the same for parameter changes in the range of +/-10%. Linearity and effects of combinations could be investigated further. An interesting question results from reverting the sensitivity analysis to find a candidate "parameter space" for a given set of (changes in) monitored signals.

We expect that presented results will guide and facilitate future adaptation of simulated patients and play a role in the creation of new patients representing a sub-population, such as pediatric or geriatric patients, or patients with a specific pathology.

Appendix
Numerical results for the sensitivity matrixes

Table A1. Numerical data of the sensitivity matrix at the basic physiological level. Values rounded to two decimal places.

Cardiovascular model parameters		Selected monitored signals: Left ventricle		Systemic circulation: Arterial			Systemic circulation: Venous	Right ventricle		Pulmonary circulation: Arterial			Pulmonary circulation: Venous	CO
		LVEDV	LVESV	SABP	MAP	DABP	CVP	RVEDV	RVESV	SPBP	MPAP	DPBP	PCWP	
Resistances	HR	-0.19	0.10	0.25	0.37	0.51	-0.30	-0.28	-0.06	-0.13	0.12	0.29	-0.26	0.41
	RLAIN	0.00	0.00	0.00	0.00	0.00	0.00	0.00	0.00	0.00	0.00	0.00	0.00	0.00
	RLAOUT	0.00	0.00	-0.01	-0.01	-0.01	0.00	0.00	0.00	0.00	0.01	0.01	0.03	-0.01
	RLV	0.00	0.00	0.00	0.00	0.00	0.00	0.00	0.00	0.00	0.00	0.00	0.00	0.00
	RETHA	0.01	0.04	0.10	0.04	0.02	-0.01	0.00	0.00	0.00	0.00	0.01	0.02	-0.01
	RSP	0.03	0.19	0.50	0.65	0.80	-0.15	-0.11	-0.06	-0.11	-0.08	-0.04	0.04	-0.18
	RETHV	-0.16	-0.07	-0.22	-0.20	-0.19	-0.27	-0.20	-0.15	-0.27	-0.27	-0.26	-0.26	-0.28
	RRAIN	0.00	0.00	0.00	0.00	0.00	0.01	0.00	0.00	0.00	0.00	0.00	0.00	0.00
	RRAOUT	-0.02	-0.01	-0.02	-0.02	-0.02	0.04	-0.02	-0.01	-0.02	-0.02	-0.02	-0.02	-0.02
	RRV	0.00	0.00	0.00	0.00	0.00	0.01	0.00	0.00	0.00	0.00	0.00	0.00	0.00
	RPP	-0.06	-0.03	-0.09	-0.08	-0.08	0.07	0.06	0.18	0.32	0.48	0.58	-0.09	-0.09
Unstressed volumes	VLAU	-0.01	-0.01	-0.02	-0.02	-0.02	-0.02	-0.01	-0.01	-0.02	-0.02	-0.02	-0.02	-0.02
	VLVU	0.35	0.67	-0.03	-0.03	-0.03	-0.04	-0.03	-0.02	-0.04	-0.03	-0.04	-0.03	-0.03
	VITHAU	-0.05	-0.03	-0.08	-0.08	-0.08	-0.08	-0.06	-0.04	-0.08	-0.08	-0.08	-0.08	-0.08
	VETHAU	-0.13	-0.07	-0.21	-0.21	-0.21	-0.22	-0.16	-0.12	-0.22	-0.21	-0.22	-0.21	-0.21
	VETHVU	-0.36	-0.19	-0.58	-0.58	-0.58	-0.58	-0.43	-0.31	-0.58	-0.58	-0.58	-0.58	-0.58
	VITHVU	-0.43	-0.22	-0.69	-0.69	-0.69	-0.69	-0.51	-0.37	-0.69	-0.69	-0.69	-0.69	-0.69
	VRAU	-0.01	-0.01	-0.02	-0.02	-0.02	-0.02	-0.02	-0.01	-0.02	-0.02	-0.02	-0.02	-0.02
	VRVU	-0.01	-0.01	-0.02	-0.02	-0.02	-0.02	0.24	0.45	-0.02	-0.02	-0.02	-0.02	-0.02
	VPAU	-0.02	-0.01	-0.03	-0.03	-0.03	-0.03	-0.02	-0.02	-0.03	-0.03	-0.03	-0.03	-0.03
	VPVU	-0.13	-0.07	-0.20	-0.20	-0.20	-0.20	-0.15	-0.11	-0.20	-0.20	-0.20	-0.20	-0.20
Elastances	ELAMIN	-0.04	-0.02	-0.06	-0.06	-0.06	-0.01	0.00	0.04	0.08	0.12	0.19	0.37	-0.06
	ELAMAX	-0.09	-0.05	-0.15	-0.15	-0.15	-0.05	-0.04	0.06	0.10	0.19	0.34	0.64	-0.15
	ELVMIN	0.02	0.01	0.15	0.04	-0.01	0.04	0.03	0.02	0.04	0.04	0.04	0.04	0.04
	ELVMAX	0.07	0.05	0.06	0.09	0.01	0.09	0.07	0.05	0.01	0.10	0.10	0.11	0.09
	EITHA	0.18	0.09	0.28	0.28	0.28	0.28	0.21	0.15	0.28	0.28	0.28	0.28	0.28
	EETHA	0.09	0.05	0.15	0.15	0.15	0.14	0.11	0.08	0.15	0.15	0.15	0.15	0.15
	EETHV	-0.09	-0.04	-0.13	-0.13	-0.12	0.36	-0.11	-0.08	-0.15	-0.15	-0.15	-0.14	-0.15
	EITHV	-0.15	-0.07	-0.22	-0.22	-0.21	0.45	-0.19	-0.14	-0.26	-0.25	-0.23	-0.24	-0.25
	ERAMIN	0.00	0.00	0.00	0.00	0.00	0.10	0.08	0.14	-0.28	0.00	0.33	0.00	0.00
	ERAMAX	0.06	0.03	0.09	0.09	0.09	0.09	0.07	0.05	0.09	0.09	0.09	0.09	0.09
	ERVMIN	0.03	0.02	0.05	0.05	0.05	0.02	0.02	-0.02	-0.03	-0.05	-0.09	-0.19	0.05
	ERVMAX	-0.14	-0.31	0.09	0.07	0.06	0.04	0.03	-0.01	-0.02	-0.05	-0.11	-0.21	0.07
	EPA	0.07	0.03	0.10	0.10	0.10	-0.18	0.08	0.06	0.11	0.11	0.11	0.11	0.11
	EPV	0.10	0.05	0.15	0.14	0.14	-0.22	-0.18	-0.46	0.16	0.16	0.15	0.16	0.16
Other	PTH	-0.09	-0.05	-0.14	-0.14	-0.14	-0.14	-0.11	-0.08	-0.14	-0.14	-0.14	-0.14	-0.14
	LETHA	0.00	-0.01	0.03	0.00	0.00	0.00	0.00	0.00	0.00	0.00	0.00	0.00	0.00
	VTOTAL	1.72	0.89	2.75	2.75	2.75	2.75	2.05	1.48	2.75	2.75	2.75	2.75	2.75

Table A2. Numerical data of the sensitivity matrix at the empirical level. Values rounded to two decimal places.

		Selected monitored signals				
		MAP	CVP	MPAP	PCWP	CO
Factors	HR_factor	0.37	-0.30	0.12	-0.26	0.41
	SVR_factor	0.52	-0.12	-0.07	0.03	-0.14
	PVR_factor	-0.07	0.06	0.38	-0.07	-0.07
	VUV_factor	-1.27	-1.27	-1.27	-1.27	-1.27
	LV_CONT_factor	0.07	0.04	-0.05	-0.21	0.07
	RV_CONT_factor	0.14	-0.22	0.16	0.16	0.16

References

1. Zijlmans M, Sá Couto CD, van Meurs WL, Goodwin JA, Andriessen P. Corrected and improved model for educational simulation of neonatal cardiovascular pathophysiology. Simul Healthc. 2009;4(1):49-53.

2. Beneken JEW: A mathematical approach to cardiovascular function. The uncontrolled human system. Ph.D. Thesis, Utrecht, The Netherlands, 1965.

3. Goodwin JA, van Meurs WL, Sá Couto CD, Beneken JEW, Graves SA. A model for educational simulation of infant cardiovascular physiology. Anest Analg. 2004; 99(6):1655-64.

4. Van Meurs WL, Neto P, Azevedo H, Sá Couto CD: "Stan Vintage": A baseline patient for the Human Patient Simulator with hemodynamic parameters from the scientific literature [abstract]. Simul Healthc. 2006;1(3):183.

5. Sá Couto CD, van Meurs WL, Goodwin JA, Andriessen P. A model for educational simulation of neonatal cardiovascular pathophysiology. Simul Healthc. 2006;1:4-12.

6. Sá Couto CD, Andriessen P, van Meurs WL, Sá Couto PM, Ayres de Campos D. A model for educational simulation of hemodynamic transitions at birth. Submitted to Pediatric Res. 2009.

7. Van Meurs WL, Euliano TY: Model driven simulators from the clinical instructor's perspective: Current status and evolving concepts, Simulators in Anesthesiology Education, editors: L. Henson, A. Lee, New-York: Plenum, Chapter 9, 65-73, 1998.

8. Öhrn MAK, van Meurs WL, Good ML: Laboratory classes: replacing animals with a patient simulator [abstract]. Anesthesiology. 1995;83(3A):A1028.

9. Euliano TY, Caton D, van Meurs WL, Good ML: Modeling obstetric cardiovascular physiology on a full-scale patient simulator. J Clin Monit. 1997;13(5): 293-297.

10. Aittokallio T, Gyllenberg M, Polo O, Virkki A. Parameter estimation of a respiratory control model from noninvasive carbon dioxide measurements during sleep. Math Med Biol. 2007;24(2):225-49.

11. Fink M, Batzel JJ, Tran H. A respiratory system model: Parameter estimation and sensitivity analysis. Cardiovasc Eng. 2008;8:120–134.

12. Ellwein LM, Tran HT, Zapata C, Novak V, Olufsen MS. Sensitivity analysis and model assessment: Mathematical models for arterial blood flow and blood pressure. Cardiovasc Eng. 2008;8:94–108.

13. Ursino M, Innocenti M: Mathematical investigation of some physiological factors involved in hemodialysis hypotension. Artif Organs. 1997;21: 891–902.

14. Cavani S, Cavalcanti S, Avanzolini G. Model based sensitivity analysis of arterial pressure response to hemodialysis induced hypovolemia. ASAIO J. 2001;47(4):377-88.

Acknowledgements

Drs. Peter Andriessen and Diogo Ayres de Campos played an essential role in establishing the general framework for this study. The results of the basic physiological analysis for larger parameter changes match unpublished results previously obtained by Alzira Mota. Pedro Sá Couto verified equations, code implementation, and correct reporting of simulation results. Early comments by Hugo Azevedo facilitated visual comparison of Figures 2 and 3.

Funding

Funded in part by the Máxima Medical Center, Veldhoven, The Netherlands and the Instituto de Engenharia Biomédica, Porto, Portugal.

Chapter 8

Concluding remarks

This closing chapter places the presented research in its model –driven simulator context, and lists the main conclusions and suggestions for future work.

General considerations

Some of the basic requirements when developing or adapting physiologic models for educational simulation are realism of baseline clinical signs and monitored signals, of their evolution, and of their responses to correct and incorrect therapeutic interventions. Finding the right balance between model complexity and realism is a major challenge. With rising complexity, models may provide increased realism, but the number of parameters also increases, making it more difficult to estimate and adjust them. Given the frequent need for adaptation of simulated patients in medical education, this challenge may be more pressing than in other areas of modeling.

Essential steps in securing sufficient realism are the verification and validation of developed models. Verification is referred to in one of the published papers, and will be further discussed below. A fundamental paradox in validation of models in this context is that many situations that are interesting to simulate from an educational point of view may involve quite extreme physiological conditions. In such conditions, little or no data may be available from controlled experiments involving human subjects. Comparison of model behavior to data from animal experiments, or its evaluation by clinical experts are other options for assessing realism. Both are applied in the presented work.

Conclusions

A consistent set of mathematical models for educational simulation of cardiovascular pathophysiology is provided. Using the same basic uncontrolled cardiovascular model, reflecting - in our opinion – an appropriate balance of complexity and realism, models for different patients (fetus, neonate, and infant), different pathologies (aortic stenosis and several other congenital heart defects), an incident (blood loss) and a natural transition (birth) are derived.

The infant model serves as a basis for the cardiovascular model of the full-body model-driven BabySIM™, commercially available from Medical Education Technologies, Inc. (METI). A screen-based demonstration prototype, including the neonatal model, was exhibited at the international Human Patient Simulator Network (HPSN) meeting in 2004. Commercialization rights to model software and simulator are property of METI.

Development of foetal and neonatal simulators at the University of Porto (Med Educ 2003;37 Suppl 1:29-33). The run-time information flow in a script-controlled model-driven medical simulator is illustrated and different types of requirements for models of physiology and pharmacology, part of the simulation engine of a medical educational simulator, are introduced.

A model for educational simulation of infant cardiovascular physiology (Anest Analg 2004;99(6):1655-64). Existing uncontrolled cardiovascular and baroreflex models for the adult are combined and described in detail, and a new parameter set representing the infant is derived. Simulated vital signs match published target data, the model reacts appropriately to blood loss, and incorporation of aortic stenosis is straightforward.

A model for educational simulation of neonatal cardiovascular pathophysiology (Simul Healthc 2006;1 Spec no.:4-9). Using the same underlying model as for the infant, a complete set of parameters reflecting a normal 1-week old neonate is derived. The hemodynamic model is then expanded to reflect selected pathologies. Simulation results for the baseline patient, blood loss, and congenital heart defects match published target data. Simulated waveforms are considered realistic enough for educational simulations.

Corrected and improved model for educational simulation of neonatal cardiovascular pathophysiology (Simul Healthc 2009;4(1):49-53). Small errors in software implementation of the previous model are identified and corrected. One of the errors masked a modeling inaccuracy, which is corrected through further investigation and adaptation of the baroreflex model. Simulation results of the corrected and improved model closely match published target data. A procedure to avoid such errors is presented. A companion editorial congratulates the authors for their "courage and integrity" and cites this paper as a "milestone for the Journal as it takes full part of the larger process of science and scholarship"[1].

A model for educational simulation of hemodynamic transitions at birth (submitted to Pediatr Res). An original combination of a physiological model with scripted parameter changes for educational simulation of hemodynamic transitions at birth is presented. Simulation results match published target data and demonstrate that the model is capable of correctly representing fetal hemodynamics and the evolution of neonatal hemodynamics during the first 24 hours of life.

Sensitivity analysis of a hemodynamic model to facilitate programming simulation patients (chapter). The recurring need for parameter estimation for new patients, and for adaptation of existing ones, prompted the presented systematic sensitivity analysis of the hemodynamic model. This first analysis involves the adult hemodynamic model in its baseline operating point. It brings out the parameters with significant and those with minor effects, and helps distinguish parameters with a more isolated effect on specific monitored signals from those that affect the entire circulation. The presented data is consistent with known aspects of human physiology.

[1] *Gaba DM. Milestones for the journal. Simul Healthc. 2009; 4(1):1-2.*

Suggestions for future work

Model-driven simulators for obstetric emergencies are currently being developed. The hemodynamic model of these simulators is not directly based on the work presented, but may benefit from incorporation of some of its elements.

Development and coupling of dependent models, such as oxygen transport and chemoreflex models, to the hemodynamic models presented in this thesis is possible, and should be relatively straightforward. Such extensions would allow for the simulation of additional monitored signals, which are educationally relevant.

Elaborating on the work presented in this thesis, the potential of educational simulation of ontogenesis and aging of the cardiovascular system could be explored. If embedded in a carefully designed educational program and with appropriate visualization of data, simulation of the (same) cardiovascular model from fetus to elderly could provide powerful insights.

The presented sensitivity analysis can be expanded for the same simulated patient by further investigation of non-linearities, changes in operating point, effect of addition of a baroreflex model, and the study of simulated drug effects. It can also be applied to hemodynamic models of other patients. Application of a similar analysis to respiratory models would further assist in programming new patients.